

Aus der Klinik für Innere Medizin IV – Nieren und Hochdruckkrankheiten

Universitätsklinikum des Saarlandes, Homburg/Saar

(Direktor: Prof. Dr. Danilo Fliser)

Substanzspezifische Toxizität intravenöser Eisenpräparate auf Monozyten, Makrophagen und Dendritische Zellen

DISSERTATION

zur Erlangung des Grades eines Doktors der Naturwissenschaften

der Medizinischen Fakultät

der UNIVERSITÄT DES SAARLANDES

2015

vorgelegt von: Lisa Fell

geb. am: 02.09.1987 in Merzig

Tag des Kolloquiums:

Dekan:

Berichterstatter:

.....

.....

Vorsitz:

Akademischer Mitarbeiter:

Inhaltsverzeichnis

Zusammenfassung	5
Summary	6
Kapitel 1: Einleitung	8
1.1 Prävalenz und Bedeutung der chronischen Nierenerkrankung	8
1.2 Pathophysiologie der Anämie der chronischen Nierenerkrankung.....	9
1.3 Therapie der Anämie bei CKD.....	11
1.4 Immunologische Toxizität intravenöser Eisenpräparate	12
1.4.1 Monozyten.....	14
1.4.2 Makrophagen.....	16
1.4.3 Dendritische Zellen	17
1.5 Fragestellung der Promotionsarbeit	19
Kapitel 2: Ergebnisse	20
2.1 Vergleich zweier Gatingstrategien zur Analyse humaner Monozytensubpopulationen	20
2.2 Mineral- und Knochenhaushalt – Die Kalzium-Phosphat-Homöostase und der neue Biomarker FGF-23	23
2.2.1 Einfluss des Kalzium-Phosphathaushalts auf die Monozytenbiologie	23
2.2.2 FGF-23 als Langzeitmarker der mittleren Plasmaphosphatspiegel bei Hämodialysepatienten	27
2.3 Substanzspezifische Toxizität intravenöser Eisenpräparate auf die Monozytenbiologie <i>in vitro</i>	30
2.3.1 Einfluss intravenöser Eisenpräparate auf die Monozytenheterogenität	30

2.3.2 Einfluss intravenöser Eisenpräparate auf die <i>in vitro</i> Differenzierung von Monozyten zu Makrophagen und Dendritischen Zellen	32
Kapitel 3: Zusammenfassung und Ausblick.....	35
Literaturverzeichnis.....	37
Abkürzungsverzeichnis	46
Abbildungsverzeichnis	49
Tabellenverzeichnis.....	49
Lebenslauf	50
Publikationen.....	50
Kongressbeiträge	52
Danksagung	53
Anhang	54
A1 Material- und Methodenteil zum „Einfluss des Kalzium-Phosphathaushalts auf die Monozytenbiologie“	54
A1-1 Material	54
A1-2 Methoden	57
A2 Publikationen.....	66

Zusammenfassung

Die Anämie der chronischen Nierenerkrankung trägt als multikausales Krankheitsbild maßgeblich zur erhöhten Morbidität und Mortalität der Patienten bei. Die Anämie geht zumeist mit einem manifesten Eisenmangel einher, der insbesondere in einer chronischen Mikroinflammation mit verringerter gastrointestinaler Eisenaufnahme begründet liegt. In der Anämietherapie wird eine Vielzahl intravenöser (*i.v.*) Eisenpräparate eingesetzt, deren potentielle Nebenwirkungen in den letzten Jahren in den Fokus von Ärzten und Wissenschaftlern gerückt sind. So sollen *i.v.* Eisenpräparate Störungen des Knochen- und Mineralhaushalts und der Immunabwehr auslösen. Dabei ist bislang unklar, ob solche Effekte klassenspezifisch durch alle *i.v.* Eisenpräparate oder substanzspezifisch nur durch einzelne Präparate induziert werden.

Vor diesem Hintergrund wurde in der vorliegenden Arbeit *in vitro* untersucht, inwiefern *i.v.* Eisenpräparate Entstehung, Phänotyp und Funktion von Monozyten, Makrophagen und Dendritischen Zellen als zentrale Mediatoren der zellulären Immunabwehr beeinflussen. Die Analysen erfolgten vor dem Hintergrund einer Monozytenheterogenität, wonach drei funktionell unabhängige Monozytensubpopulationen (klassische, intermediäre und nicht-klassische Monozyten) definiert werden. Die Einteilung der Monozytensubpopulationen erfolgte durchflusszytometrisch nach einem Messprotokoll, welches zu Beginn der Arbeit am Patientenkollektiv der CARE FOR HOME Studie validiert wurde.

Als zentrales Ergebnis der *in vitro* Studien wurde erkannt, dass *i.v.* Eisenpräparate – in Abhängigkeit ihrer Stabilität und Ferrokinetik – eine starke substanzspezifische Toxizität aufweisen. Während stabilere Eisenpräparate wie Eisen-Isomaltosid 1000 immunologisch weitgehend neutral waren, wiesen weniger stabile Eisenpräparate wie Eisen-Saccharose jedoch bereits in therapeutischen Dosierungen ein hohes immunmodulatorisches Potential auf. Dies äußerte sich einerseits in einer stark veränderten *in vitro* Differenzierung von Monozyten und ihren myeloiden Nachkommen, den Makrophagen und Dendritischen Zellen. Andererseits konnten starke phänotypische und funktionelle Veränderungen der Immunzellen erkannt werden, welche mit einer Dysregulation von microRNAs als zentrale posttranskriptionelle Regulation der Genexpression assoziiert werden konnten.

Die Ergebnisse können zu einem besseren pathophysiologischen Verständnis der Nebenwirkungen von *i.v.* Eisenpräparaten beitragen. Zukünftig sollten in einer klinischen

Studie die *in vitro* beobachteten immunmodulatorischen Effekte *in vivo* bei chronisch nierenkranken Patienten überprüft werden, um mittels Optimierung der Anämietherapie eine Verbesserung der Lebensqualität und Sicherheit von nierenkranken Patienten zu erreichen.

Summary

As a multicausal disease, anemia of chronic kidney disease contributes to the high morbidity and mortality of patients with impaired renal function. This anemia of chronic kidney disease is associated with iron deficiency, resulting from chronic microinflammation with reduced gastrointestinal iron uptake. Several intravenous (*i.v.*) iron preparations are available for anemia therapy, the adverse reactions of which – comprising mineral- and bone disorders and immunological effects – have gained substantial interest in recent years. It is still unknown whether these adverse effects occur with all *i.v.* iron preparations, or whether they are substance-specifically caused by distinct preparations.

Against this background, this thesis aimed to assess the impact of different *i.v.* iron preparations on *in vitro* development, phenotype and function of monocytes and their progenies, macrophages and dendritic cells, which are central regulators of host defence. The studies particularly acknowledged monocyte heterogeneity and analysed three monocyte subsets flow-cytometrically (classical, intermediate and nonclassical monocytes). The applied gating strategy was *a priori* validated in our CARE FOR HOME cohort.

Our *in vitro* studies demonstrated that – depending on their stability and ferrokinetics – specific *i.v.* iron preparations exert relevant toxic effects on monocyte biology. In contrast to more stable *i.v.* iron preparations such as iron isomaltoside 1000, which were immunologically neutral, less stable preparations such as iron sucrose and sodium ferric gluconate strongly affected differentiation of monocytes, macrophages and dendritic cells *in vitro*. Moreover, they induced strong phenotypical and functional changes that could be associated with dysregulation of microRNAs as central posttranscriptional regulators of gene expression.

These data may broaden our pathophysiologic understanding of side effects of *i.v.* iron therapy. Future clinical trials should delineate in how far these *in vitro* observations will

translate into clinically relevant immune responses, aiming to optimize anemia therapy and to improve quality of life and safety for our chronic kidney disease patients.

Kapitel 1: Einleitung

1.1 Prävalenz und Bedeutung der chronischen Nierenerkrankung

Die chronische Nierenerkrankung (CKD) stellt weltweit eine zunehmende medizinische und auch ökonomische Herausforderung dar. Definiert man die chronische Nierenerkrankung gemäß den KDIGO-Leitlinien als strukturelle oder funktionelle renale Veränderungen, die über mindestens drei Monate vorliegen (KDIGO, 2012), so wiesen im Jahr 2003 laut bevölkerungsbasierter US-amerikanischer Studien wie NHANES III etwa 11% der amerikanischen Allgemeinbevölkerung über 18 Jahre eine CKD auf; zwischen 2007 und 2010 stieg die Prävalenz der CKD auf 14% an (CORESH et al., 2003; STAUFFER, FAN, 2014). Daten aus Deutschland zeigten für den Zeitraum von 1997 bis 2006 einen jährlichen Zuwachs der Anzahl der Patienten, die eine chronische Nierenersatztherapie benötigen, von durchschnittlich 4,4% (FREI, H.-J., 2008).

Die chronische Nierenerkrankung ist durch einen langsam voranschreitenden Verlust der Nierenfunktion charakterisiert, welcher im Endstadium in einer Nierenersatztherapie mündet. Die Klassifizierung der CKD erfolgt anhand der glomerulären Filtrationsrate (GFR) und der Albuminurie (A), durch welche man die Patienten in unterschiedliche CKD Stadien (Stadien G1 bis G5 und A1 bis A3) stratifizieren kann.

Im Vergleich zur nierengesunden Allgemeinbevölkerung ist das Risiko eines CKD-Patienten für kardiovaskuläre Ereignisse um das Zehn- bis Zwanzigfache erhöht. Dieser Anstieg trägt zur hohen Mortalität chronisch nierenkranker Menschen bei (DE JAGER et al., 2009). Dabei tragen neben klassischen kardiovaskulären Risikofaktoren, wie Alter, Hypercholesterinämie, Bluthochdruck, Nikotinkonsum oder Diabetes mellitus, auch nicht-klassische Risikofaktoren signifikant zur erhöhten kardiovaskulären Co-Morbidität bei (SARNAK et al., 2003). Zu den nicht-klassischen Risikofaktoren zählen der dysregulierte Kalzium-Phosphat-Stoffwechsel, welcher insbesondere durch eine Hyperphosphatämie, eine verminderte Vitamin D-Aktivierung sowie einen Anstieg der phosphaturischen Hormone Fibroblasten Wachstumsfaktor-23 (FGF-23) und Parathormon (PTH), eine chronische Mikroinflammation und möglicherweise die CKD-assoziierte Anämie charakterisiert ist (SARNAK et al., 2003; SEILER et al., 2013).

1.2 Pathophysiologie der Anämie der chronischen Nierenerkrankung

Eine Anämie definiert sich laut WHO-Empfehlungen als Hämoglobinwert < 13 g/dL bei Männern und < 12 g/dL bei Frauen. Im Rahmen der chronischen Nierenerkrankung steigt die Prävalenz einer Anämie mit zunehmender renaler Dysfunktion an (LANKHORST, WISH, 2010). Prospektive Kohortenstudien zeigen, dass die Anämie mit der erhöhten Morbidität und Mortalität der CKD Patienten assoziiert ist. So konnte das Ausmaß der Anämie als ein unabhängiger prognostischer Faktor für die Progredienz einer chronischen Nierenerkrankung zur Dialysepflichtigkeit (KEANE et al., 2003), für kardiovaskuläre Ereignisse (VLAGOPOULOS et al., 2005) und für die Gesamtmortalität (LOCATELLI et al., 2004) erkannt werden. Die Anämie der chronischen Nierenerkrankung resultiert aus multifaktoriellen Ursachen: Durch Verlust intakten Nierengewebes nimmt die Produktion des renalen Hormons Erythropoetin ab; daneben beeinflussen urämische Toxine und die chronische Mikroinflammation direkt einerseits die Erythrozyten-Proliferation und -Lebensdauer, andererseits die Eisenhomöostase, welche in der Ausbildung einer Eisenmangelanämie münden kann (WEISS, GOODNOUGH, 2005).

Als essentielles Mineral ist Eisen Baustein vieler Proteine, die etwa an der Atmungskette und Biosynthese beteiligt sind (GOZZELINO et al., 2010; SHEFTEL et al., 2010). Aus der Nahrung wird Eisen über die Enterozyten des Duodenums und oberen Jejunums als anorganisches Salz über den bivalenten Metalltransporter-1 (DMT-1) oder in organischer gebundener Form, beispielsweise als Häm-Eisen über den Häm-Transporter-1 (HCP-1) absorbiert (FRAZER, ANDERSON, 2005; LATUNDE-DADA et al., 2008; THEIL, 2011).

Während Eisen in der Nahrung zumeist dreiwertig (Fe^{3+}) vorliegt, welches zunächst im Darmlumen reduziert wird, tritt es intrazellulär als zweiwertiges Eisen (Fe^{2+}) in den zellulären „labilen Eisenpool“ ein. Von dort aus wird Fe^{2+} entweder für intrazelluläre Prozesse wie die Häm-Synthese genutzt, als Ferritin gespeichert oder über das Membranprotein Ferroportin in das Interstitium transportiert, von wo es in die Blutzirkulation übertreten kann. Ferroportin ist ein Eisentransporter von Enterozyten und Makrophagen, dessen Expression über das hepatische Akut-Phase-Protein Hepcidin reguliert wird (EVSTATIEV, GASCHÉ, 2011). Während des Transports wird Fe^{2+} zu Fe^{3+} oxidiert und an Apotransferrin gebunden, welches anschließend als Transferrin über den Transferrinrezeptor-1 in Makrophagen oder Erythroblasten aufgenommen werden kann.

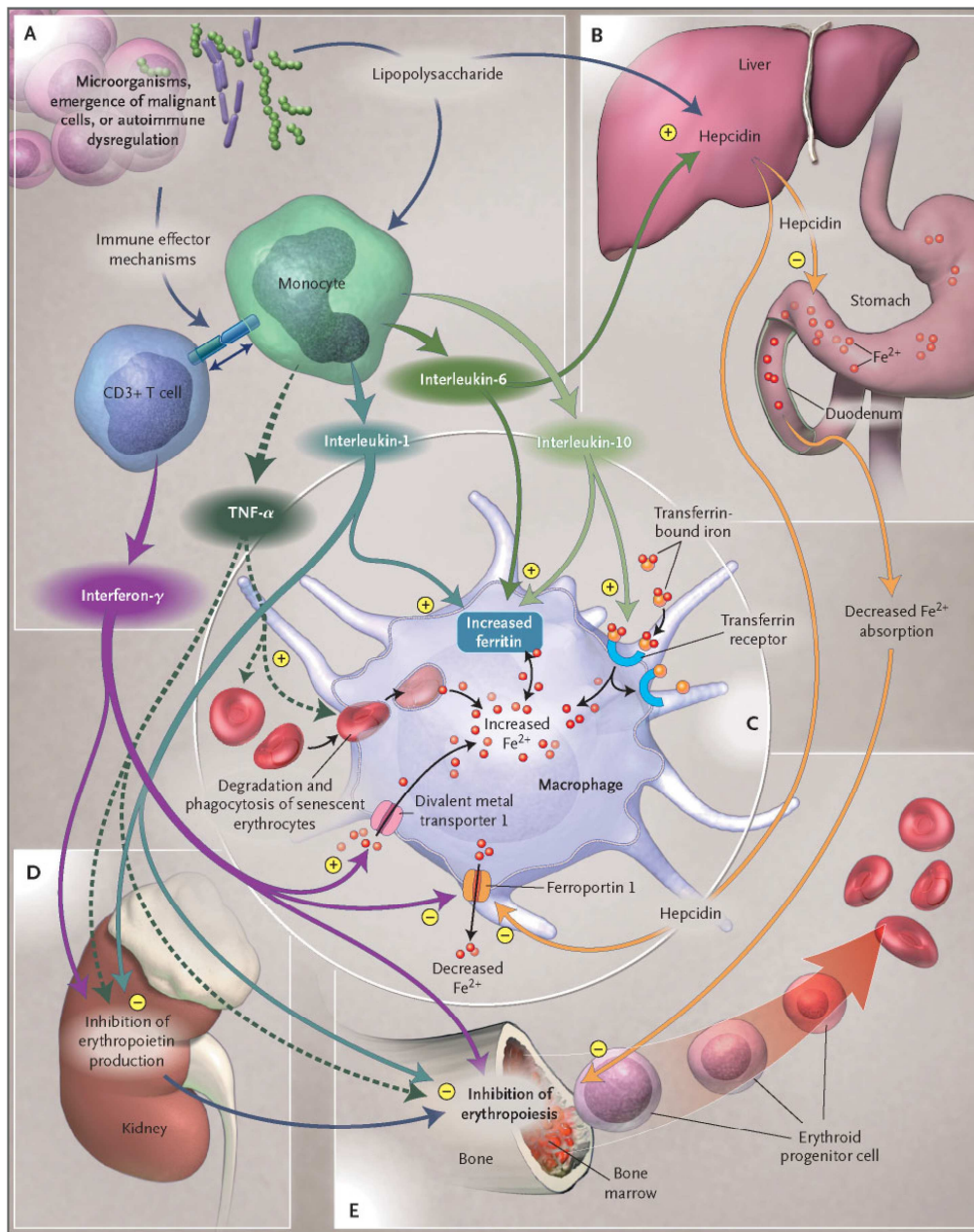


Abbildung 1: Pathophysiologische Mechanismen der Anämie der chronischen Nierenerkrankung

A: Aktivierung von T-Zellen und Monozyten: Induktion von Effektormechanismen, die eine Produktion von Zytokinen wie Interferon- γ , Tumornekrosefaktor- α und die Interleukine-1, -6, und -10 zur Folge haben. **B:** Minderung der duodenalen Eisenabsorption: Hemmung des Eisentransporters Ferroportin-1 durch Interleukin-6- und Lipopolysaccharid-vermittelte Stimulation der hepatischen Hepcidinexpression. **C:** Mangelnde Eisenversorgung erythroider Zellen durch Eisenakkumulation in den Makrophagen: Erhöhte Eisenaufnahme durch verstärkte Expression des bivalenten Metalltransporters-1 und Transferrinrezeptors und Phagozytose seneszenten Erythrozyten; erhöhte Eisenretention durch verstärkte Ferritinexpression und verminderte Eisenabgabe durch Minderexpression von Ferroportin-1. **D, E:** Inhibition der Erythropoietin-Synthese und demnach der Differenzierung und Proliferation erythroider Zellen durch Tumornekrosefaktor- α , Interferon- γ und Interleukin-1. Reproduced with permission from Weiss and Goodnough (WEISS, GOODNOUGH, 2005), Copyright Massachusetts Medical Society.

Während die Erythroblasten das Eisen zur Hämoglobinsynthese nutzen, dienen Makrophagen hauptsächlich der Speicherung des Eisens, welches sie neben Transferrin auch über Phagozytose seneszenten Erythrozyten aufnehmen und dem Organismus als Transferrin und Ferritin erneut zur Verfügung stellen (COHEN et al., 2010; MOURA et al., 2015).

Bei chronischer Nierenerkrankung beeinflusst die erhöhte Sekretion von Zytokinen wie Interferon- γ (IFN- γ), Tumornekrosefaktor- α (TNF- α) und der Interleukine (IL) IL-1, IL-6 und IL-10 die Eisenhomöostase (**Abbildung 1**). Diese regulieren die Expression von Eisentransportproteinen sowohl direkt als auch indirekt durch Stimulation der Hepcidinexpression, wodurch einerseits eine verminderte Absorption des Nahrungseisens, andererseits eine verstärkte Eisenaufnahme und -retention in Makrophagen resultiert. Zusätzlich erhöhen sie die Expression des Eisenspeichers Ferritin in den Makrophagen. TNF- α bewirkt zudem eine Schädigung der Erythrozytenmembran und stimuliert so deren Degradation und Phagozytose durch Makrophagen. Zusammenfassend gipfelt die geringe Eisenverfügbarkeit für den Organismus in einer verminderten Erythropoese und dem Auftreten einer Eisenmangelanämie (WEISS, GOODNOUGH, 2005).

1.3 Therapie der Anämie bei CKD

Im Zentrum der Anämietherapie bei CKD Patienten standen in den letzten zwei Jahrzehnten Erythropoetin (EPO) und andere Erythropoese-stimulierenden Agenzien (ESAs). Diese erlauben eine Normalisierung des Hämoglobinwertes bei chronisch nierenkranken Patienten; dennoch erbrachte weder die EPO-Behandlung in den CHOIR- und CREATE-Studien (DRUEKE et al., 2006; SINGH et al., 2006) noch die ESA-Behandlung in der TREAT-Studie (PFEFFER et al., 2009) einen prognostischen Benefit hinsichtlich des Auftretens kardiovaskulärer Ereignisse. Im Gegenteil wurde in der TREAT-Studie vielmehr ein Anstieg des Schlaganfallrisikos beobachtet (PFEFFER et al., 2009). Basierend auf dieser Datenlage wird in den aktuellen KDIGO-Leitlinien geraten, den Einsatz von EPO und ESAs möglichst gering zu halten und stattdessen die Normalisierung des Eisenmangels in den Fokus der Anämietherapie zu rücken (KDIGO, 2012).

Aufgrund der zuvor beschriebenen Dysregulation der Eisenhomöostase mit verminderter Eisenabsorption über die Enterozyten wird zumindest bei fortgeschrittener CKD die Therapie mit intravenösen (*i.v.*) anstelle von oralen Eisenpräparaten empfohlen (KDIGO, 2012). Dies bestätigen auch aktuelle randomisierte Vergleichsstudien: So zeigte eine intravenöse

Eisensubstitution einen schnelleren Therapieerfolg als eine orale Eisentherapie, obgleich eine mehrmonatige orale Substitution zumindest bei Patienten in frühen Stadien der chronischen Nierenerkrankung ebenso zu einer Normalisierung der Eisenspeicher führen kann (ROZEN-ZVI et al., 2008). Daneben wird als neue Form der Eisentherapie bei Dialysepatienten eine Substitution von Eisen Pyrophosphat Citrat diskutiert (FELL et al., 2015).

1.4 Immunologische Toxizität intravenöser Eisenpräparate

Zur *i.v.* Eisentherapie sind verschiedene Eisenpräparate zugelassen, die zumeist aus einem Ferritin-ähnlichen Kern und einer Präparat-spezifischen Kohlenhydrathülle aufgebaut sind (Tabelle 1); strukturell unterscheidet sich lediglich MonoFer[®] als Eisen-Isomaltosid-Verbindung mit seiner Bilayer Struktur deutlich. Die Kohlenhydrathülle bedingt die physiochemischen und pharmakokinetischen Parameter der Präparate wie das Molekulargewicht und die Reaktivität sowie die thermodynamische Stabilität (JAHN et al., 2011; MACDOUGALL, GEISSER, 2013).

Tabelle 1: *I.v.* Eisenpräparate und ausgewählte Eigenschaften

Verbindung	Natrium-Eisen-Gluconat	Eisen-Saccharose	Eisen-Oxytol	Eisen-Carboxy-maltose	LMW Eisen-Dextran	Eisen-Isomaltosid
Handelsname	Ferrlecit [®]	Venofer [®] FerMed [®]	Rienso [®]	Ferinject [®]	CosmoFer [®]	MonoFer [®]
Konzentration	12,5 mg/ml	20 mg/ml	30 mg/ml	50 mg/ml	50 mg/ml	100 mg/ml
Höchstosis	62,5 mg	500 mg	1020 mg	1000 mg	20 mg pro kg KG	2000 mg
Molekulargewicht	164 kDa	140 kDa	276 kDa	233 kDa	165 kDa	150 kDa
Stabilität	Schwach		Moderat		Hoch	
Halbwertszeit	1,4 h	5,3 h	14,7 h	7,4-9,4 h	27-30 h	23,2 h

LMW = low molecular weight (niedermolekular), KG = Körpergewicht; Daten nach (GEISSER, BURCKHARDT, 2011; JAHN et al., 2011; MACDOUGALL, GEISSER, 2013; NORDFJELD et al., 2012).

Nachdem die CHOIR, CREATE und TREAT Studien keinen prognostischen Vorteil einer EPO- oder ESA-Therapie (DRUEKE et al., 2006; PFEFFER et al., 2009; SINGH et al., 2006) aufzeigten, entwickelte sich ein Trend zur *i.v.* Eisentherapie insbesondere bei Patienten mit

fortgeschrittener CKD vor Einsetzen der Dialysepflichtigkeit (PADHI et al., 2015; WINKELMAYER et al., 2014).

Mit der wachsenden klinischen Bedeutung rücken jedoch auch Meldungen über potentielle systemische Nebenwirkungen der *i.v.* Eisenpräparate in den Fokus von Ärzten und Wissenschaftlern. So wurden *i.v.* Eisenpräparate mit renalen, kardiovaskulären, endokrinologischen und vor allem auch immunologischen Nebenwirkungen assoziiert, welche in aktuellen Übersichtsartikeln zusammengefasst wurden (FISHBANE et al., 2014; MACDOUGALL, GEISSER, 2013; VAZIRI, 2013). Hinsichtlich renalier Nebenwirkungen wurde die Applikation intravenöser Eisenpartikel als prooxidative Agentien mit der Induktion eines tubulären und endothelialen Zelltods in Verbindung gebracht (ZAGER et al., 2002). Kardiovaskulär wurde postuliert, dass die injizierten *i.v.* Eisenpräparate *in vitro* eine endotheliale Dysfunktion (KAMANNA et al., 2012) und *in vivo* eine beschleunigte Atherosklerose bedingen können (DRUEKE et al., 2006). Endokrinologisch interagieren zumindest einzelne *i.v.* Präparate mit dem Mineral- und Knochenhaushalt, indem sie eine erhöhte Sekretion des phosphaturischen Hormons FGF-23 und damit eine Hypophosphatämie induzieren (BRANDENBURG et al., 2014; WOLF et al., 2013).

Im Zentrum der Toxizität stehen jedoch vermutlich immunologische Effekte, welche aus der Wirkung von *i.v.* Eisenpräparaten auf Immunzellen – etwa auf Granulozyten und auf Monozyten – resultieren. So induzierten *i.v.* Eisenpräparate eine verminderte Proliferationsrate und Phagozytoseleistung der Granulozyten, bei gleichzeitig erhöhter Apoptose (DEICHER et al., 2003; ICHII et al., 2012). Hinsichtlich ihrer Wirkung auf Monozyten konnte gezeigt werden, dass diese *i.v.* verabreichtes Eisen aufnehmen und speichern, wodurch es zu einer Beeinflussung von monozytären Effektorfunktionen kommt (SONNWEBER et al., 2011; YOSHIMURA et al., 2005). In Einklang damit konnte in Serumproben von Patienten nach *i.v.* Eisentherapie ein vermehrtes bakterielles Wachstum *in vitro* aufgezeigt werden, welches mit einem erhöhten Infektionsrisiko *in vivo* assoziiert ist (PARKKINEN et al., 2000).

Ursächlich erscheint hierbei insbesondere eine toxische Rolle von nicht-Transferrin gebundenem Eisen (NTBI). NTBI entsteht bei Überangebot an Eisen nach Erreichen der Transferrinsättigung, wie es durch die Injektion hoher Dosen von *i.v.* Eisenpräparaten auftritt, und ist maßgeblich an der Induktion von reaktiven Sauerstoffspezies (ROS) beteiligt (BRISSOT et al., 2012; GEISSER, BURCKHARDT, 2011; PAI et al., 2011; SHE et al., 2002; ZAGER et al., 2002), welche insbesondere Lipidmembranen, Proteine und DNA

schädigen und somit an der Ausbildung von Inflamationsreaktionen beteiligt sind (EVANS et al., 2008).

Solche immunologischen Nebenwirkungen von *i.v.* Eisenpräparaten haben bei chronisch nierenkranken Patienten eine besondere Bedeutung, da diese Patienten bereits im Rahmen ihrer nephrologischen Grunderkrankung eine chronische Mikroinflammation aufweisen. Diese chronische Mikroinflammation kann zur Pathophysiologie zweier zentraler extrarenaler Komorbiditäten – der deutlich erhöhten kardiovaskulären Morbidität und einer erhöhten Prävalenz von Infektionserkrankungen – beitragen (DE JAGER et al., 2009). In diesem Kontext erscheinen die immunologischen Nebenwirkungen der *i.v.* Eisenpräparate bei chronischer Nierenerkrankung von besonderer potentieller Bedeutung.

Daher soll diese Dissertationsschrift auf die Toxizität von *i.v.* Eisenpräparaten auf einzelne Leukozytensubpopulationen fokussieren, die in den folgenden Abschnitten kurz charakterisiert werden sollen.

1.4.1 Monozyten

Monozyten sind zentrale Komponenten des angeborenen Immunsystems. Sie entstehen aus myeloiden Stammzellen im Knochenmark und zirkulieren im Blut, wo sie funktionell an der Phagozytose, Antigenpräsentation und Sezernierung pro- und antiinflammatorischer Zytokine beteiligt sind.

Monozyten stellen eine heterogene Zellpopulation dar, die den LPS-Rezeptor (CD14) auf ihrer Oberfläche tragen und phänotypisch anhand der Expressionsstärke des Fcγ-Rezeptors Typ III (CD16) zunächst in zwei Subpopulationen eingeteilt wurden: CD14⁺⁺CD16⁻ und CD16⁺ Monozyten (PASSLICK et al., 1989), wobei der Anteil CD16⁺ Monozyten lediglich 5-20% der Gesamtmonozyten ausmacht. Beide Subpopulationen unterscheiden sich auch hinsichtlich ihrer Morphologie und Zytokinexpression. So sind CD16⁺ Monozyten kleiner, besitzen eine größere Granularität als CD16⁻ Monozyten (PASSLICK et al., 1989) und sezernieren vermehrt proinflammatorische Zytokine. In zahlreichen inflammatorischen Erkrankungen steigt die Anzahl CD16⁺ Monozyten an (KAWANAKA et al., 2002; NOCKHER, SCHERBERICH, 1998; ZIEGLER-HEITBROCK, 2007), weshalb sie als proinflammatorische Monozyten betrachtet werden (BELGE et al., 2002; SKINNER et al., 2005; ZIEGLER-HEITBROCK, 2007).

Innerhalb der Gesamtpopulation der CD16⁺ Monozyten gelang es im Jahr 2010 zwei phänotypisch und funktionell distinkte Subpopulationen zu identifizieren, die sich morphologisch anhand der CD14-Expressionsstärke unterscheiden: die CD14⁺⁺CD16⁺ und CD14⁺CD16⁺⁺ Monozyten (ANCUTA et al., 2003; ZIEGLER-HEITBROCK et al., 2010). Basierend auf diesen Beobachtungen wurde von der IUIS (*Nomenclature Committee of the international Union of Immunological Societies*) eine offizielle Nomenklatur für Monozyten veröffentlicht, welche die Gesamtmonozyten in die drei Subpopulationen

- klassische (CD14⁺⁺CD16⁻) Monozyten,
- intermediäre (CD14⁺⁺CD16⁺) Monozyten und
- nicht-klassische (CD14⁺CD16⁺⁺) Monozyten

differenziert (ZIEGLER-HEITBROCK et al., 2010), ohne dass ein Konsens bezüglich der exakten Gatingstrategie zur durchflusszytometrischen Einteilung der Monozytensubpopulationen erzielt wurde.

In epidemiologischen Untersuchungen konnten intermediäre Monozyten als unabhängige Prädiktoren für kardiovaskuläre Ereignisse bei Dialysepatienten (HEINE et al., 2008), bei chronisch nierenkranken, nicht-dialysepflichtigen Patienten (ROGACEV et al., 2010) sowie bei kardiovaskulären Risikopatienten (ROGACEV et al., 2012) beschrieben werden. Experimentelle Studien haben gezeigt, dass sie eine erhöhte Expression proatherogener und proinflammatorischer Rezeptoren (CCR5, TLR2, ACE) aufweisen (ROGACEV et al., 2011; ULRICH et al., 2006) und selektiv ROS produzieren (ZAWADA et al., 2011). Zudem sind intermediäre Monozyten durch eine erhöhte Sekretion proinflammatorischer Zytokine, wie TNF- α , IL-1 β und IL-6 (CROS et al., 2010) charakterisiert, die im Rahmen der Immunantwort weitere Immunzellen aber auch Endothelzellen der Gefäßwand aktivieren.

Aktivierte Endothelzellen exprimieren verstärkt Adhäsionsmoleküle wie ICAM-1 (intrazelluläres Adhäsionsmolekül-1) und VCAM-1 (vaskuläres Zelladhäsionsmolekül-1), welche zusammen mit der chemotaktischen Wirkung von MCP-1 (Monozyten-chemotaktisches Protein-1) Monozyten anlocken und deren Adhäsion und Einwanderung in die Intima ermöglichen. Dort induzieren Zytokine, wie M-CSF (Makrophagen Koloniestimulierender Faktor) und GM-CSF (Granulozyten und Makrophagen Koloniestimulierender Faktor) eine Differenzierung der Monozyten zu Makrophagen oder Dendritischen Zellen (DC) (KRYCHTIUK et al., 2015; LIBBY et al., 2002).

1.4.2 Makrophagen

Makrophagen sind Teil der angeborenen Immunabwehr, deren Hauptaufgaben in der Phagozytose und Sezernierung pro- und antiinflammatorischer Zytokine, aber auch in der Antigenpräsentation liegen. Traditionell werden reife Makrophagen in zwei Populationen eingeteilt: die klassisch aktivierten M1-Makrophagen und die alternativ aktivierten M2-Makrophagen. Während der Differenzierung hin zu Makrophagen wird der Monozytenmarker CD14 herunterreguliert und der Makrophagenmarker CD68, welcher Bestandteil intrazellulärer lysosomaler Membranproteine ist, verstärkt exprimiert (BROWN et al., 2009; GORDON, TAYLOR, 2005; MARTINEZ, GORDON, 2014).

M1-Makrophagen dienen im Wesentlichen der Abwehr von Mikroorganismen und entwickeln sich nach Stimulation mit IFN- γ und LPS. Als Effektorzellen exprimieren sie den Oberflächenmarker CD16, welcher der Phagozytose opsonierter Zellen, Bakterien und sonstiger Mikropartikel dient, sowie HLA-DR, CD80 und CD86, welche zur Antigenpräsentation und Kostimulation von T-Zellen dienen. Zusätzlich sezernieren sie verschiedene proinflammatorische Zytokine wie IL-1, IL-12 und TNF- α und produzieren Stickstoff- und Sauerstoffradikale (MANTOVANI et al., 2007; MANTOVANI et al., 2004; MOSSER, EDWARDS, 2008; VERRECK et al., 2004; VERRECK et al., 2006).

Im Gegensatz zu den M1-Makrophagen sind M2-Makrophagen eine sehr heterogene Zellpopulation, die immunsuppressiv wirkt und an der Beseitigung von Zelltrümmern, aber auch an der Wundheilung und Angiogenese beteiligt ist. In Abhängigkeit der einwirkenden Differenzierungssignale werden die drei unterschiedlichen Subtypen M2a, M2b und M2c ausgebildet (MANTOVANI et al., 2007; MANTOVANI et al., 2004). M2-Makrophagen können durch spezifische Zytokine und Oberflächenmarker von M1-Makrophagen unterschieden werden. So sezernieren sie hohe Spiegel an IL-10, CCL2 und CCL18 und exprimieren Scavenger (CD163)- und Mannose (CD206)-Rezeptoren. Funktionell dienen sie hauptsächlich der Phagozytose und weniger der Antigenpräsentation (MARTINEZ et al., 2006; MARTINEZ et al., 2009; VARIN et al., 2010; VERRECK et al., 2006).

Im Rahmen der chronischen Nierenerkrankung führt die chronische Inflammation zu einer vermehrten Differenzierung und Einwanderung von M1- und M2-Makrophagen in die Gefäßwände, wo sie die Ausbildung atherosklerotischer Plaques begünstigen. Diese Plaques bedingen eine Einengung des Gefäßlumens, was eine konsekutive Flusslimitierung und dadurch eine Ischämie von nachgeschalteten Gefäßsegmenten zur Folge hat. Im Falle einer

Beteiligung von Koronargefäßen droht als schwerwiegendste Komplikation eine Plaqueruptur, bei welcher der stark thrombogene Inhalt des Plaques zu einem thrombotischen Verschluss eines Koronargefäßes und damit zu einem akuten Myokardinfarkt führen kann. Da M1-Makrophagen mit einer Plaquestabilisierung, Ruptur und konsekutiver Thrombose in Verbindung gebracht werden, M2-Makrophagen hingegen mit der Steigerung der Plaquestabilität, konnte gezeigt werden, dass das Zusammenspiel und die Balance zwischen M1- und M2-Makrophagen innerhalb solcher atherosklerotischer Plaques entscheidend für die Progression der Atherosklerose ist (BOBRY SHEV et al., 2013; GUI et al., 2012; KRYCHTIUK et al., 2015; ZAWADA et al., 2012).

1.4.3 Dendritische Zellen

Neben Monozyten und Makrophagen spielen auch DCs des peripheren Blutes eine Schlüsselrolle in der Atherogenese. DCs sind hochspezialisierte, antigenpräsentierende Zellen, die als reife DCs (mDC) über MHC (Haupthistokompatibilitätskomplex)-Moleküle und kostimulatorische Oberflächenmarker wie CD40, CD80, CD83 und CD86 T-Zellen aktivieren und so Inflamationsreaktionen verstärken können (HEATH, CARBONE, 2009; NI, O'NEILL, 1997).

Im Rahmen der Atherogenese bedingen DCs – ähnlich der M1-Makrophagen – eine erhöhte Plaquestabilisierung durch verstärkte Einwanderung und Akkumulation in atherosklerotische Plaques (NIESSNER et al., 2006; WEBER, NOELS, 2011; YILMAZ et al., 2004). Daneben sollen DCs auch die Pathogenese der CKD durch Akkumulation im Nierenparenchym beeinflussen. Dort sollen sie durch potentiell pathogene Proteine, die im Rahmen der Entzündungsreaktion und Proteinurie auftreten, aktiviert werden und wandern in die peripheren Lymphknoten (NOESSNER et al., 2011). Weitere Tiermodelle zeigen, dass während einer renalen Ischämie hauptsächlich DCs proinflammatorische Zytokine wie TNF, IL-6 und MCP-1 sezernieren (DONG et al., 2007). Diese rekrutieren und aktivieren CD4⁺ und CD8⁺ T-Gedächtniszellen, die die Inflamationsreaktion verstärken und zu einer weiteren Schädigung des Gewebes führen (DONG et al., 2008; HEYMANN et al., 2009).

DCs des peripheren Blutes können in die zwei Subtypen der myeloiden DCs (welche auch als klassische DCs bezeichnet werden) und der plasmacytoiden DCs eingeteilt werden. Während sich myeloide DCs aus Monozyten differenzieren können, haben plasmacytoide DCs lymphoiden Ursprung und sind hauptsächlich an Immunreaktionen gegen virale Pathogene

und an der Stimulation regulatorischer T-Zellen beteiligt. Humane myeloide DCs exprimieren einige myeloide Antigene wie CD11c, CD13, CD33 und CD11b, während monozytäre Oberflächenmarker wie CD14 und CD16 herunterreguliert werden.

In der Literatur werden myeloide DCs häufig in die zwei phänotypisch und funktionell unterschiedlichen Subpopulationen der CD1c⁺ und CD141⁺ DCs unterteilt (SATPATHY et al., 2012; STEINMAN, BANCHEREAU, 2007; ZIEGLER-HEITBROCK et al., 2010). Diese Unterscheidung findet sich auch bei murinen DCs, wobei die humanen CD1c⁺ DCs Charakteristika der murinen CD11b⁺ DCs und die humanen CD141⁺ DCs Charakteristika der murinen CD8⁺/CD103⁺ DCs teilen (CROZAT et al., 2010; POULIN et al., 2010; ROBBINS et al., 2008). Während CD1c⁺ DCs hohe Mengen an CD86 exprimieren (HANIFFA et al., 2012) und überwiegend CD4⁺ T-Zellen über MHC-II stimulieren, aktivieren CD141⁺ DCs verstärkt CD8⁺ T-Zellen wie zytotoxische T-Zellen (CTL) über MHC-I, was CD141⁺ DCs zu potenten Immunzellen in der Abwehr viraler Infekte macht (BERKE, 1994; JONGBLOED et al., 2010).

1.5 Fragestellung der Promotionsarbeit

Vor diesem Hintergrund soll in der vorgelegten Dissertationsarbeit der Einfluss von *i.v.* Eisenpräparaten auf die immunologische Dysregulation chronisch nierenkranker Menschen untersucht werden. Die Arbeit fokussiert auf die Effekte dieser Präparate auf Monozytensubpopulationen und deren zelluläre Nachfolger, Makrophagen und DCs.

Als Grundlage der Untersuchungen soll zunächst in einer methodischen Arbeit die Einteilung der Monozyten in die drei Subpopulationen (klassische $CD14^{++}CD16^{-}$, intermediäre $CD14^{++}CD16^{+}$ und nicht-klassische $CD14^{+}CD16^{++}$ Monozyten) im Vergleich von zwei verschiedene Gatingstrategien am Patientenkollektiv der CARE FOR HOME Studie überprüft werden. In dieser Kohorte konnten zuvor intermediäre Monozyten als unabhängige Prädiktoren kardiovaskulärer Ereignisse identifiziert werden.

In ergänzenden Untersuchungen soll nachfolgend die Interaktion zwischen CKD-assoziierten Störungen des Mineral- und Knochenhaushalts und der Monozytenbiologie untersucht und verschiedene Komponenten des Mineral- und Knochenhaushalts hinsichtlich ihrer prognostischen Bedeutung im klinischen Alltag verglichen werden.

Nachfolgend soll der Einfluss verschiedener *i.v.* Eisenpräparate auf die Monozytenbiologie, insbesondere auf die Heterogenität der Monozyten und deren myeloide Differenzierung aus hämatopoetischen Stammzellen sowie die Makrophagen- und DC-Differenzierung, charakterisiert werden. Das immunmodulatorische Potential der Eisenpräparate auf isolierten und *in vitro* ausdifferenzierten Immunzellen soll durch Charakterisierung des Phänotyps insbesondere mittels Expressionsanalyse spezifischer Oberflächenmarker und durch funktionelle Untersuchungen wie Zytokinbildung, Bestimmung von Phagozytosekapazität und T-Zell-Stimulation untersucht werden. Mit Hilfe eines microRNA-Expressionsprofils der reifen DCs soll die Wirkung intravenöser Eisenpräparate auch auf molekulargenetischer Ebene analysiert werden.

So soll ermittelt werden, ob die Immunmodulation durch Eisenpräparate nicht klassenspezifisch, sondern substanzspezifisch auftritt. Diese Fragestellung besitzt potentielle klinische Relevanz, da im Falle einer substanzspezifischen Eisentoxizität durch Einsatz von weniger toxischen Präparaten eine sicherere Anämietherapie erreicht werden könnte.

Kapitel 2: Ergebnisse

2.1 Vergleich zweier Gatingstrategien zur Analyse humaner Monozytensubpopulationen

Diese Arbeit wurde wie folgt publiziert:

Adam M. Zawada*, Lisa H. Fell*, Kathrin Untersteller, Sarah Seiler, Kyrill S. Rogacev, Danilo Fliser, Loems Ziegler-Heitbrock, Gunnar H. Heine (2015) Comparison of two different strategies for human monocyte subsets gating within the large-scale prospective CARE FOR HOME study. Cytometry A, 87(8):750-8 (*geteilte Erstautorenschaft)

Zusammenfassung

Monozyten werden anhand der Expression des LPS-Rezeptors CD14 und des Fc γ -Rezeptors CD16 klassifiziert und in drei funktionell unabhängige Subtypen, die klassischen (CD14⁺⁺CD16⁻), intermediären (CD14⁺⁺CD16⁺) und nicht-klassischen (CD14⁺CD16⁺⁺) Monozyten, eingeteilt (PASSLICK et al., 1989; ZIEGLER-HEITBROCK et al., 2010). Dabei sind die als proinflammatorisch geltenden intermediären Monozyten (CROS et al., 2010; ZAWADA et al., 2011) unabhängige Prädiktoren für kardiovaskuläre Ereignisse chronisch nierenkranker Patienten (HEINE et al., 2008; ROGACEV et al., 2011; ROGACEV et al., 2014). Allerdings divergiert die durchflusszytometrische Gatingstrategie verschiedener Forschergruppen hinsichtlich der genauen Abgrenzung intermediärer von nicht-klassischen Monozyten. So werden hauptsächlich zwei Gatingstrategien unterschieden: die rechteckige Gatingstrategie (RG-Strategie) und die trapezförmige Gatingstrategie (TG-Strategie), die im Vergleich zur RG-Strategie weniger intermediäre Monozyten inkludiert und dadurch den Anteil nicht-klassischer Monozyten erweitert (**Abbildung 2**). Die beiden Gatingstrategien sollten nun erstmals innerhalb der CARE FOR HOME Kohorte verglichen und hinsichtlich ihrer Aussagekraft als Prädiktor klinischer Ereignisse evaluiert werden.

Unsere CARE FOR HOME-Studie schließt CKD Patienten in den Stadien G2 bis G4 ein und soll prospektiv Risikofaktoren für renale und kardiovaskuläre Ereignisse evaluieren (ROGACEV et al., 2014). In der vorliegenden Analyse wurde nach der genannten RG- und der TG-Strategie bei 416 Patienten dieses Studienkollektivs die Zellzahlen der Monozytensubpopulationen bestimmt, um zu untersuchen, ob die Gatingstrategie einen

Einfluss auf die prädiktive Rolle der Zellzahlen insbesondere der intermediären Monozyten zur Vorhersage kardiovaskulärer Ereignisse aufweist. Zusätzlich wurde die Expressionsstärke spezifischer Oberflächenmarker wie des Chemokinrezeptors CCR2, des Angiotensin-konvertierenden Enzyms (ACE) und des Toll-like-Rezeptors-2 (TLR2) auf einzelnen Monozytensubpopulationen, die nach RG- und TG-Strategie definiert wurden, untersucht.

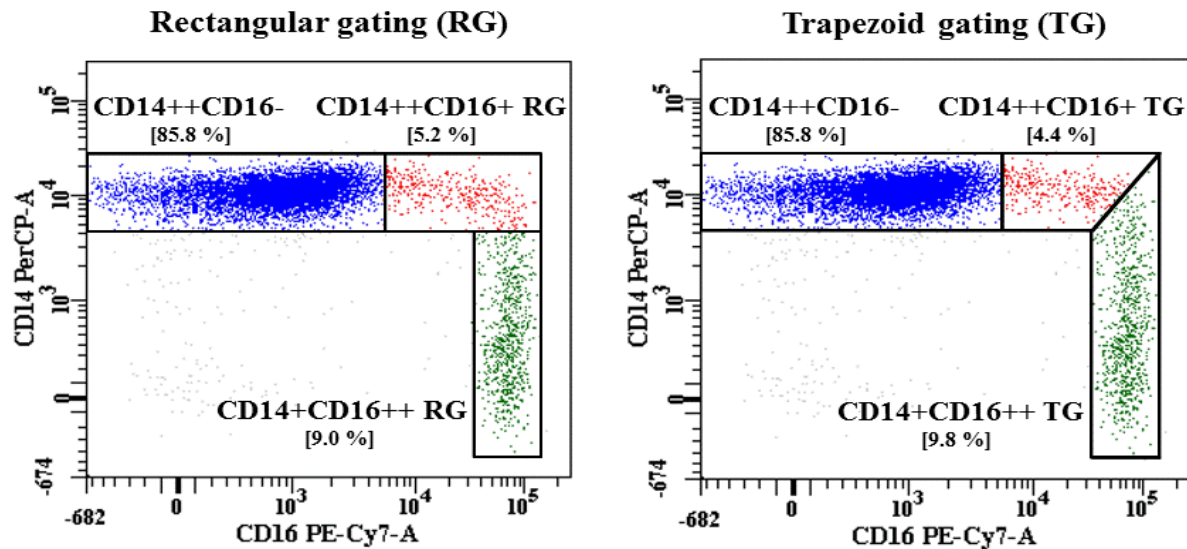


Abbildung 2: Gatingstrategien zur Einteilung von Monozytensubpopulationen

Die Abgrenzung intermediärer (rot) von nicht-klassischen (grün) Monozyten kann durch rechteckiges Gating (RG, *rectangular gating*) oder durch trapezförmiges Gating (TG, *trapezoid gating*) erfolgen. Die klassischen Monozyten, die durch die beiden Strategien nicht betroffen sind, sind in blau abgebildet.

Wir konnten zeigen, dass die erhöhte Anzahl intermediärer Monozyten unabhängig von der angewandten Gatingstrategie mit dem Auftreten kardiovaskulärer Endpunkte in Kaplan-Meier-Analysen assoziiert ist. In multivariaten Cox-Regressions-Analysen blieb die Zellzahl intermediärer Monozyten auch nach Korrektur für kardiovaskuläre Risikofaktoren (Alter, Geschlecht, prävalente kardiovaskuläre Vorerkrankungen, eGFR, Cholesteroll, Blutdruck, C-reaktives Protein, Diabetes mellitus) unabhängiger Prädiktor für ein ereignisfreies Überleben (HR = 1,013 [95% CI: 1,006-1,020; P < 0,001] mit RG; HR = 1,015 [95% CI: 1,006-1,024; P = 0,001] mit TG). Hierbei konnte mittels ROC-Analyse gezeigt werden, dass die Spezifität und Sensitivität intermediärer Monozyten zur Prädiktion kardiovaskulärer Ereignisse nach beiden Strategien gleich hoch war.

In Reklassifikationsanalysen zeigte sich nach Einteilung der Patienten gemäß der nach RG- und TG-Strategie bestimmten Anzahl intermediärer Monozyten in Quartile, kein relevanter Unterschied zwischen beiden Gatingstrategien. In Expressionsanalysen konnte zusätzlich aufgezeigt werden, dass die im Grenzbereich liegenden Monozyten, die nach RG-Strategie als

intermediäre und nach TG-Strategie als nicht-klassische Monozyten klassifiziert wurden, Charakteristika beider Subpopulationen teilen. So zeigten sie eine starke Expression von ACE, TLR2 und CCR5, während sie gleichzeitig auch CX₃CR1 stark exprimierten.

Auf Basis dieser Vergleichsstudie konnten RG- und TG-Strategien als gleichwertige Gatingverfahren zur Einteilung der Monozyten in die drei Subpopulationen bewertet werden. Dabei gelang es – unabhängig von den angewandten Gatingstrategien – intermediäre Monozyten als unabhängige Prädiktoren für kardiovaskuläre Ereignisse chronisch nierenkranker Menschen zu identifizieren, was ihre Voraussagekraft als Biomarker zusätzlich unterstreicht. Die Expressionsanalysen der Oberflächenmarker zeigten jedoch auch, dass eine exakte Abgrenzung intermediärer von nicht-klassischen Monozyten eine weitere Charakterisierung dieser Zellen notwendig macht.

Auf Grundlage dieser Daten wird für die folgenden Teilprojekte weiterhin die RG-Strategie verwendet, da sie der TG-Strategie nicht unterlegen ist, gleichzeitig jedoch die Vergleichbarkeit mit früheren Analysen gewährleistet und auch in der Literatur eine breitere Anwendung findet.

2.2 Mineral- und Knochenhaushalt – Die Kalzium-Phosphat-Homöostase und der neue Biomarker FGF-23

2.2.1 Einfluss des Kalzium-Phosphathaushalts auf die Monozytenbiologie

Nachdem die erhöhte kardiovaskuläre Morbidität und Mortalität chronisch nierenkranker Patienten einerseits mit der Anzahl intermediärer Monozyten, andererseits mit Parametern des Mineral- und Knochenhaushalts assoziiert ist, haben wir nachfolgend einen möglichen direkten Zusammenhang zwischen Monozytenheterogenität und dem Mineral- und Knochenhaushalt untersucht (KETTELER et al., 2013). Da CKD-assoziierte Störungen des Mineral- und Knochenhaushalts neben einer akzelerierten vaskulären Kalzifikation und einer renalen Osteodystrophie insbesondere durch stark erhöhten Plasmaphosphatspiegel und eine systemische Kalziumüberladung charakterisiert werden können (BLOCK et al., 2004; TENTORI et al., 2008; WALD et al., 2008), haben wir den direkten Zusammenhang zwischen veränderten Kalzium- und Phosphatspiegeln und der erhöhten Zellzahl intermediärer Monozyten analysiert.

Dazu stimulierten wir zum einen zirkulierende Monozyten im Vollblut und zum anderen hämatopoetische Stammzellen während ihrer Differenzierung zu Monozyten mit unterschiedlichen Kalzium- und/oder Phosphatkonzentrationen *in vitro*. Mit Hilfe der Durchflusszytometrie charakterisierten wir die Monozytensubpopulationen nach Verteilung, Phänotyp und Funktion. Phänotypisch wurden die Monozyten hinsichtlich der Expression spezifischer Oberflächenmarker (CD80, CD86, CCR2, CCR5, CX₃CR1) und proinflammatorischer Zytokine charakterisiert, funktionell über ihre Phagozytosekapazität.

Dabei fanden wir heraus, dass erhöhte Kalzium- und Phosphatspiegel im Vollblut keinen Einfluss auf die Monozytensubpopulationen hatten. Im Gegensatz dazu ergab sich bei der Differenzierung hämatopoetischer Stammzellen zu intermediären Monozyten ein durch steigende Phosphatkonzentrationen induzierter fünffacher Anstieg des prozentualen Anteils intermediärer Monozyten (**Abbildung 3**); erhöhte Kalziumkonzentrationen nahmen dabei keinen Einfluss.

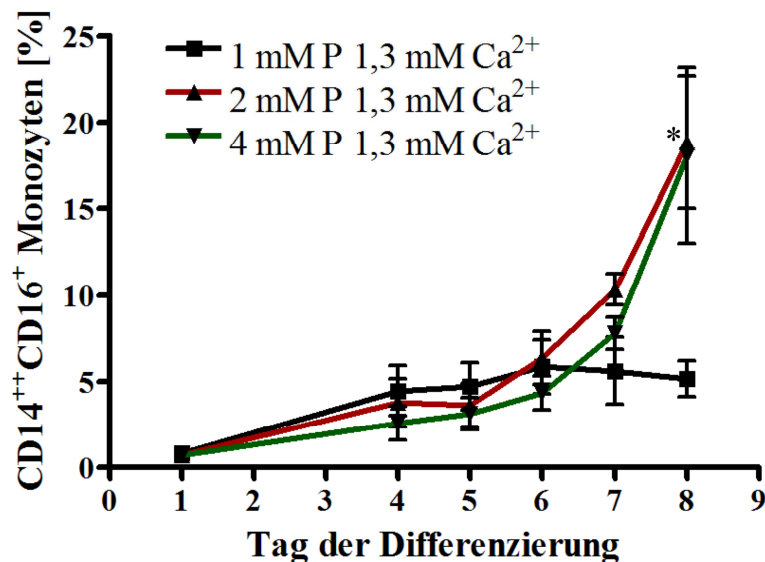


Abbildung 3: Differenzierung hämatopoetischer Stammzellen zu CD14⁺⁺CD16⁺ Monozyten

Prozentualer Anteil von CD14⁺⁺CD16⁺ Monozyten während einer achttägiger *in vitro* Differenzierung hämatopoetischer CD34⁺ Stammzellen unter Simulation mit 1 mM (schwarz), 2 mM (rot) bzw. 4 mM (grün) Phosphat [(PO₄)³⁻]. Stammzellen wurden aus dem Blut gesunder Probanden isoliert. Die statistische Auswertung erfolgte mittels einfaktorieller Varianzanalyse (ANOVA) und nachfolgendem Dunnett-Test als post hoc Analyse. Darstellt sind Mittelwerte ± Standardfehler; n = 5; *P < 0,05.

Diese intermediären Monozyten zeigten zudem starke phänotypische Veränderungen wie eine gesteigerte Oberflächenexpression von CD16, CD86, CCR2 sowie CX₃CR1, wohingegen CD80 und CCR5 vermindert exprimiert wurden (**Abbildung 4**). Im Gegensatz dazu hatten veränderte Kalzium- und Phosphatkonzentrationen keinen Einfluss auf die monozytäre Produktion proinflammatorischer Zytokine wie TNF-α, IL-1β und IL-6 und reaktiver Sauerstoffspezies, ebenso zeigten sie funktionell keine Veränderungen hinsichtlich ihrer Phagozytosekapazität (Daten nicht gezeigt).

Zusammenfassend haben diese Stammzellexperimente einen direkten Zusammenhang zwischen erhöhten Phosphatkonzentrationen und der gesteigerten Ausbildung proinflammatorischer intermediärer Monozyten *in vitro* aufzeigen können. Übertragen auf den klinischen Alltag suggeriert dieses Ergebnis, dass eine ausgeprägte Hyperphosphatämie bei Patienten mit chronischer Nierenerkrankung eine Zunahme der intermediären Monozyten induziert, welche ihrerseits zu einem höheren Risiko für kardiovaskuläre Ereignisse führen kann.

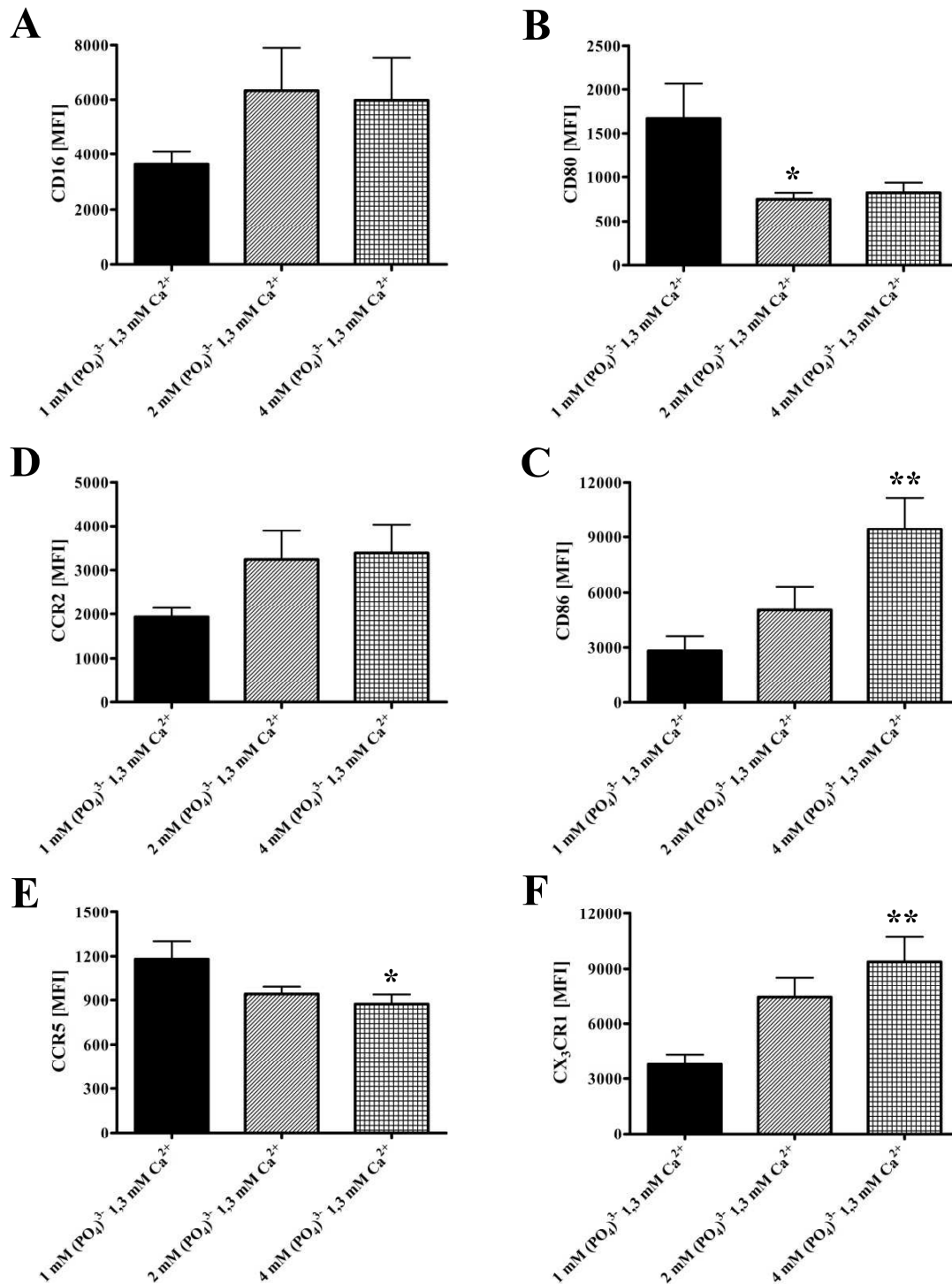


Abbildung 4: Expressionsanalyse spezifischer Oberflächenmarker *in vitro* differenzierter CD14⁺⁺CD16⁺ Monozyten

Oberflächenexpression von CD16 (A), CD80 (B), CCR2 (C), CD86 (D), CCR5 (E), CX₃CR1 (F) auf CD14⁺⁺CD16⁺ Monozyten nach achttägiger *in vitro* Differenzierung aus hämatopoetischen CD34⁺ Stammzellen unter Simulation mit 1 mM, 2 mM bzw. 4 mM Phosphat. Stammzellen wurden aus dem Blut gesunder Probanden isoliert. Die statistische Auswertung erfolgte mittels einfaktorieller Varianzanalyse (ANOVA) mit nachfolgendem Dunnett-Test zur anschließenden post hoc Analyse. Darstellt sind Mittelwerte ± Standardfehler; n = 5; *P < 0,05, **P < 0,01.

Die *in vivo* Relevanz dieser Ergebnisse konnte jedoch in einer post hoc Analyse der HOM SWEET HOME Studie nicht bestätigt werden. Die HOM SWEET HOME Kohorte inkludierte 1309 Patienten, die sich in der Klinik für Innere Medizin III – Kardiologie, Angiologie und Internistische Intensivmedizin – am Universitätsklinikum des Saarlandes zu einer elektiven Koronarangiographie vorstellten (ROGACEV et al., 2012). Wir stratifizierten diese Patienten nach ihrem Plasmaphosphat Spiegel in vier Quartile. Bei Vergleich der Anzahl intermediärer Monozyten in den einzelnen Quartilen zeigte sich jedoch kein Unterschied (**Abbildung 5**).

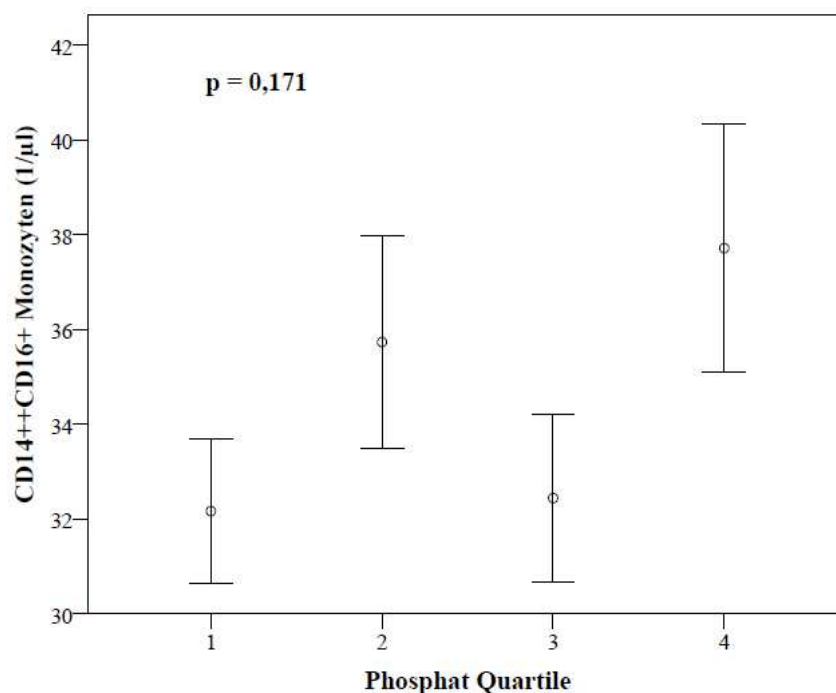


Abbildung 5: Assoziation zwischen intermediären Monozyten und Phosphatspiegeln

1309 Patienten der HOM SWEET HOME Kohorte wurden bezüglich ihrer Plasmaphosphat Spiegel in Quartile stratifiziert. Die statistische Auswertung erfolgte mittels einfaktorieller Varianzanalyse (ANOVA). Darstellt sind Mittelwerte \pm Standardabweichung.

Zusammenfassend können diese epidemiologischen Daten somit unsere experimentellen Daten nicht bestätigen, so dass eine Zunahme von intermediären Monozyten aufgrund einer Hyperphosphatämie nicht von klinischer Bedeutung zu sein scheint.

2.2.2 FGF-23 als Langzeitmarker der mittleren Plasmaphosphatspiegel bei Hämodialysepatienten

Diese Arbeit wurde wie folgt publiziert:

Sarah Seiler*, Gaetano Lucisano*, Philipp Ege, Lisa H. Fell, Kyrill S. Rogacev, Anne Lerner-Gräber, Matthias Klingele, Matthias Ziegler, Danilo Fliser, Gunnar H. Heine (2013) Single FGF-23 Measurement and Time-Averaged Plasma Phosphate Levels in Hemodialysis Patients. Clin J Am Soc Nephrol 8(10): 1764-72 (*geteilte Erstautorenschaft)

Zusammenfassung

Zu Beginn des 21. Jahrhunderts wurde mit FGF-23 ein weiterer zentraler Regulator der Kalzium-Phosphathomöostase charakterisiert (WEBER et al., 2003). FGF-23 wird nach Stimulation durch Kalzitriol und PTH zumeist von Osteoblasten und Osteozyten sezerniert und bewirkt die Senkung des Phosphatspiegels, indem es die gastrointestinale Phosphatabsorption vermindert und gleichzeitig die renale Phosphatausscheidung erhöht (KAWATA et al., 2007; LIU et al., 2006; SEILER et al., 2009). Zudem vermindert FGF-23 die renale Vitamin D-Aktivierung, was sich durch die Suppression des Vitamin D-aktivierenden Enzyms 1α -Hydroxylase erklären lässt (HEINE et al., 2012; SEILER et al., 2009). Aktuelle Studien suggerieren darüberhinaus, dass FGF-23 immunologisch eine Monozytenaktivierung und weitere proinflammatorische Signalkaskaden induziert (BACCHETTA et al., 2013; SHIMADA et al., 2004).

Epidemiologische Daten unserer HOM SWEET HOME Studie zeigten eine starke Assoziation zwischen den Zellzahlen intermediärer Monozyten und den Plasmaspiegeln von C-terminalem FGF-23 (cFGF-23); ein direkter Effekt von FGF-23 auf die Monozytenbiologie wie auf die Expression von spezifischen Markern, auf funktionelle Charakteristika und auf die monozytäre Differenzierung, wurde *in vitro* dagegen nicht bestätigt (LUTHE, 2015).

In Gegensatz zu diesen kontrovers diskutierten immunologischen Effekten erscheint ein Zusammenhang zwischen FGF-23 und kardiovaskulärer Erkrankung unzweifelhaft. So konnte in der HOM SWEET HOME Studie in Querschnittsanalysen ein Zusammenhang zwischen FGF-23, linksventrikulärer Dysfunktion und Vorhofflimmern aufgezeigt werden. Prospektive klinische Studien bei chronisch nierenkranken Menschen wie die HEMO Studie konnten starke Assoziationen hoher cFGF-23-Plasmaspiegel mit einem erhöhten Risiko für kardiale Todesfälle darstellen (CHONCHOL et al., 2015). Allerdings ist unklar, ob FGF-23 direkt

kardiotoxische Eigenschaften hat oder ein bloßer Indikator des derangierten Phosphathaushalts ist und eine chronische Hyperphosphatämie der eigentliche Schädigungsfaktor ist (HEINE et al., 2012).

So konnten zahlreiche epidemiologische Studien wie die interkontinentale DOPPS-Studie zweifelsfrei aufzeigen, dass eine Hyperphosphatämie zu der schlechten kardiovaskulären Prognose von Dialysepatienten beiträgt (TENTORI et al., 2008). Daher empfehlen die aktuellen Leitlinien der KDIGO Expertengruppe zur Behandlung von CKD-assoziierten Störungen des Mineral- und Knochenhaushalts eine Normalisierung des Plasmaphosphatspiegels durch eine diätetische Phosphatrestriktion und durch die Einnahme oraler Phosphatbinder (KDIGO, 2009). Im klinischen Alltag jedoch gestaltet sich die Adjustierung des Plasmaphosphatspiegels von Dialysepatienten wegen hoher zirkadianer und infradianer Schwankungen als schwierig, weshalb nach stabileren Markern mit höherer Aussagekraft gesucht wird (LEVITT et al., 2009; RING et al., 1995).

Daher wurde postuliert, dass ein erhöhter Plasmaspiegel von FGF-23 einen Langzeitindikator der Hyperphosphatämie darstellt (PARKER et al., 2010), ähnlich wie HbA1c ein Marker der chronischen Hyperglykämie ist.

Daran anknüpfend sollte in einer weiteren klinischen Studie überprüft werden, ob cFGF-23-Plasmaspiegel stabilere Marker CKD-assoziiierter Störungen des Mineral- und Knochenhaushalts als Plasmaphosphatspiegel sind, und ob ein einmalig bestimmter cFGF-23-Plasmaspiegel Reflektor der Plasmaphosphatspiegel der Vorwochen ist. Daher initiierten wir die DIAL HOME Studie, in welche insgesamt 40 Hämodialysepatienten eingeschlossen wurden, die über 28 Tage nachverfolgt wurden. In diesem Zeitraum wurden zu definierten Zeitpunkten die Spiegel zentraler Marker des Mineral- und Knochenhaushalts wie des cFGF-23, PTH, der alkalischen Phosphatase und des Vitamins D und deren intraindividuelle Variabilität bestimmt. Zudem untersuchten wir, ob ein einmalig bestimmtes Plasma-cFGF-23 am Ende der vierwöchigen Untersuchungszeit mit den mittleren Plasmaphosphatspiegeln der vorherigen Wochen stärker assoziiert ist als mit einem einmaligen Plasmaphosphat bei Untersuchungsende. Die durchschnittliche diätetische Kalorien- und Phosphataufnahme wurde mit Hilfe eines Ernährungsfragebogens evaluiert.

Die Ergebnisse zeigten, dass entgegen der Erwartung die intraindividuelle Variabilität von cFGF-23 innerhalb der vierwöchigen Studiendauer nicht geringer war als die des Plasmaphosphatspiegels und weiterer Marker des Mineral- und Knochenhaushalts wie PTH,

Kalzium und der alkalischen Phosphatase. Das zu Studienende bestimmte Plasma-FGF-23 war nicht stärker mit dem durchschnittlichen Plasmaphosphat als mit einem einmalig bestimmten FGF-23 korreliert. Zudem war diese Korrelation nicht hochgradig, sodass Patienten mit ähnlichem cFGF-23-Spiegel sehr unterschiedliche Phosphatspiegel aufwiesen. Die Analyse der Ernährungsfragebogen erbrachte, dass die Phosphataufnahme weder mit dem Plasmaphosphatspiegel noch mit Plasma-cFGF-23 korrelierte.

Zusammenfassend konnte die Auswertung der DIAL HOME Studie zeigen, dass cFGF-23 wegen seiner geringen intraindividuellen Stabilität und nur moderater Assoziation mit den mittleren Phosphatwerten der Vorwochen kein verlässlicher Marker der zeitlich gemittelten Plasmaphosphatspiegel ist und somit als Routineparameter im klinischen Alltag zum aktuellen Zeitpunkt keinen Mehrwert bringt.

Eine Limitation dieser Studie war die alleinige Bestimmung der cFGF-23-Spiegel, da verlässliche Testmethoden für das intakte FGF-23 (iFGF-23) auch wegen dessen geringerer Stabilität zum Zeitpunkt der Studie nicht verfügbar waren. Zudem ging man davon aus, dass sich die Spiegel des inaktiven Spaltprodukts cFGF-23 proportional zu dem phosphaturisch aktiven iFGF-23 verhalten.

Neuere Studien zeigten jedoch zumindest bei spezifischen Krankheitsentitäten eine klare Divergenz zwischen cFGF-23 und iFGF-23-Spiegeln im Plasma. So wiesen eisendefiziente Wildtyp-Mäuse aufgrund einer erhöhten *fgf23*-Transkription und Spaltaktivität sehr hohe Spiegel an cFGF-23 auf, während die iFGF-23-Spiegel jedoch unverändert blieben und sich auch keine Hypophosphatämie ausbildete (FARROW et al., 2011). Dieser Zusammenhang wurde in einer klinischen Studie bestätigt, in der Frauen mit ausgeprägter Eisenmangelanämie stark erhöhte cFGF-23-Spiegel, jedoch unauffällige iFGF-23-Spiegel, aufwiesen. So verstärkte der Eisenmangel gleichermaßen *FGF23*-Transkription und -Abbau; eine Behandlung mit intravenösen Eisenpräparaten wie Eisen-Dextran oder Eisen-Carboxymaltose hingegen normalisierte die Transkription und führte so zu einer 80%igen Reduktion der cFGF-23-Spiegel. Dabei wiesen Patientinnen, die mit Eisen-Carboxymaltose therapiert wurden, nicht jedoch Patientinnen unter Behandlung mit Eisen-Dextran, deutlich höhere Plasmalevel an iFGF-23, welches eine Hypophosphatämie induzierte (WOLF et al., 2013).

2.3 Substanzspezifische Toxizität intravenöser Eisenpräparate auf die Monozytenbiologie *in vitro*

Wie bereits einleitend dargestellt, wurde im Kontext der hohen Prävalenz der Anämie der chronischen Nierenerkrankung in den letzten Jahren einerseits eine intravenöse Eisentherapie in den Mittelpunkt nephrologischer Therapiestrategien gerückt (KDIGO, 2012; PADHI et al., 2015) und andererseits potentielle renale, kardiovaskuläre und immunologische Nebenwirkungen dieser Therapiestrategien kritischer diskutiert (FISHBANE et al., 2014; MACDOUGALL, GEISSER, 2013; VAZIRI, 2013), ohne dass hinreichend untersucht wurde, ob diese Nebenwirkungen klassenspezifisch oder substanzspezifisch durch einzelne *i.v.* Eisenpräparate auftreten.

Klinische und experimentelle Studien testen zumeist ältere Präparate geringerer Stabilität, wie Eisen-Saccharose oder Natrium-Eisen-Glukonat, und vergleichen diese überwiegend mit oralen Präparaten oder eisenfreien Kontrollansätzen, weshalb Daten zu neueren, zumeist stabileren *i.v.* Eisenpräparaten, wie Eisen-Carboxymaltose und Eisen-Isomaltosid 1000, weitgehend fehlen.

Vor diesem Hintergrund untersuchten wir verschiedene *i.v.* Eisenpräparate hinsichtlich ihrer potentiell substanzspezifischen Toxizität auf Immunzellen wie Monozyten, Makrophagen und DCs *in vitro*.

2.3.1 Einfluss intravenöser Eisenpräparate auf die Monozytenheterogenität

Diese Arbeit wurde wie folgt publiziert:

Lisa H. Fell, Adam M. Zawada, Kyrill S. Rogacev, Sarah Seiler, Danilo Fliser, Gunnar H. Heine (2014) Distinct immunologic effects of different intravenous iron preparations on monocytes. *Nephrol Dial Transplant* 29(4): 809-22

Zusammenfassung

Vor dem Hintergrund der zentralen Bedeutung von Monozyten als Mediatoren der körpereigenen Immunabwehr wurde der Einfluss verschiedener *i.v.* Eisenpräparate auf die Monozytenheterogenität untersucht. Dazu wurden zirkulierende Monozyten und hämatopoetische CD34⁺ Stammzellen während ihrer Differenzierung zu Monozyten mit

unterschiedlichen Eisenpräparaten stimuliert und anschließend die Monozytensubpopulationen hinsichtlich Verteilung, Phänotyp und Funktion, sowie Viabilität und Eisengehalt charakterisiert. Phänotypisch wurde die Expression spezifischer Oberflächenmarker (CD14, CD16, CD86, CCR5, CX₃CR1) und proinflammatorischer Zytokine (IL-1 β , TNF- α) sowie die ROS-Produktion der einzelnen Monozytensubpopulationen analysiert, funktionell ihre Phagozytosekapazität und Fähigkeit zur T-Zell-Stimulation. Für die Stimulationen wurden fünf *i.v.* Eisenpräparate (Eisen-Saccharose, Eisen-Carboxymaltose, Eisen-Isomaltosid 1000, niedermolekulares Eisen-Dextran, Eisenoxytol, siehe auch **Tabelle 1**) und Blut gesunder Kontrollprobanden sowie CKD-Patienten (Stadium G4 – G5) in den drei Konzentrationen 0,133 mg/ml, 0,266 mg/ml und 0,533 mg/ml eingesetzt. Im klinischen Alltag entsprechen diese Konzentrationen, bezogen auf einen 70 kg schweren Patienten, Eisendosen von etwa 400 mg, 800 mg bzw. 1600 mg.

Erste Hinweise auf eine substanzspezifische Immunmodulation der Eisenpräparate zeigten durchflusszytometrische Expressionsanalysen proinflammatorischer und proatherogener Oberflächenmarker ausgereifter Monozyten. So wies von den getesteten Substanzen nur Eisen-Saccharose substanzspezifische Effekte auf die Monozytensubpopulationen auf. Daneben kam es bereits bei geringen Dosierungen – entsprechend therapeutisch zugelassener Präparatmengen – an Eisen-Saccharose zu einem deutlichen Anstieg des Eisengehalts in den drei Monozytensubpopulationen, was eine substanzspezifische Aufnahme der Eisen-Saccharose suggeriert. Eisen-Saccharose bewirkte nachfolgend eine verminderte Oberflächenexpression von CD14, CD16 und CX₃CR1, während CD86 vermehrt exprimiert wurde. Zudem zeigten sich veränderte IL-1 β -Spiegel, die mit einer erhöhten ROS-Produktion einhergingen. In weiteren Analysen bedingte Eisen-Saccharose dosisabhängig eine substantiell verminderte Phagozytoseleistung klassischer Monozyten und beeinträchtigte zudem die monozytäre Differenzierung hämatopoetischer Stammzellen zu klassischen und intermediären Monozyten. Im Gegensatz dazu zeigten die übrigen Präparate keinerlei Effekte auf monozytäre Charakteristika, Differenzierung und Eisenaufnahme.

2.3.2 Einfluss intravenöser Eisenpräparate auf die *in vitro* Differenzierung von Monozyten zu Makrophagen und Dendritischen Zellen

Das Manuskript dieser Arbeit wurde wie folgt eingereicht:

Lisa H. Fell, Sarah Seiler, Björn Rotter, Peter Winter, Martina Sester, Danilo Fliser, Gunnar H. Heine*, Adam M. Zawada* (2015) Impact of individual intravenous iron preparations on the differentiation of monocytes towards macrophages and dendritic cells. (*geteilte Letztautorenschaft)

Zusammenfassung

In der angeborenen Immunabwehr agieren Monozyten in direktem Zusammenspiel mit ihren zellulären Nachkommen, den Makrophagen und DCs. Dabei gelten die Adhäsion der zirkulierenden Monozyten an den Endothelzellen und die Transmigration ins Gewebe als initiale Schritte ihrer Differenzierung. Darauf basierend wurde der Einfluss intravenöser Eisenpräparate auf das Adhäsions- und Migrationspotential der Monozyten und deren myeloide Differenzierung zu Makrophagen und DCs *in vitro* evaluiert. Weiterhin sollte erstmals untersucht werden, inwieweit einzelne Präparate das Expressionsmuster der microRNAs (miRNAs) modifizieren, da miRNAs als kleine nicht-kodierende Oligonukleotide, die die Genexpression posttranskriptionell steuern, eine zentrale Bedeutung für die zelluläre Regulation von Inflammationsreaktionen haben (DAVIS, CLARKE, 2013; O'CONNELL et al., 2007; WEI et al., 2013).

Für die Experimente wurden Monozyten aus dem Blut gesunder Kontrollprobanden isoliert und erneut mit 0,133 mg/mL, 0,266 mg/mL bzw. 0,533 mg/mL Eisen-Saccharose, Eisen-Carboxymaltose, Eisen-Isomaltosid 1000 und zusätzlich Natrium-Eisen-Glukonat stimuliert. Das Adhäsions- und Migrationspotential wurde mikroskopisch durch Auszählen der an Endothelzellen haftenden bzw. durch 8 µm große Membranporen migrierten Monozyten überprüft. Nach Differenzierung der Monozyten zu M1 und M2 Makrophagen bzw. reifen DCs (mDCs) wurden diese phänotypisch und funktionell charakterisiert. Dazu wurde die Expression spezifischer Oberflächenmarker (M1-Marker: CD40, CD64, CD80, CD86; M2-Marker: CD14, CD16, CD32, CD163, CD206; M1/M2-Marker: CD68; DC-Marker: CD1c, CD141, CD80, CD83, CD86, CD1a, CD40, HLA-DR) sowie die Phagozytosekapazität der Makrophagen und die Fähigkeit der mDCs zur T-Zell-Aktivierung bestimmt. Zur Überprüfung, ob diese Einflüsse molekulargenetisch nachweisbar sind, wurde das miRNA-

Expressionsprofil der *in vitro* differenzierten mDCs unter Kontrollbedingungen und unter 0.266 mg/mL Eisen-Saccharose bzw. Eisen-Isomaltosid 1000 bestimmt.

Die Ergebnisse zeigten, dass Eisen-Saccharose und ebenso Natrium-Eisen-Glukonat starke substanzspezifische Effekte auf die *in vitro* Differenzierung von Monozyten zu Makrophagen und mDCs hatten. Sie steigerten das Adhäsionsverhalten von Monozyten zwar nur leicht, bedingten jedoch starke phänotypische und funktionelle Veränderungen der ausdifferenzierten Makrophagen und mDCs. So exprimierten die unter Eisen-Saccharose oder Natrium-Eisen-Glukonat ausdifferenzierten M1-Makrophagen weniger CD40, die M2-Makrophagen weniger CD16 und CD163 auf ihrer Zelloberfläche. Zudem wiesen die M1 und M2 Makrophagen selbst bei geringen Dosen von Eisen-Saccharose oder Natrium-Eisen-Glukonat eine stark reduzierte Phagozytosekapazität auf. Hinsichtlich der mDC-Differenzierung bewirkten die beiden Eisenpräparate phänotypisch eine stark verminderte Oberflächenexpressionen von CD1c, CD11b, CD40, CD80 und CD86, während CD141 und HLA-DR verstärkt exprimiert wurden. Funktionell verstärkte eine Stimulation mit allen *i.v.* Eisenpräparaten die durch mDCs induzierte Proliferation nicht-selektierter T-Zellen, während die Proliferation des CD8⁺ T-Zell-Subtyps selektiv durch Eisen-Saccharose, Natrium-Eisen-Glukonat und Eisen-Carboxymaltose verstärkt wurde.

Im Gegensatz zu Eisen-Saccharose und Natrium-Eisen-Glukonat bewirkte Eisen-Carboxymaltose deutlich schwächere phänotypische und funktionelle Veränderungen von Makrophagen und mDCs, während Eisen-Isomaltosid 1000 in den verwendeten Assays meistens immunologisch neutral war.

Dies bestätigten auch die Ergebnisse der miRNA-Expressionsanalyse der unter Eisen-Saccharose bzw. Eisen-Isomaltosid 1000 ausdifferenzierten mDCs. 108 von 631 analysierten miRNAs wurden nach Eisen-Saccharose-Stimulation dysreguliert; nur 25 dieser 108 miRNAs wurden auch durch Eisen-Isomaltosid 1000 beeinflusst, wenngleich in niedrigerer Effektstärke. Lediglich acht miRNAs wurden selektiv durch Eisen-Isomaltosid 1000, nicht jedoch durch Eisen-Saccharose dysreguliert.

Die vorgestellten *in vitro* Ergebnisse unterstreichen die substanzspezifische Toxizität intravenöser Eisenpräparate und deuten auf eine selektive Immunmodulation durch Eisen-Saccharose und/oder Natrium-Eisen-Glukonat hin, während die übrigen Eisenpräparate immunologisch weitgehend neutral erscheinen. Eine mögliche Ursache dieser Effekte stellt die ferrokinetische Divergenz der einzelnen Eisenpräparate aufgrund stark unterschiedlicher

physiochemischer und pharmakokinetischer Eigenschaften dar. So konnte in Vorarbeiten bereits gezeigt werden, dass Eisen-Saccharose und Natrium-Eisen-Glukonat im Vergleich zu den übrigen Präparaten die geringste Halbwertszeit und Stabilität aufweisen, was zu einer erhöhten Abspaltung freier und hoch reaktiver Eisenionen führt (JAHN et al., 2011; MACDOUGALL, GEISSER, 2013). Dieses „labile“ Eisen wird von den Zellen aufgenommen, steigert die intrazelluläre ROS-Produktion und Lipidperoxidation und initiiert somit Inflamationsreaktionen (EVANS et al., 2008). Daran anknüpfend konnten unsere *in vitro* Studien zeigen, dass die substanzspezifische Immunmodulation labiler *i.v.* Eisenpräparate auch eine Inhibition der Funktion zirkulierender Monozytensubpopulationen und eine Modifikation der Differenzierung zu Makrophagen und mDCs umfasst. Interessanterweise traten solch starke Effekte in den Differenzierungsexperimenten auch nach mehrtägiger Stimulation und somit nach Überschreitung der physiologischen Halbwertszeit stabilerer Eisenpräparate nicht auf.

Kapitel 3: Zusammenfassung und Ausblick

Im Rahmen dieser Dissertationsarbeit konnte erstmals eine substanzspezifische Wirkweise intravenöser Eisenpräparate auf die Monozytenbiologie *in vitro* aufgezeigt werden. Dabei wiesen vor allem weniger stabile Eisenpräparate, wie Eisen-Saccharose und Natrium-Eisen-Glukonat, das höchste immunmodulatorische Potential auf. Dies zeigte sich in stark ausgeprägten phänotypischen, aber auch funktionellen Veränderungen von Monozyten und ihren zellulären Nachfolgern, den Makrophagen und DCs. Übertragen auf die Anämitherapie chronisch nierenkranker Menschen, könnte die Behandlung mit labileren Eisenpräparaten eine zusätzliche Schwächung der Immunabwehr induzieren und somit die Infektanfälligkeit erhöhen. Jedoch ist die klinische Relevanz dieser *in vitro* Daten derzeit noch unklar und soll mit Hilfe der in dieser Arbeit identifizierten Biomarker und etablierten Messmethoden in zukünftigen klinischen Studien unserer Arbeitsgruppe überprüft werden.

Dazu sollte zunächst in einer umschriebenen Kohorte von chronisch nierenkranken Patienten mit Eisenmangel und klinischer Indikation zur intravenösen Eisentherapie untersucht werden, ob die nachgewiesenen *in vitro* Effekte von Eisen-Saccharose und Natrium-Eisen-Glukonat mit den in der vorgelegten Dissertationsarbeit angewendeten Methoden auch für klinische Untersuchungen bestätigt werden können.

Auf Grundlage dessen könnte ein Studienprotokoll für eine randomisierte Studie erstellt werden, welche den Vergleich zweier *i.v.* Eisenpräparate unterschiedlicher Stabilität – wie beispielsweise Eisen-Saccharose und Eisen-Isomaltosid 1000 – hinsichtlich immunologischer Parameter und klinischer Endpunkte ermöglicht. Diese Studien könnten die *in vitro* gezeigte Überlegenheit stabilerer Eisenpräparate, wie Eisen-Isomaltosid 1000, *in vivo* überprüfen. Zusätzlich zu diesen immunologischen Aspekten erlaubte dieses Studiendesign, durch Bestimmung zentraler Parameter des Kalzium-Phosphathaushalts, wie Plasmaphosphat, FGF-23, Vitamin D und PTH, das Wissen zur substanzspezifischen Wirkweisen von *i.v.* Eisenpräparaten auf die Kalzium-Phosphathomöostase zu ergänzen (WOLF et al., 2013).

In weiteren experimentellen Studien sollte die Pathogenese der Anämie der chronischen Nierenerkrankung vor allem hinsichtlich der Bedeutung des Hepcidins für die Eisenhomöostase genauer untersucht werden. In diesem Zusammenhang sollte überprüft werden, inwieweit die Wahl des eingesetzten *i.v.* Eisenpräparats die Eisenaufnahme und Eisenretention von Makrophagen und damit die Eisenverfügbarkeit beeinflussen kann, wobei

insbesondere untersucht werden sollte, inwieweit erhöhte Hepcidinspiegel die Expression von Eisentransportern wie Ferroportin und DMT-1 und des Transferrinrezeptors, auf Makrophagen von chronisch nierenkranken Menschen beeinflussen. Zusätzlich sollte analysiert werden, ob sich mit Hilfe eines Hepcidin-Inhibitors die Dysregulation der Eisenhomöostase in Makrophagen aufheben lässt.

Mit Hilfe dieser weiteren Untersuchungen soll die Sicherheit und Verträglichkeit der intravenösen Eisentherapie chronisch nierenkranker Patienten hinsichtlich immunologischer Aspekte, aber auch vor dem Hintergrund CKD-assoziiierter Störungen des Mineral- und Knochenhaushalts und der Eisenhomöostase, verbessert werden. Als Resultat könnte der Therapieerfolg bei Anämie durch die Wahl des geeigneten *i.v.* Eisenpräparats optimiert und dadurch die Lebensqualität der Patienten deutlich erhöht werden.

Literaturverzeichnis

1. Ancuta P, Rao R, Moses A, Mehle A, Shaw SK, Luscinskas FW, Gabuzda D (2003) Fractalkine preferentially mediates arrest and migration of CD16+ monocytes. *J Exp Med* 197:1701-1707
2. Bacchetta J, Sea JL, Chun RF, Lisse TS, Wesseling-Perry K, Gales B, Adams JS, Salusky IB, Hewison M (2013) Fibroblast growth factor 23 inhibits extrarenal synthesis of 1,25-dihydroxyvitamin D in human monocytes. *J Bone Miner Res* 28:46-55
3. Belge KU, Dayyani F, Horelt A, Siedlar M, Frankenberger M, Frankenberger B, Espevik T, Ziegler-Heitbrock L (2002) The proinflammatory CD14+CD16+DR++ monocytes are a major source of TNF. *J Immunol* 168:3536-3542
4. Berke G (1994) The binding and lysis of target cells by cytotoxic lymphocytes: molecular and cellular aspects. *Annu Rev Immunol* 12:735-773
5. Block GA, Klassen PS, Lazarus JM, Ofsthun N, Lowrie EG, Chertow GM (2004) Mineral metabolism, mortality, and morbidity in maintenance hemodialysis. *J Am Soc Nephrol* 15:2208-2218
6. Bobryshev YV, Shchelkunova TA, Morozov IA, Rubtsov PM, Sobenin IA, Orekhov AN, Smirnov AN (2013) Changes of lysosomes in the earliest stages of the development of atherosclerosis. *J Cell Mol Med* 17:626-635
7. Brandenburg VM, Kleber ME, Vervloet MG, Tomaschitz A, Pilz S, Stojakovic T, Delgado G, Grammer TB, Marx N, Marx W, Scharnagl H (2014) Fibroblast growth factor 23 (FGF23) and mortality: the Ludwigshafen Risk and Cardiovascular Health Study. *Atherosclerosis* 237:53-59
8. Brissot P, Ropert M, Le Lan C, Loreal O (2012) Non-transferrin bound iron: a key role in iron overload and iron toxicity. *Biochim Biophys Acta* 1820:403-410
9. Brown BN, Valentin JE, Stewart-Akers AM, McCabe GP, Badylak SF (2009) Macrophage phenotype and remodeling outcomes in response to biologic scaffolds with and without a cellular component. *Biomaterials* 30:1482-1491
10. Chonchol M, Greene T, Zhang Y, Hoofnagle AN, Cheung AK (2015) Low Vitamin D and High Fibroblast Growth Factor 23 Serum Levels Associate with Infectious and Cardiac Deaths in the HEMO Study. *J Am Soc Nephrol*:in print
11. Cohen LA, Gutierrez L, Weiss A, Leichtmann-Bardoogo Y, Zhang DL, Crooks DR, Sougrat R, Morgenstern A, Galy B, Hentze MW, Lazaro FJ, Rouault TA, Meyron-Holtz EG (2010) Serum ferritin is derived primarily from macrophages through a nonclassical secretory pathway. *Blood* 116:1574-1584
12. Coresh J, Astor BC, Greene T, Eknoyan G, Levey AS (2003) Prevalence of chronic kidney disease and decreased kidney function in the adult US population: Third National Health and Nutrition Examination Survey. *Am J Kidney Dis* 41:1-12

13. Cros J, Cagnard N, Woollard K, Patey N, Zhang SY, Senechal B, Puel A, Biswas SK, Moshous D, Picard C, Jais JP, D'Cruz D, Casanova JL, Trouillet C, Geissmann F (2010) Human CD14dim monocytes patrol and sense nucleic acids and viruses via TLR7 and TLR8 receptors. *Immunity* 33:375-386
14. Crozat K, Guiton R, Williams M, Henri S, Baranek T, Schwartz-Cornil I, Malissen B, Dalod M (2010) Comparative genomics as a tool to reveal functional equivalences between human and mouse dendritic cell subsets. *Immunol Rev* 234:177-198
15. Davis M, Clarke S (2013) Influence of microRNA on the maintenance of human iron metabolism. *Nutrients* 5:2611-2628
16. de Jager DJ, Grootendorst DC, Jager KJ, van Dijk PC, Tomas LM, Ansell D, Collart F, Finne P, Heaf JG, De Meester J, Wetzels JF, Rosendaal FR, Dekker FW (2009) Cardiovascular and noncardiovascular mortality among patients starting dialysis. *JAMA* 302:1782-1789
17. Deicher R, Ziai F, Cohen G, Mullner M, Horl WH (2003) High-dose parenteral iron sucrose depresses neutrophil intracellular killing capacity. *Kidney Int* 64:728-736
18. Dong X, Swaminathan S, Bachman LA, Croatt AJ, Nath KA, Griffin MD (2007) Resident dendritic cells are the predominant TNF-secreting cell in early renal ischemia-reperfusion injury. *Kidney Int* 71:619-628
19. Dong X, Bachman LA, Miller MN, Nath KA, Griffin MD (2008) Dendritic cells facilitate accumulation of IL-17 T cells in the kidney following acute renal obstruction. *Kidney Int* 74:1294-1309
20. Drueke TB, Locatelli F, Clyne N, Eckardt KU, Macdougall IC, Tsakiris D, Burger HU, Scherhag A (2006) Normalization of hemoglobin level in patients with chronic kidney disease and anemia. *N Engl J Med* 355:2071-2084
21. Evans RW, Rafique R, Zarea A, Rapisarda C, Cammack R, Evans PJ, Porter JB, Hider RC (2008) Nature of non-transferrin-bound iron: studies on iron citrate complexes and thalassemic sera. *J Biol Inorg Chem* 13:57-74
22. Evstatiev R, Gasche C (2011) Iron sensing and signalling. *Gut* 61:933-952
23. Farrow EG, Yu X, Summers LJ, Davis SI, Fleet JC, Allen MR, Robling AG, Stayrook KR, Jideonwo V, Magers MJ, Garringer HJ, Vidal R, Chan RJ, Goodwin CB, Hui SL, Peacock M, White KE (2011) Iron deficiency drives an autosomal dominant hypophosphatemic rickets (ADHR) phenotype in fibroblast growth factor-23 (Fgf23) knock-in mice. *Proc Natl Acad Sci U S A* 108:E1146-1155
24. Fell LH, Fliser D, Heine GH (2015) Ferric pyrophosphate: good things come to those who wait? *Nephrol Dial Transplant*
25. Fishbane S, Mathew A, Vaziri ND (2014) Iron toxicity: relevance for dialysis patients. *Nephrol Dial Transplant* 29:255-259
26. Frazer DM, Anderson GJ (2005) Iron imports. I. Intestinal iron absorption and its regulation. *Am J Physiol Gastrointest Liver Physiol* 289:G631-635

27. Frei U, H.-J. S-H (2008). Nierenersatztherapie in Deutschland - Bericht 2006/2007 (QuaSi-Niere gGmbH, Berlin)
28. Geisser P, Burckhardt S (2011) The Pharmacokinetics and Pharmacodynamics of Iron Preparations. *Pharmaceutics* 3:12-33
29. Gordon S, Taylor PR (2005) Monocyte and macrophage heterogeneity. *Nat Rev Immunol* 5:953-964
30. Gozzelino R, Jeney V, Soares MP (2010) Mechanisms of cell protection by heme oxygenase-1. *Annu Rev Pharmacol Toxicol* 50:323-354
31. Gui T, Shimokado A, Sun Y, Akasaka T, Muragaki Y (2012) Diverse roles of macrophages in atherosclerosis: from inflammatory biology to biomarker discovery. *Mediators Inflamm* 2012:1-14
32. Haniffa M, Shin A, Bigley V, McGovern N, Teo P, See P, Wasan PS, Wang XN, Malinarich F, Malleret B, Larbi A, Tan P, Zhao H, Poidinger M, Pagan S, Cookson S, Dickinson R, Dimmick I, Jarrett RF, Renia L, Tam J, Song C, Connolly J, Chan JK, Gehring A, Bertolotti A, Collin M, Ginhoux F (2012) Human tissues contain CD141hi cross-presenting dendritic cells with functional homology to mouse CD103+ nonlymphoid dendritic cells. *Immunity* 37:60-73
33. Heath WR, Carbone FR (2009) Dendritic cell subsets in primary and secondary T cell responses at body surfaces. *Nat Immunol* 10:1237-1244
34. Heine GH, Ulrich C, Seibert E, Seiler S, Marell J, Reichart B, Krause M, Schlitt A, Kohler H, Girndt M (2008) CD14(++)CD16+ monocytes but not total monocyte numbers predict cardiovascular events in dialysis patients. *Kidney Int* 73:622-629
35. Heine GH, Seiler S, Fliser D (2012) FGF-23: the rise of a novel cardiovascular risk marker in CKD. *Nephrol Dial Transplant* 27:3072-3081
36. Heymann F, Meyer-Schwesinger C, Hamilton-Williams EE, Hammerich L, Panzer U, Kaden S, Quaggin SE, Floege J, Grone HJ, Kurts C (2009) Kidney dendritic cell activation is required for progression of renal disease in a mouse model of glomerular injury. *J Clin Invest* 119:1286-1297
37. Ichii H, Masuda Y, Hassanzadeh T, Saffarian M, Gollapudi S, Vaziri ND (2012) Iron sucrose impairs phagocytic function and promotes apoptosis in polymorphonuclear leukocytes. *Am J Nephrol* 36:50-57
38. Jahn MR, Andreasen HB, Futterer S, Nawroth T, Schunemann V, Kolb U, Hofmeister W, Munoz M, Bock K, Meldal M, Langguth P (2011) A comparative study of the physicochemical properties of iron isomaltoside 1000 (Monofer), a new intravenous iron preparation and its clinical implications. *Eur J Pharm Biopharm* 78:480-491
39. Jongbloed SL, Kassianos AJ, McDonald KJ, Clark GJ, Ju X, Angel CE, Chen CJ, Dunbar PR, Wadley RB, Jeet V, Vulink AJ, Hart DN, Radford KJ (2010) Human CD141+ (BDCA-3)+ dendritic cells (DCs) represent a unique myeloid DC subset that cross-presents necrotic cell antigens. *J Exp Med* 207:1247-1260

40. Kamanna VS, Ganji SH, Shelkovnikov S, Norris K, Vaziri ND (2012) Iron sucrose promotes endothelial injury and dysfunction and monocyte adhesion/infiltration. *Am J Nephrol* 35:114-119
41. Kawanaka N, Yamamura M, Aita T, Morita Y, Okamoto A, Kawashima M, Iwahashi M, Ueno A, Ohmoto Y, Makino H (2002) CD14+,CD16+ blood monocytes and joint inflammation in rheumatoid arthritis. *Arthritis Rheum* 46:2578-2586
42. Kawata T, Imanishi Y, Kobayashi K, Miki T, Arnold A, Inaba M, Nishizawa Y (2007) Parathyroid hormone regulates fibroblast growth factor-23 in a mouse model of primary hyperparathyroidism. *J Am Soc Nephrol* 18:2683-2688
43. KDIGO KDIGOCKDMBDWG (2009) KDIGO clinical practice guideline for the diagnosis, evaluation, prevention, and treatment of Chronic Kidney Disease-Mineral and Bone Disorder (CKD-MBD). *Kidney Int Suppl*:S1-130
44. KDIGO KDIGOKAWG (2012) KDIGO Clinical Practice Guideline for Anemia in Chronic Kidney Disease. *Kidney inter, Suppl* 2:279-335
45. Keane WF, Brenner BM, de Zeeuw D, Grunfeld JP, McGill J, Mitch WE, Ribeiro AB, Shahinfar S, Simpson RL, Snapinn SM, Toto R, Investigators RS (2003) The risk of developing end-stage renal disease in patients with type 2 diabetes and nephropathy: the RENAAL study. *Kidney Int* 63:1499-1507
46. Ketteler M, Wolf M, Hahn K, Ritz E (2013) Phosphate: a novel cardiovascular risk factor. *Eur Heart J* 34:1099-1101
47. Krychtiuk KA, Kastl SP, Wojta J (2015) Entzündung und Atherosklerose - Update 2015. *Journal für Kardiologie - Austrian Journal of Cardiology* 22:6-14
48. Lankhorst CE, Wish JB (2010) Anemia in renal disease: diagnosis and management. *Blood Rev* 24:39-47
49. Latunde-Dada GO, Simpson RJ, McKie AT (2008) Duodenal cytochrome B expression stimulates iron uptake by human intestinal epithelial cells. *J Nutr* 138:991-995
50. Levitt H, Smith KG, Rosner MH (2009) Variability in calcium, phosphorus, and parathyroid hormone in patients on hemodialysis. *Hemodial Int* 13:518-525
51. Libby P, Ridker PM, Maseri A (2002) Inflammation and atherosclerosis. *Circulation* 105:1135-1143
52. Liu S, Tang W, Zhou J, Stubbs JR, Luo Q, Pi M, Quarles LD (2006) Fibroblast growth factor 23 is a counter-regulatory phosphaturic hormone for vitamin D. *J Am Soc Nephrol* 17:1305-1315
53. Locatelli F, Pisoni RL, Combe C, Bommer J, Andreucci VE, Piera L, Greenwood R, Feldman HI, Port FK, Held PJ (2004) Anaemia in haemodialysis patients of five European countries: association with morbidity and mortality in the Dialysis Outcomes and Practice Patterns Study (DOPPS). *Nephrol Dial Transplant* 19:121-132

54. Luthe A (2015) Bedingt ein Hyperphosphatönismus die Monozytendysfunktion chronisch nierenkranker Menschen?, Saarland University Medical Center and Saarland University Faculty of Medicine, Homburg.
55. Macdougall IC, Geisser P (2013) Use of intravenous iron supplementation in chronic kidney disease: an update. *Iran J Kidney Dis* 7:9-22
56. Mantovani A, Sica A, Sozzani S, Allavena P, Vecchi A, Locati M (2004) The chemokine system in diverse forms of macrophage activation and polarization. *Trends Immunol* 25:677-686
57. Mantovani A, Sica A, Locati M (2007) New vistas on macrophage differentiation and activation. *Eur J Immunol* 37:14-16
58. Martinez FO, Gordon S, Locati M, Mantovani A (2006) Transcriptional profiling of the human monocyte-to-macrophage differentiation and polarization: new molecules and patterns of gene expression. *J Immunol* 177:7303-7311
59. Martinez FO, Helming L, Gordon S (2009) Alternative activation of macrophages: an immunologic functional perspective. *Annu Rev Immunol* 27:451-483
60. Martinez FO, Gordon S (2014) The M1 and M2 paradigm of macrophage activation: time for reassessment. *F1000Prime Rep* 6:13
61. Mosser DM, Edwards JP (2008) Exploring the full spectrum of macrophage activation. *Nat Rev Immunol* 8:958-969
62. Moura IC, Hermine O, Lacombe C, Mayeux P (2015) Erythropoiesis and transferrin receptors. *Curr Opin Hematol* 22:193-198
63. Ni K, O'Neill HC (1997) The role of dendritic cells in T cell activation. *Immunol Cell Biol* 75:223-230
64. Niessner A, Sato K, Chaikof EL, Colmegna I, Goronzy JJ, Weyand CM (2006) Pathogen-sensing plasmacytoid dendritic cells stimulate cytotoxic T-cell function in the atherosclerotic plaque through interferon-alpha. *Circulation* 114:2482-2489
65. Nockher WA, Scherberich JE (1998) Expanded CD14⁺ CD16⁺ monocyte subpopulation in patients with acute and chronic infections undergoing hemodialysis. *Infect Immun* 66:2782-2790
66. Noessner E, Lindenmeyer M, Nelson PJ, Segerer S (2011) Dendritic cells in human renal inflammation--Part II. *Nephron Exp Nephrol* 119:e91-98
67. Nordfjeld K, Andreassen H, Thomsen LL (2012) Pharmacokinetics of iron isomaltoside 1000 in patients with inflammatory bowel disease. *Drug Des Devel Ther* 6:43-51
68. O'Connell RM, Taganov KD, Boldin MP, Cheng G, Baltimore D (2007) MicroRNA-155 is induced during the macrophage inflammatory response. *Proc Natl Acad Sci U S A* 104:1604-1609

69. Padhi S, Glen J, Pordes BA, Thomas ME, Guideline Development G (2015) Management of anaemia in chronic kidney disease: summary of updated NICE guidance. *BMJ* 350:h2258
70. Pai AB, Conner T, McQuade CR, Olp J, Hicks P (2011) Non-transferrin bound iron, cytokine activation and intracellular reactive oxygen species generation in hemodialysis patients receiving intravenous iron dextran or iron sucrose. *Biometals* 24:603-613
71. Parker BD, Schurgers LJ, Brandenburg VM, Christenson RH, Vermeer C, Ketteler M, Shlipak MG, Whooley MA, Ix JH (2010) The associations of fibroblast growth factor 23 and uncarboxylated matrix Gla protein with mortality in coronary artery disease: the Heart and Soul Study. *Ann Intern Med* 152:640-648
72. Parkkinen J, von Bonsdorff L, Peltonen S, Gronhagen-Riska C, Rosenlof K (2000) Catalytically active iron and bacterial growth in serum of haemodialysis patients after i.v. iron-saccharate administration. *Nephrol Dial Transplant* 15:1827-1834
73. Passlick B, Flieger D, Ziegler-Heitbrock HW (1989) Identification and characterization of a novel monocyte subpopulation in human peripheral blood. *Blood* 74:2527-2534
74. Pfeffer MA, Burdmann EA, Chen CY, Cooper ME, de Zeeuw D, Eckardt KU, Feyzi JM, Ivanovich P, Kewalramani R, Levey AS, Lewis EF, McGill JB, McMurray JJ, Parfrey P, Parving HH, Remuzzi G, Singh AK, Solomon SD, Toto R (2009) A trial of darbepoetin alfa in type 2 diabetes and chronic kidney disease. *N Engl J Med* 361:2019-2032
75. Poulin LF, Salio M, Griessinger E, Anjos-Afonso F, Craciun L, Chen JL, Keller AM, Joffre O, Zelenay S, Nye E, Le Moine A, Faure F, Donckier V, Sancho D, Cerundolo V, Bonnet D, Reis e Sousa C (2010) Characterization of human DNGR-1+ BDCA3+ leukocytes as putative equivalents of mouse CD8alpha+ dendritic cells. *J Exp Med* 207:1261-1271
76. Ring T, Sanden AK, Hansen HH, Halkier P, Nielsen C, Fog L (1995) Ultradian variation in serum phosphate concentration in patients on haemodialysis. *Nephrol Dial Transplant* 10:59-63
77. Robbins SH, Walzer T, Dembele D, Thibault C, Defays A, Bessou G, Xu H, Vivier E, Sellars M, Pierre P, Sharp FR, Chan S, Kastner P, Dalod M (2008) Novel insights into the relationships between dendritic cell subsets in human and mouse revealed by genome-wide expression profiling. *Genome Biol* 9:R17
78. Rogacev KS, Ulrich C, Blomer L, Hornof F, Oster K, Ziegelin M, Cremers B, Grenner Y, Geisel J, Schlitt A, Kohler H, Fliser D, Girndt M, Heine GH (2010) Monocyte heterogeneity in obesity and subclinical atherosclerosis. *Eur Heart J* 31:369-376
79. Rogacev KS, Seiler S, Zawada AM, Reichart B, Herath E, Roth D, Ulrich C, Fliser D, Heine GH (2011) CD14++CD16+ monocytes and cardiovascular outcome in patients with chronic kidney disease. *Eur Heart J* 32:84-92
80. Rogacev KS, Cremers B, Zawada AM, Seiler S, Binder N, Ege P, Grosse-Dunker G, Heisel I, Hornof F, Jeken J, Rebling NM, Ulrich C, Scheller B, Bohm M, Fliser D,

- Heine GH (2012) CD14++CD16+ monocytes independently predict cardiovascular events: a cohort study of 951 patients referred for elective coronary angiography. *J Am Coll Cardiol* 60:1512-1520
81. Rogacev KS, Zawada AM, Emrich I, Seiler S, Bohm M, Fliser D, Woollard KJ, Heine GH (2014) Lower Apo A-I and lower HDL-C levels are associated with higher intermediate CD14++CD16+ monocyte counts that predict cardiovascular events in chronic kidney disease. *Arterioscler Thromb Vasc Biol* 34:2120-2127
 82. Rozen-Zvi B, Gafter-Gvili A, Paul M, Leibovici L, Shpilberg O, Gafter U (2008) Intravenous versus oral iron supplementation for the treatment of anemia in CKD: systematic review and meta-analysis. *Am J Kidney Dis* 52:897-906
 83. Sarnak MJ, Levey AS, Schoolwerth AC, Coresh J, Culleton B, Hamm LL, McCullough PA, Kasiske BL, Kelepouris E, Klag MJ, Parfrey P, Pfeffer M, Raij L, Spinosa DJ, Wilson PW, American Heart Association Councils on Kidney in Cardiovascular Disease HBPRCC, Epidemiology, Prevention (2003) Kidney disease as a risk factor for development of cardiovascular disease: a statement from the American Heart Association Councils on Kidney in Cardiovascular Disease, High Blood Pressure Research, Clinical Cardiology, and Epidemiology and Prevention. *Circulation* 108:2154-2169
 84. Satpathy AT, Wu X, Albring JC, Murphy KM (2012) Re(de)fining the dendritic cell lineage. *Nat Immunol* 13:1145-1154
 85. Seiler S, Heine GH, Fliser D (2009) Clinical relevance of FGF-23 in chronic kidney disease. *Kidney Int Suppl*:S34-42
 86. Seiler S, Lucisano G, Ege P, Fell LH, Rogacev KS, Lerner-Graber A, Klingele M, Ziegler M, Fliser D, Heine GH (2013) Single FGF-23 measurement and time-averaged plasma phosphate levels in hemodialysis patients. *Clin J Am Soc Nephrol* 8:1764-1772
 87. She H, Xiong S, Lin M, Zandi E, Giulivi C, Tsukamoto H (2002) Iron activates NF-kappaB in Kupffer cells. *Am J Physiol Gastrointest Liver Physiol* 283:G719-726
 88. Sheftel A, Stehling O, Lill R (2010) Iron-sulfur proteins in health and disease. *Trends Endocrinol Metab* 21:302-314
 89. Shimada T, Hasegawa H, Yamazaki Y, Muto T, Hino R, Takeuchi Y, Fujita T, Nakahara K, Fukumoto S, Yamashita T (2004) FGF-23 is a potent regulator of vitamin D metabolism and phosphate homeostasis. *J Bone Miner Res* 19:429-435
 90. Singh AK, Szczech L, Tang KL, Barnhart H, Sapp S, Wolfson M, Reddan D (2006) Correction of anemia with epoetin alfa in chronic kidney disease. *N Engl J Med* 355:2085-2098
 91. Skinner NA, MacIsaac CM, Hamilton JA, Visvanathan K (2005) Regulation of Toll-like receptor (TLR)2 and TLR4 on CD14dimCD16+ monocytes in response to sepsis-related antigens. *Clin Exp Immunol* 141:270-278

92. Sonnweber T, Theurl I, Seifert M, Schroll A, Eder S, Mayer G, Weiss G (2011) Impact of iron treatment on immune effector function and cellular iron status of circulating monocytes in dialysis patients. *Nephrol Dial Transplant* 26:977-987
93. Stauffer ME, Fan T (2014) Prevalence of anemia in chronic kidney disease in the United States. *PLoS One* 9:e84943
94. Steinman RM, Banchereau J (2007) Taking dendritic cells into medicine. *Nature* 449:419-426
95. Tentori F, Blayney MJ, Albert JM, Gillespie BW, Kerr PG, Bommer J, Young EW, Akizawa T, Akiba T, Pisoni RL, Robinson BM, Port FK (2008) Mortality risk for dialysis patients with different levels of serum calcium, phosphorus, and PTH: the Dialysis Outcomes and Practice Patterns Study (DOPPS). *Am J Kidney Dis* 52:519-530
96. Theil EC (2011) Iron homeostasis and nutritional iron deficiency. *J Nutr* 141:724S-728S
97. Ulrich C, Heine GH, Garcia P, Reichart B, Georg T, Krause M, Kohler H, Girndt M (2006) Increased expression of monocytic angiotensin-converting enzyme in dialysis patients with cardiovascular disease. *Nephrol Dial Transplant* 21:1596-1602
98. Varin A, Mukhopadhyay S, Herbein G, Gordon S (2010) Alternative activation of macrophages by IL-4 impairs phagocytosis of pathogens but potentiates microbial-induced signalling and cytokine secretion. *Blood* 115:353-362
99. Vaziri ND (2013) Understanding iron: promoting its safe use in patients with chronic kidney failure treated by hemodialysis. *Am J Kidney Dis* 61:992-1000
100. Verreck FA, de Boer T, Langenberg DM, Hoeve MA, Kramer M, Vaisberg E, Kastelein R, Kolk A, de Waal-Malefyt R, Ottenhoff TH (2004) Human IL-23-producing type 1 macrophages promote but IL-10-producing type 2 macrophages subvert immunity to (myco)bacteria. *Proc Natl Acad Sci U S A* 101:4560-4565
101. Verreck FA, de Boer T, Langenberg DM, van der Zanden L, Ottenhoff TH (2006) Phenotypic and functional profiling of human proinflammatory type-1 and anti-inflammatory type-2 macrophages in response to microbial antigens and IFN-gamma- and CD40L-mediated costimulation. *J Leukoc Biol* 79:285-293
102. Vlagopoulos PT, Tighiouart H, Weiner DE, Griffith J, Pettitt D, Salem DN, Levey AS, Sarnak MJ (2005) Anemia as a risk factor for cardiovascular disease and all-cause mortality in diabetes: the impact of chronic kidney disease. *J Am Soc Nephrol* 16:3403-3410
103. Wald R, Sarnak MJ, Tighiouart H, Cheung AK, Levey AS, Eknoyan G, Miskulin DC (2008) Disordered mineral metabolism in hemodialysis patients: an analysis of cumulative effects in the Hemodialysis (HEMO) Study. *Am J Kidney Dis* 52:531-540
104. Weber C, Noels H (2011) Atherosclerosis: current pathogenesis and therapeutic options. *Nat Med* 17:1410-1422

105. Weber TJ, Liu S, Indridason OS, Quarles LD (2003) Serum FGF23 levels in normal and disordered phosphorus homeostasis. *J Bone Miner Res* 18:1227-1234
106. Wei Y, Nazari-Jahantigh M, Chan L, Zhu M, Heyll K, Corbalan-Campos J, Hartmann P, Thiemann A, Weber C, Schober A (2013) The microRNA-342-5p fosters inflammatory macrophage activation through an Akt1- and microRNA-155-dependent pathway during atherosclerosis. *Circulation* 127:1609-1619
107. Weiss G, Goodnough LT (2005) Anemia of chronic disease. *N Engl J Med* 352:1011-1023
108. Winkelmayer WC, Mitani AA, Goldstein BA, Brookhart MA, Chertow GM (2014) Trends in anemia care in older patients approaching end-stage renal disease in the United States (1995-2010). *JAMA Intern Med* 174:699-707
109. Wolf M, Koch TA, Bregman DB (2013) Effects of iron deficiency anemia and its treatment on fibroblast growth factor 23 and phosphate homeostasis in women. *J Bone Miner Res* 28:1793-1803
110. Yilmaz A, Lochno M, Traeg F, Cicha I, Reiss C, Stumpf C, Raaz D, Anger T, Amann K, Probst T, Ludwig J, Daniel WG, Garlischs CD (2004) Emergence of dendritic cells in rupture-prone regions of vulnerable carotid plaques. *Atherosclerosis* 176:101-110
111. Yoshimura K, Nakano H, Yokoyama K, Nakayama M (2005) High iron storage levels are associated with increased DNA oxidative injury in patients on regular hemodialysis. *Clin Exp Nephrol* 9:158-163
112. Zager RA, Johnson AC, Hanson SY, Wasse H (2002) Parenteral iron formulations: a comparative toxicologic analysis and mechanisms of cell injury. *Am J Kidney Dis* 40:90-103
113. Zawada AM, Rogacev KS, Rotter B, Winter P, Marell RR, Fliser D, Heine GH (2011) SuperSAGE evidence for CD14⁺⁺CD16⁺ monocytes as a third monocyte subset. *Blood* 118:e50-61
114. Zawada AM, Rogacev KS, Schirmer SH, Sester M, Bohm M, Fliser D, Heine GH (2012) Monocyte heterogeneity in human cardiovascular disease. *Immunobiology* 217:1273-1284
115. Ziegler-Heitbrock L (2007) The CD14⁺ CD16⁺ blood monocytes: their role in infection and inflammation. *J Leukoc Biol* 81:584-592
116. Ziegler-Heitbrock L, Ancuta P, Crowe S, Dalod M, Grau V, Hart DN, Leenen PJ, Liu YJ, MacPherson G, Randolph GJ, Scherberich J, Schmitz J, Shortman K, Sozzani S, Strobl H, Zembala M, Austyn JM, Lutz MB (2010) Nomenclature of monocytes and dendritic cells in blood. *Blood* 116:e74-80

Abkürzungsverzeichnis

%	Prozent
A	Albuminurie
ACE	Angiotensin-converting enzyme, Angiotensin-konvertierendes Enzym
ANOVA	Analysis of variance, Varianzanalyse
Ca.	Circa
Ca ²⁺	Zweiwertiges (freies) Kalzium
CARE FOR HOME	Cardiovascular and renal outcome in CKD 2-4 patients - The forth Homburg evaluation
CCL	C-C Chemokin-Ligand
CCR	C-C Chemokin-Rezeptor
CD	Cluster of differentiation
cFGF-23	C-terminales FGF-23
CD14 ⁺⁺ CD16 ⁻ Monozyten	Klassische Monozyten
CD14 ⁺⁺ CD16 ⁺ Monozyten	Intermediäre Monozyten
CD14 ⁺ CD16 ⁺⁺ Monozyten	Nicht-klassische Monozyten
CHOIR	Correction of hemoglobin outcomes in renal insufficiency study
CI	Konfidenzintervall
CKD	Chronic kidney disease, Chronische Nierenerkrankung
CREATE	Cardiovascular risk reduction by early anemia treatment with Epoetin Beta trail
CTL	Cytotoxic T-lymphocyte, zytotoxischer T-Lymphozyt
CX ₃ CR1	C-X3-C Chemokin-Rezeptor 1
DC	Dendritic cell, Dendritische Zelle
DIAL HOME	Dialysis in Homburg evaluation
dL	Deziliter
DMT-1	Divalent metal transporter-1, Bivalenter Metalltransporter-1
DNA	Deoxyribonucleic acid, Desoxyribonukleinsäure
DOPPS	The Dialysis Outcomes and Practice Patterns Study
EPO	Erythropoetin
ESA	Erythropoese-stimulierendes Agens
FCS	Fetal calf serum, fetales Kälberserum
Fe ²⁺ , Fe ³⁺	Zweiwertiges Eisen, dreiwertiges Eisen
FGF-23	Fibroblast growth factor-23, Fibroblastischer Wachstumsfaktor-23
FSC	Forward scatter, Vorwärtsstreulicht

G	Gramm bzw. Erdbeschleunigung
GFR	Glomeruläre Filtrationsrate
GM-CSF	Granulocyte macrophage colony-stimulating factor, Granulozyten Makrophagen Koloniestimulierender Faktor
H	Stunde
HCP-1	Haem carrier protein-1, Häm-Transporter-1
HEMO study	Hemodialysis study
HLA-DR	Human leukocyte antigen-DR, Humanes Leukozytenantigen-DR
HOM SWEET HOMe	Heterogeneity of monocytes in subjects who undergo elective coronary angiography – The Homburg evaluation
HR	Hazard ratio
ICAM-1	Intracellular adhesion molecule-1, intrazelluläres Adhäsionsmolekül-1
iFGF23	Intaktes FGF-23
IL	Interleukin
IFN- γ	Interferon- γ
IUIS	Nomenclature Committee of the international Union of Immunological Societies
i.v.	Intravenös
KDIGO	Kidney Disease Improving Global Outcomes
Kg	Kilogramm
KG	Körpergewicht
LPS	Lipopolysaccharid
MCP-1	Monocyte chemoattractant protein-1, Monozyten-chemotaktisches Protein-1, CCL2
M-CSF	Macrophage-colony stimulating factor, Makrophagen Koloniestimulierender Faktor
mDC	Mature dendritic cell, reife Dendritische Zelle
MFI	Mean fluorescence intensity, mittlere Fluoreszenzintensität
Mg	Milligramm
MHC	Major histocompatibility complex, Haupthistokompatibilitätskomplex
mL	Milliliter
Min	Minute
N	Anzahl
NHANES	National Health and Nutrition Survey
NICE	The National Institute for Health and Care Excellence
NTBI	Non-transferrin bound iron, Nicht-Transferrin-gebundenes Eisen
P	P-Wert

PBMC	Peripheral blood mononuclear cell, Periphere mononukleare Blutzelle
$(\text{PO}_4)^{3-}$	Phosphat
PSGL-1	P-Selektin Glykoprotein Ligand-1
PTH	Parathormon
MFI	Mediane Fluoreszenzintensität
miRNA	MikroRNA (Ribonukleinsäure)
RG	Rechteckiges Gating
ROC	Receiver Operating Characteristic, Grenzwertoptimierung
ROS	Reactive oxygen species, Reaktive Sauerstoffspezies
SSC	Sideward scatter, Seitwärtsstreulicht
TG	Trapezförmiges Gating
Th1/2	T-Helferzelle vom Typ 1/2
TLR	Toll-like Rezeptor
TNF- α	Tumornekrosefaktor- α
TREAT	Trial to reduce cardiovascular events with Aranesp therapy
μL	Mikroliter
VCAM-1	Vascular cell adhesion molecule-1, Vaskuläres Zelladhäsionsmolekül-1
VEGFR	Vasucular endothelial growth factor receptor, Vaskulärer endothelialer Wachstumsfaktor-Rezeptor
WHO	World Health Organisation, Weltgesundheitsorganisation

Abbildungsverzeichnis

Abbildung 1:	Pathophysiologische Mechanismen der Anämie der chronischen Nierenerkrankung	10
Abbildung 2:	Gatingstrategien zur Einteilung von Monozytensubpopulationen.....	21
Abbildung 3:	Differenzierung hämatopoetischer Stammzellen zu CD14 ⁺⁺ CD16 ⁺ Monozyten	24
Abbildung 4:	Expressionsanalyse spezifischer Oberflächenmarker <i>in vitro</i> differenzierter CD14 ⁺⁺ CD16 ⁺ Monozyten.....	25
Abbildung 5:	Assoziation zwischen intermediären Monozyten und Phosphatspiegeln	26
Abbildung A1-1:	Einteilung humaner Monozytensubpopulationen in Vollblut.....	62

Tabellenverzeichnis

Tabelle 1:	<i>I.v.</i> Eisenpräparate und ausgewählte Eigenschaften	12
Tabelle A1-1:	In der Durchflusszytometrie verwendete Antikörper	55
Tabelle. A1-2:	Kalzium- und Phosphat-Stimulation.....	58
Tabelle A1-3:	Antikörpermix zur Charakterisierung von Monozytensubpopulationen im Vollblut	63
Tabelle A1-4:	Antikörpermix zur Charakterisierung hämatopoetischer Stammzellen.....	63
Tabelle A1-5:	Antikörpermix zur Charakterisierung intrazellulärer Zytokine	64

Lebenslauf

Der Lebenslauf ist nicht Teil der elektronischen Version.

Publikationen

Fell L. H., Seiler S., Rotter B., Winter P., Sester M., Fliser D., Heine G. H., Zawada A. M. (2015). Impact of individual *i.v.* iron preparations on the differentiation of monocytes toward macrophages and dendritic cells. Zur Publikation eingereicht

Fell L. H., Fliser D., Heine G. H. (2015). Ferric pyrophosphate: good things come to those who wait? *Nephrol Dial Transplant*, im Druck

Zawada A. M.*, **Fell L. H.***, Untersteller K., Seiler S., Rogacev K. S., Fliser D., Ziegler-Heitbrock L., Heine G. H. (2015). Comparison of two different strategies for human monocyte subsets gating within the large-scale prospective CARE FOR HOME study. *Cytometry A*. 87(8):750-8, *geteilte Erstautorenschaft.

Karaca I., Tamboli I. Y., Glebov K., Richter J., **Fell L. H.**, Grimm M. O., Haupenthal V. J., Hartmann T., Gräler M. H., van Echten-Deckert G., Walter J. (2014). S1P-lyase deficiency impairs lysosomal metabolism of the amyloid precursor protein. *J Biol Chem*, 289, 16761-16772

Fell L. H., Zawada A. M., Rogacev K. S., Seiler S., Fliser D., Heine G. H. (2014). Distinct immunologic effects of different intravenous iron preparations on monocytes. *Nephrol Dial Transplant*, 29, 809-822.

Seiler S., Lucisano G., Ege P., **Fell L. H.**, Rogacev K. S., Lerner-Gräber A., Klingele M., Ziegler M., Fliser D., Heine, G. H. (2013). Single FGF-23 measurement and time-averaged plasma phosphate levels in hemodialysis patients. *Clin J Am Soc Nephrol*, 8, 1764–1772.

Kongressbeiträge

Freie Vorträge

Fell L. H., Seiler S., Sester M., Fliser D., Zawada A. M., Heine G. H. (2015). Impact of individual *i.v.* iron preparations on differentiation of macrophages and dendritic cells. Kongress für Nephrologie – 7. Jahrestagung der Deutschen Gesellschaft für Nephrologie, Berlin.

Fell L. H., Zawada A. M., Seiler S., Untersteller K., Fliser D., Heine G. H. (2015). Impact of individual *i.v.* iron preparations on differentiation of macrophages and dendritic cells. 52nd ERA-EDTA Congress London, United Kingdom [ausgezeichnet mit einem *travel grant* als einer der elf besten Abstracts].

Posterpräsentationen

Zawada A. M., **Fell L. H.**, Untersteller K., Seiler S., Rogacev K. S., Fliser D., Ziegler-Heitbrock L., Heine G. H. (2015). Gating strategy for the identification of intermediate monocytes. Präsentation durch Zawada A. M. auf dem 21th Leipziger Workshop ‘Cytomics’, Leipzig.

Fell L. H., Seiler S., Zawada A. M., Rogacev K. S., Sester M., Fliser D., Heine, G. H. (2014). Einfluss der Hyperphosphatämie auf die myeloide Differenzierung hämatopoetischer Stammzellen. Kongress für Nephrologie – 6. Jahrestagung der Deutschen Gesellschaft für Nephrologie, Berlin.

Fell L. H., Zawada A. M., Rogacev K. S., Seiler S., Fliser D., Heine G. H. (2013). Distinct immunologic effects of individual *i.v.* iron formulations on monocytes. 50th ERA-EDTA Congress, Istanbul, Turkey.

Fell L. H., Zawada A. M., Rogacev K. S., Seiler S., Fliser D., Heine G. H. (2013). Distinct immunologic effects of individual *i.v.* iron formulations on monocytes. Kongress für Nephrologie – 5. Jahrestagung der Deutschen Gesellschaft für Nephrologie, Berlin.

Danksagung

Ich möchte denjenigen danken, die mich in den letzten Jahren auf meinem Weg beruflich und privat begleitet haben und zum Gelingen dieser Dissertationsschrift beigetragen haben.

Zunächst danke ich Frau Professor Martina Sester und Herrn Professor Gunnar Heine sowie Herrn Professor Fliser, die mich als naturwissenschaftliche Doktorandin und Mitarbeiterin aufnahmen und mir ein Promotionsthema zur Verfügung stellten. In den letzten Jahren standen sie mir stets mit immensem Fachwissen zur Seite, unterstützen mich mit wertvollen Anregungen und Ideen, und boten mir zudem die Möglichkeit, meine Ergebnisse auf nationalen und internationalen Kongressen zu präsentieren.

Besonders danke ich auch Frau Privatdozentin Sarah Seiler, deren Engagement und Ehrgeiz meine Stelle ermöglichten und auf deren Hilfe ich bei beruflichen wie auch privaten Fragen und Problemen immer bauen durfte.

Als Laborkollege, enthusiastischer Mensagefährte, aber vor allem auch direkter wissenschaftlicher Ansprechpartner möchte ich Herrn Dr. Adam Zawada für all seine Unterstützung, Diskussionsbereitschaft und Geduld danken.

Ein weiterer Dank gilt allen Mitgliedern der AG1 und AG1a, mit denen ich auf Kongressen und Seminaren, aber auch bei nicht-wissenschaftlichen Events, eine tolle Zeit verbringen durfte. Danken möchte ich auch allen Blutspendern und ganz besonders dem gesamten Ambulanzteam der Klinik für Innere Medizin IV, die die Blutentnahmen für die Experimente mit viel Erfahrung und Geschick durchführten. Ich danke auch Frau Offenhäuser, Herrn Kunter, Herrn Lizzi und natürlich Herrn Schmid, für ihre Hilfe bei administrativen, wissenschaftlichen und technischen Fragen.

Danken möchte ich auch der Medizinischen Fakultät der Universität des Saarlandes, deren Homburger Forschungsförderungsprogramm (HOMFOR) die Finanzierung meiner Stelle und Forschung ermöglichte.

Zutiefst danke ich auch meiner Familie, meinem Partner und meinen Freunden, die mir stets Mut zusprachen, mich in meiner Arbeit bestärkten und ein niemals enden wollendes Verständnis zeigten.

Anhang

A1 Material- und Methodenteil zum „Einfluss des Kalzium-Phosphathaushalts auf die Monozytenbiologie“

A1-1 Material

A1-1.1 Geräte

Durchflusszytometer BD FACS Canto II	BD Biosciences, Heidelberg
Zellseparationsmagnete OctoMACS/QuadroMACS	Miltenyi Biotec, Bergisch-Gladbach

A1-1.2 Software

GraphPad Prism 4	GraphPad Software, La Jolla, CA
FACSDiva 6	BD Biosciences, Heidelberg

A1-1.3 Chemikalien

Bovines Serumalbumin (BSA)	Serva, Heidelberg
Calciumchlorid-Dihydrat ($\text{CaCl}_2 \times 2\text{H}_2\text{O}$)	Sigma-Aldrich, Taufkirchen
Cytokine Mix E for HPC-Expansion Medium DXF	PromoCell, Heidelberg
D(+) Glukose	Sigma-Aldrich, Taufkirchen
Essigsäure (100 %)	Roth, Karlsruhe
Ethylendiamintetraessigsäure (EDTA)	Sigma-Aldrich, Taufkirchen
Fetales Kälberserum (FCS)	Fisher Scientific, Schwerte
Fluoresbrite YG Carboxylate Microspheres (0,75 μm) ($1,08 \times 10^{11}$ Partikel/ml)	Polysciences Inc., Eppelheim
Humanes Serumalbumin (HSA)	Sigma-Aldrich, Taufkirchen
Kaliumhydrogenphosphat (KH_2PO_4)	Sigma-Aldrich, Taufkirchen
Natriumazid (NaN_3)	Serva, Heidelberg
Paraformaldehyd (PFA)	Sigma-Aldrich, Taufkirchen
Saponin	Sigma-Aldrich, Taufkirchen

A1-1.4 Reaktionskits

CD34 Microbead Kit, human

Miltenyi Biotec, Bergisch-Gladbach

A1-1.5 Antikörper

Die in dem Kalzium-Phosphat-Teil verwendeten Antikörper sind in **Tabelle A1-1** aufgelistet.

Tabelle A1-1: In der Durchflusszytometrie verwendete Antikörper

Zielantigen	Fluorochrom	Klon	Ig-Klasse	Host	Firma
CD14	PerCP	MΦP9	IgG _{2b} κ	Maus	BD Pharmingen
CD16	PE/Cy7	3G8	IgG ₁ κ	Maus	BD Pharmingen
CD34	APC	581	IgG ₁ κ	Maus	BD Pharmingen
CD45	PE	HI30	IgG ₁ κ	Maus	BD Biosciences
CD80	FITC	2D10	IgG ₁ κ	Maus	Biolegend
CD86	PE	HA5.2B7	IgG _{2b}	Maus	Beckman Coulter
CD195	APC	2D7/CCR5	IgG _{2a} κ	Maus	BD Pharmingen
CX₃CR1	FITC	2A9-1	IgG _{2b} fE	Ratte	Biozol
TNF	FITC	MAb11	IgG ₁ κ	Maus	BD Pharmingen
IL-1β	Alexa Fluor 647	JK1B-1	IgG ₁	Maus	Biolegend
IL-6	FITC	MQ2-13A5	IgG ₁ κ	Ratte	Biolegend

A1-1.6 Gebrauchsfertige Medien, Puffer und Lösungen

BD FACS™ Lysing Solution

BD Biosciences, Heidelberg

FACS-Clean

BD Biosciences, Heidelberg

FACS-Flow

BD Biosciences, Heidelberg

FACS-Rinse

BD Biosciences, Heidelberg

Hematopoietic Progenitor Cell Expansion Medium DXF

PromoCell, Heidelberg

Hematopoietic Progenitor Medium

PromoCell, Heidelberg

LSM 1077 Lymphocyte Separation Medium

PAA Laboratories, Cölbe

Medium 199 (M199)

Biozym, Hessisch Oldendorf

PBS (ohne Ca und Mg)

Life Technologies, Darmstadt

PBS (mit Ca und Mg)

PAA Laboratories, Cölbe

A1-1.7 Medien, Puffer und Lösungen

Kalzium-Phosphat-Stimulation

M199/FCS	5% (v/v)	FCS in M199
Kalzium-Stocklösung	40 mM	CaCl ₂ in M199/FCS bzw. Wachstumsmedium bzw. Hematopoietic Progenitor Medium
Phosphat-Stocklösung	40 mM	Na ₂ HPO ₄ in M199/FCS bzw. Wachstumsmedium bzw. Hematopoietic Progenitor Medium

Zellisolation

PBS/EDTA	5 mM	EDTA in PBS (ohne Ca und Mg)
MACS-Puffer	0,6% (v/v)	HSA in PBS/EDTA

Zellkultur

Essigsäure (3 %)	3% (v/v)	Essigsäure (100%) in ddH ₂ O
------------------	----------	---

Durchflusszytometrie

FACS-Puffer	5% (v/v)	FCS
	0,5% (w/v)	BSA
	0,02% (v/v)	EDTA [10%ig (w/v) in PBS (ohne Ca und Mg)]
	0,07% (v/v)	NaN ₃ [10%ig (w/v) in PBS (ohne Ca und Mg)] In PBS (ohne Ca und Mg)
Saponinpuffer	0,1% (w/v)	Saponin in FACS-Puffer

Lysepuffer	10% (v/v)	BD FACS™ Lysing Solution in ddH ₂ O
PFA (4%ig)	4% (w/v)	PFA in PBS (ohne Ca und Mg); PH 7,5
PFA (1%ig)	25% (v/v)	PFA (4%ig) in PBS (ohne Ca und Mg)
Krebs-Ringer Lösung	20 mL 20,4 mg	PBS (mit Ca und Mg) D(+) Glukose

Die Medien, Puffer und Lösungen wurden bei 4°C gelagert.

A1-1.8 Probanden

Für die *in vitro* Experimente wurde Blut gesunder Probanden, im Alter zwischen 20 und 60 Jahren und ohne anamnestischen Hinweis auf kardiovaskuläre oder renale Komorbiditäten (Kreatinin < 1,5 mg) verwendet.

A1-2 Methoden

A1-2.1 Stimulation mit Kalzium und Phosphat *in vitro*

Zur Stimulation mit Kalzium- und Phosphat wurden die verwendeten Medien entsprechend ihrer Ausgangskonzentration an freiem Kalzium (Ca²⁺) und Phosphat sowie der gewünschten Endkonzentrationen individuell mit kalzium- und phosphathaltigen Stocklösungen eingestellt (**Tabelle A1-2**).

Die Vollblutstimulation erfolgte in Reagiergefäßen aus Polypropylen in einem Gesamtvolumen von 450 µL, bei 37°C und 5% CO₂ in einem Inkubator. Dazu wurden zur Expressionsanalyse der Oberflächenmarker 150 µL EDTA-antikoaguliertes Vollblut und zur Bestimmung der Phagozytosekapazität 150 µL Citrat-antikoaguliertes Vollblut mit M199 und den kalzium- und phosphathaltigen Stocklösungen (**Tabelle A1-2**) vermengt und 5 h inkubiert.

Zur Expressionsanalyse intrazellulärer Zytokine wurde 150 μL Lithium-Heparin-antikoaguliertes Vollblut verwendet; die Ansätze wurden zunächst 2 h und nach Zugabe von 10 $\mu\text{g/ml}$ Brefeldin A nochmals 1 h bei 37°C und 5% CO_2 inkubiert. Brefeldin A blockiert den Golgi-Apparat der Zellen, wodurch die Zytokine nicht mehr sezerniert werden können und im Endoplasmatischen Retikulum akkumulieren.

Nach Stimulation wurde 2 mL FACS-Puffer hinzugegeben, die Blutbestandteile bei 300 x g 7 min abzentrifugiert und für die weiteren Analysen verwendet.

Tabelle. A1-2: Kalzium- und Phosphat-Stimulation

Experiment (Gesamtvolumen)	Ansatz	Kalzium- Stocklösung [μL]	Phosphat- Stocklösung [μL]
Vollblutstimulation (450 μL)	1 mM $(\text{PO}_4)^{3-}$ /1,3 mM Ca^{2+}	0	1,50
	2 mM $(\text{PO}_4)^{3-}$ /1,3 mM Ca^{2+}	0	13,48
	4 mM $(\text{PO}_4)^{3-}$ /1,3 mM Ca^{2+}	0	40,86
	4 mM $(\text{PO}_4)^{3-}$ /1,8 mM Ca^{2+}	17,71	40,87
Differenzierung hämatopoetischer Stammzellen (5 ml)	1 mM $(\text{PO}_4)^{3-}$ /1,3 mM Ca^{2+}	0	0
	1 mM $(\text{PO}_4)^{3-}$ /1,8 mM Ca^{2+}	141,25	0
	2 mM $(\text{PO}_4)^{3-}$ /1,3 mM Ca^{2+}	0	80
	2 mM $(\text{PO}_4)^{3-}$ /1,8 mM Ca^{2+}	153,75	80
	4 mM $(\text{PO}_4)^{3-}$ /1,3 mM Ca^{2+}	0	330
	4 mM $(\text{PO}_4)^{3-}$ /1,8 mM Ca^{2+}	191,25	330

A1-2.2 Zellisolation

Isolation von peripheren mononukleären Zellen aus Vollblut

Periphere mononukleare Blutzellen (PBMCs) wurden aus EDTA-antikoaguliertem Vollblut mit Hilfe einer Dichtegradientenzentrifugation isoliert. Dabei ergeben je nach Spender aus 9 mL EDTA-antikoaguliertem Vollblut zwischen 10 und 20 Mio. PBMCs.

Zur Isolation wurde bis zu 18 mL EDTA-antikoaguliertes Vollblut pro 50 mL Reagiergefäß mit PBS/EDTA auf 35 mL verdünnt und auf 13 mL Separationsmedium (Ficoll-Paque) geschichtet, so dass eine Phasentrennung sichtbar wurde. Die Auftrennung der Blutzellen erfolgte während einer ungebremsten Zentrifugation innerhalb von 35 min bei 410 x g und 20°C. Währenddessen durchwandern Erythrozyten, Granulozyten und tote Zellen aufgrund ihrer höheren Dichte das Separationsmedium und bilden die unterste Phase. Die

Thrombozyten befinden sich in der obersten Schicht in einem Gemisch aus Plasma und PBS/EDTA. Die PBMCs bilden eine weißliche Interphase, die dem Separationsmedium aufliegt.

Zur Isolation der PBMCs wurden 10 mL der oberen Phase abgesaugt und die PBMCs mit einer Pipette abgenommen. Die abgenommenen Zellen wurden in einem 50 mL Reagiergefäß mit PBS/EDTA gemischt und bei 300 x g für 20 min bei 4°C abzentrifugiert. Anschließend wurde der Überstand verworfen, das Zellpellet je nach Experiment in einem entsprechendem Medium oder Puffer resuspendiert und die PBMCs für weitere Experimente verwendet.

Isolation CD34⁺ hämatopoetischer Stammzellen aus Vollblut

Hämatopoetische Stammzellen sind CD34⁺ blutbildende Vorläuferzellen, die durch Positivselektion mit Hilfe des CD34 MicroBead Kit und dem MACS-System von Miltenyi Biotec isoliert wurden. Dazu wurden PBMCs aus EDTA-antikoaguliertem Vollblut isoliert, in 10 mL PBS/EDTA aufgenommen und in ein 15 mL Reaktionsgefäß überführt. Die Zellzahl wurde nach Neubauer bestimmt und die Zellen anschließend bei 300 x g 10 min abzentrifugiert. Der Überstand wurde verworfen, das Zellpellet in 300 µL MACS-Puffer pro 10⁸ Zellen resuspendiert und mit je 100 µL FcR Blocking Reagent und CD34 MicroBead pro 10⁸ Zellen gemischt. Die Ansätze wurden 30 min bei 4°C inkubiert. Dabei wurden die CD34⁺ Zellen mit spezifischen Magnetpartikeln gegen CD34 markiert und konnten anschließend durch magnetische Separation von den übrigen Zellen getrennt werden.

Die magnetische Auftrennung erfolgte mit Hilfe eines QuadroMACS- und OctoMACS-Magneten und je einer LS- und MS-Säule. Dazu wurden die Zellen zunächst in 10 mL MACS-Puffer gewaschen, bei 300 x g und 4°C 10 min abzentrifugiert und anschließend in 500 µL MACS-Puffer resuspendiert. Zur Separation wurde die LS-Säule in den QuadroMACS-Magnet eingespannt und mit 3 mL MACS-Puffer äquilibriert. Anschließend wurde die Zellsuspension durchlaufen gelassen und die Säule dreimal mit je 3 mL MACS-Puffer gespült. Die Säule wurde dem Magneten entnommen und die CD34⁺-Zellen nach Zugabe von 5 mL MACS-Puffer mit Hilfe eines Stößels aus der Säule in ein 15 mL Reagiergefäß gedrückt. Die isolierten Zellen wurde bei 300 x g 10 min bei 4°C abzentrifugiert und das Zellpellet erneut in 500 µL MACS-Puffer resuspendiert. Zur Aufreinigung der CD34⁺ Zellen wurde nun mit der MS-Säule und dem OctoMACS-Magnet gleichermaßen verfahren. Hierbei wurden 500 µL MACS-Puffer zum Äquilibrieren und Spülen und 1 mL zur

Gewinnung der Zellen verwendet. Die Reinheit wurde durchflusszytometrisch durch Färbung von CD34 und CD45 (**siehe A1-2.4**) überprüft und die hämatopoetischen Stammzellen für weitere Experimente verwendet.

A1-2.3 Zellkultur

Zellzählung nach Neubauer

Die Zellzählung erfolgte mit Hilfe einer Neubauer-Zählkammer. Dabei wurde 10 µL der Zellsuspension 1:10 mit Essigsäure (3%) verdünnt, wovon 10 µL in eine Zählkammer pipettiert wurden. Unter einem Mikroskop wurden die Zellen in den vier Quadranten (inklusive zwei der vier Ränder) ausgezählt (n_1 - n_4). Um die absolute Zellzahl zu erhalten, wurde der arithmetische Mittelwert der vier Zellzahlen gebildet und mit dem Verdünnungsfaktor (10), dem Kammerfaktor (10^4) und dem Volumen an Zellsuspension (V) multipliziert.

$$\text{Kurz: } N_{\text{absolut}} = \frac{1}{4} \sum_{i=1}^4 n_i \times 10 \times 10^4 \times V$$

Expansion und Differenzierung hämatopoetischer Stammzellen

Zur Expansion der CD34⁺ hämatopoetischen Stammzellen wurden diese zunächst in 5 mL Hematopoietic Progenitor Expansion Medium aufgenommen, mit 50 µL Cytokine Mix E supplementiert und in die Vertiefung einer 6Well-Platte gegeben. Nach einer siebentägigen Inkubation bei 37°C und 5% CO₂ wurde das Medium gewechselt. Dazu wurde die gesamte Zellsuspension in ein 15 mL Reagiergefäß überführt und die Zellen bei 300 x g 10 min abzentrifugiert. Die Zellen wurden in 5 mL Hematopoietic Progenitor Expansion Medium resuspendiert, in die Vertiefung einer 6Well-Platte pipettiert und mit 50 µL Cytokine Mix E weitere 7 Tage bei 37°C und 5% CO₂ kultiviert.

Zur anschließenden Differenzierung wurden die Zellen in ein 15 mL Reagiergefäß überführt, bei 300 x g 10 min abzentrifugiert, in kalzium- und phosphathaltigem Hematopoietic Progenitor Medium (**Tabelle A1-2**) in 6Well-Platten ausgesät und 8 Tage bei 37°C und 5% CO₂ inkubiert. Während dieser Zeit wurden die Zellen täglich phänotypisch und am letzten Tag zusätzlich funktionell untersucht.

A1-2.4 Durchflusszytometrie

Die Durchflusszytometrie ist ein Verfahren zur quantitativen Bestimmung von Oberflächenmolekülen und intrazellulären Proteinen, Peptiden und DNA. Grundlage hierfür ist die Detektion der optischen Signale fluoreszenzmarkierter Zellen, die einzeln durch eine Kapillare gesaugt werden und in der Durchflusszelle eine ausgesandte Laserstrahlung passieren. Dabei wird der Fluoreszenzfarbstoff des Antikörpers durch Laserlicht angeregt und dessen Fluoreszenzintensität detektiert. Diese gibt Auskunft über die Expressionsstärke des markierten Proteins. Detektiert wird zudem die Lichtstreuung als Vorwärts- und Seitwärtsstreuung. Das Vorwärtsstreulicht (FSC) ist ein Maß für die Beugung des Lichts im flachen Winkel und hängt vom Volumen der Zelle ab. Das Seitwärtsstreulicht (SSC) ist ein Maß für die Brechung des Lichts im rechten Winkel, die von der Granularität der Zelle, der Größe und Struktur ihres Zellkerns sowie der Menge der Vesikel in einer Zelle beeinflusst wird.

Zur Auswertung der durchflusszytometrischen Analyse können die registrierten optischen Signale in Punktdiagrammen (*Dotplots*) und Histogrammen dargestellt und die gesuchte Zellpopulation nach ihren Eigenschaften zusammengefasst (*gated*) werden. Anschließend kann für jede ausgewählte Zellpopulation der prozentuale Anteil sowie für jedes Fluorophor die mediane Fluoreszenzintensität (MFI) angegeben werden.

Bestimmung der Expression von Oberflächenmarkern

Die Einteilung der Monozyten in die drei Monozytensubpopulationen der klassischen, intermediären und nicht-klassischen Monozyten erfolgte nach dem in **Abbildung A1-1** dargestellten Schema. Dabei wurden zunächst alle Zellen in einem SSC/CD86 Dotplot dargestellt und die Monozyten mit Hilfe der CD86-Expression von den übrigen Zellpopulationen wie Lymphozyten und Granulozyten abgegrenzt (**A**). Anschließend wurden die CD86⁺-Zellen selektiv in einem FSC/SSC Dotplot dargestellt, der eine weitere Eingrenzung der präsumtiven Monozyten nach ihren charakteristischen Streulichteigenschaften ermöglichte (**B**). Innerhalb dieser vordefinierten Monozyten wurden die drei Subpopulationen nach der Expression ihrer Oberflächenrezeptoren CD14 und CD16 definiert (**C**).

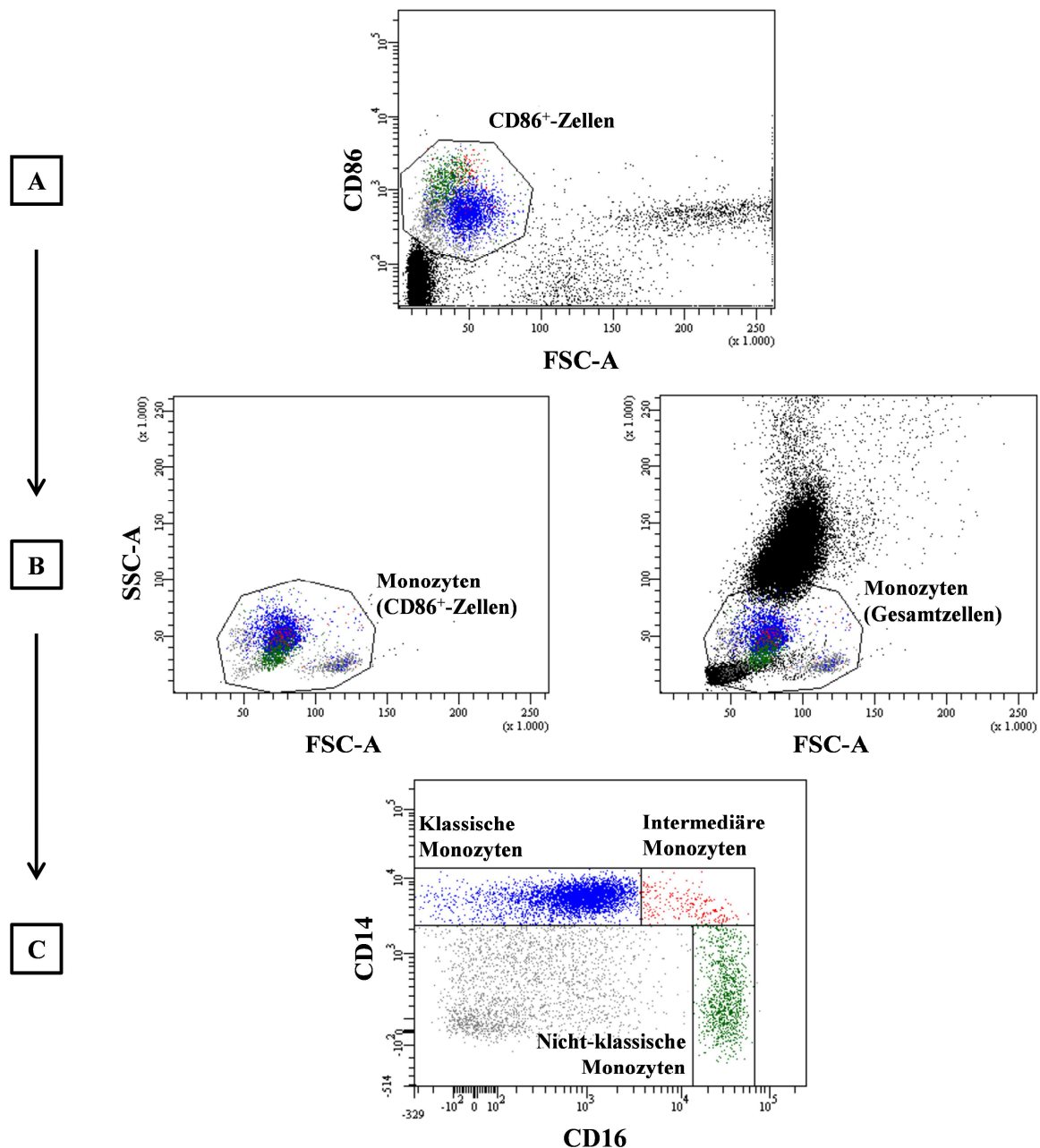


Abbildung A1-1: Einteilung humaner Monozytensubpopulationen in Vollblut (ZAWADA et al., 2012)

Im Vollblut wurden Blutzellen mit fluoreszenzgekoppelten Antikörpern gegen CD14, CD16 und CD86 markiert und durchflusszytometrisch vermessen. **A:** Abgrenzung der Monozyten von anderen Leukozyten durch Gating der CD86⁺-Zellen in einem SSC/CD86-Dotplot. **B:** Darstellung der CD86⁺ Zellen und Gesamtzellen aus A in einem FSC/SSC-Dotplot und Gating der Monozyten anhand ihrer charakteristischen Größe und Granularität. **C:** Darstellung aus A und B erhaltenen CD86⁺ Monozyten und Einteilung der klassischen, intermediären und nicht-klassischen Monozytensubpopulationen nach der Oberflächenexpression von CD14 und CD16.

Zur Charakterisierung von Monozytensubpopulationen im Vollblut wurden die Blutzellen in 2 mL FACS-Puffer gewaschen, bei 300 x g 7 min abzentrifugiert und mit Antikörpern aus Mix 1 und Mix 2 (**Tabelle A1-3**) für 30 min bei 4°C gefärbt. Anschließend wurden die Erythrozyten in 2 mL Lysepuffer 10 min bei Raumtemperatur im Dunkeln lysiert. Die

verbleibenden Blutzellen wurden bei 300 x g 7 min abzentrifugiert und in 2 mL FACS-Puffer gewaschen, nochmals bei 300 x g 7 min abzentrifugiert. Anschließend wurden die Zellen durch Zugabe von PFA (1%) fixiert und konnten durchflusszytometrisch gemessen werden.

Tabelle A1-3: Antikörpermix zur Charakterisierung von Monozytensubpopulationen im Vollblut

Mix 1	Antikörper	Menge	Mix 2	Antikörper	Menge
	CD14	4 µL		CD14	4 µL
	CD16	0,5 µL		CD16	0,5 µL
	CD86	5 µL		CD86	5 µL
				CCR5	20 µL
				CX3CR1	1 µL
	FACS-Puffer	ad 70 µL		FACS-Puffer	ad 70 µL

Zur Überprüfung der Reinheit hämatopoetischer Stammzellen wurde nach der Isolation die Expression der Oberflächenproteine CD34 und CD45 durchflusszytometrisch überprüft. Dazu wurden 100 µL Zellsuspension mit Antikörpern gegen CD34 und CD45 aus Mix 1 (**Tabelle A1-4**) für 15 min bei 4°C gefärbt. Anschließend wurden die Zellen in 2 mL FACS-Puffer gewaschen und bei 300 x g 7 min abzentrifugiert. Die Zellen wurden mit PFA (1%) fixiert und die Expression von CD34 und CD45 im Durchflusszytometer bestimmt.

Tabelle A1-4: Antikörpermix zur Charakterisierung hämatopoetischer Stammzellen

Mix 1	Antikörper	Menge	Mix 2	Antikörper	Menge
	CD34	20 µL		CD14	3 µL
	CD45	20 µL		CD16	0,25 µL
				CD86	4 µL
	FACS-Puffer	ad 70 µL		FACS-Puffer	ad 70 µL

Mix 3	Antikörper	Menge	Mix 4	Antikörper	Menge
	CD14	3 µL		CD14	3 µL
	CD16	0,25 µL		CD16	0,25 µL
	CD86	4 µL		CD86	4 µL
	CCR5	20 µL		CD80	5 µL
	CX3CR1	1 µL		CCR2	20 µL
	FACS-Puffer	ad 70 µL		FACS-Puffer	ad 70 µL

Zur phänotypischen Charakterisierung hämatopoetischer Stammzellen und *in vitro* differenzierter Monozyten wurde die Expression von CD14, CD16 und CD86 an jedem Tag der Differenzierung und am letzten Tag zusätzlich die Expression von CCR5 und CX₃CR1 sowie von CD80 und CCR2 bestimmt. Dazu wurden je 100 µL Zellsuspension mit Antikörpern aus Mix 2, Mix 3 und Mix 4 (**Tabelle A1-4**) für 15 min bei 4°C gefärbt, anschließend in 2 mL FACS-Puffer gewaschen und bei 300 x g 7 min abzentrifugiert. Die Zellen wurden in PFA (1%) fixiert und die Expression der Oberflächenmarker durchflusszytometrisch vermessen.

Bestimmung der Expression intrazellulärer Zytokine

Für die Expressionsanalyse intrazellulärer Zytokine wurde die Zellmembran mit Hilfe eines saponinhaltigen Puffers perforiert. Saponin beeinflusst die Membranpermeabilität durch Interaktion mit Cholesterol in der Zellmembran. Dabei entfernt es das Cholesterol selektiv und schafft so Freiräume, durch die die Zelle Antikörper aufnehmen kann.

Tabelle A1-5: Antikörpermix zur Charakterisierung intrazellulärer Zytokine

Mix 1	Antikörper	Menge	Mix 2	Antikörper	Menge
	TNF	2 µL		IL-6	5 µL
	IL-1β	2 µL			
	Saponinpuffer	ad 70 µL		Saponinpuffer	ad 70 µL

Für die Expressionsanalyse von TNF, IL-1β und IL-6 wurden die Monozyten zunächst wie bereits beschrieben mit Antikörpern gegen CD14, CD16 und CD86 gefärbt, anschließend in 100 µL PFA (4%) 5 min bei Raumtemperatur fixiert und weitere 10 min in 2 mL Saponinpuffer inkubiert. Die Zellen wurden bei 300 x g 7 min abzentrifugiert und mit Antikörpern aus Mix 1 und Mix 2 (**Tabelle A1-5**) gegen TNF und IL-1β sowie gegen IL-6 45 min bei Raumtemperatur im Dunkeln gefärbt. Danach wurden die Zellen in 2 mL FACS-Puffer gewaschen, bei 300 x g 7 min abzentrifugiert und in 100 µL PFA (1%) fixiert. Abschließend konnte die Zytokinexpression durchflusszytometrisch bestimmt werden.

Phagozytose-Assay

Zur Bestimmung der Phagozytosekapazität wurden grün fluoreszierende Latexpartikel (Fluoresbrite Yellow Green (YG) Carboxylate Microspheres) verwendet. Diese wurden zunächst opsoniert, indem 1,5 µL Latexpartikel mit 500 µL humanem Serum (aus drei

humanen Seren gemischt) und 500 μL Krebs-Ringer PBS (Endkonzentration $1,5 \times 10^8$ Partikel/mL) gemischt und unter Schütteln für 30 min bei 37°C im Wasserbad inkubiert wurden. Die Analyse der monozytären Phagozytosekapazität erfolgte nach Vollblutstimulation und nach Differenzierung hämatopoetischer Stammzellen. Dazu wurde zu jedem 450 μL Vollblut-Ansatz 50 μL opsonierte Latexpartikel und zu 100 μL Zellsuspension 10 μL Latexpartikel zugegeben. Die Ansätze wurden 30 min bei 37°C unter leichtem Schütteln im Wasserbad inkubiert, anschließend in 2 mL FACS-Puffer gewaschen und bei $300 \times g$ 7 min abzentrifugiert. Die Zellen wurden wie bereits beschrieben mit Antikörpern gegen CD14, CD16 und CD86 markiert und durchflusszytometrisch vermessen. Nach Einteilung der Monozyten in die drei Subpopulationen konnten die phagozytierenden Monozyten in jeder Subpopulation als FITC-positive Zellen identifiziert werden.

A1-2.5 Statistische Auswertung der Daten

Die statistische Analyse und graphische Darstellung der Ergebnisse erfolgte mittels Graphpad Prism 4 (La Jolla, USA) über einfaktorielle Varianzanalyse (ANOVA) und wo angegeben mit nachfolgendem Dunnett-Test als post hoc Analyse. Als Signifikanzniveau wurde dabei $P < 0,05$ definiert.

A2 Publikationen

Die im Rahmen dieser Promotionsarbeit veröffentlichten Publikationen sind im Folgenden angehängt.

Beitrag der Mitautoren für die Arbeit:

Adam M. Zawada*, Lisa H. Fell*, Kathrin Untersteller, Sarah Seiler, Kyrill S. Rogacev, Danilo Fliser, Loems Ziegler-Heitbrock, Gunnar H. Heine (2015) Comparison of two different strategies for human monocyte subsets gating within large-scale prospective CARE FOR HOME study. Cytometry A, 87(8):750-8 (*geteilte Erstautorenschaft)

Diese Studie wurde von Herrn Dr. Adam Zawada, Frau Lisa Fell, Herrn Prof. Dr. Danilo Fliser, Herrn Prof. Dr. Loems Ziegler-Heitbrock und Herrn Prof. Dr. Gunnar Heine entworfen und geplant. Die Patienten wurden durch Frau Kathrin Untersteller, Frau PD Dr. Sarah Seiler, Herrn PD Dr. Kyrill Rogacev sowie durch Herrn Prof. Dr. Gunnar Heine rekrutiert. Die Auswertung der FACS-Daten erfolgte durch Frau Lisa Fell und Frau Kathrin Untersteller. Herr Dr. Adam Zawada, Frau Lisa Fell und Herr Prof. Dr. Gunnar Heine führten die statistische Auswertung der Daten durch und deren Interpretation in Zusammenarbeit mit Herrn Prof. Dr. Danilo Fliser und Herrn Prof. Dr. Loems Ziegler-Heitbrock. Das Manuskript wurde von Herrn Dr. Adam Zawada, Frau Lisa Fell und Herrn Prof. Dr. Gunnar Heine geschrieben.

Die oben aufgeführten Autoren haben die finale Version des Manuskripts gelesen, kritisch überarbeitet und ihr zugestimmt.

Comparison of Two Different Strategies for Human Monocyte Subsets Gating Within the Large-Scale Prospective CARE FOR HOME Study

Adam M. Zawada,^{1†} Lisa H. Fell,^{1†} Kathrin Untersteller,¹ Sarah Seiler,¹ Kyrill S. Rogacev,¹ Danilo Fliser,¹ Loems Ziegler-Heitbrock,² Gunnar H. Heine^{1*}

¹Department of Internal Medicine IV - Nephrology and Hypertension, Saarland University Medical Center, Homburg, Germany

²EvA Study Center, Comprehensive Pneumology Center Helmholtz Zentrum München—German Research Center for Environmental Health, Gauting, Germany

Received 11 March 2015; Revised 23 April 2015; Accepted 18 May 2015

Grant sponsor: Else Kröner-Fresenius-Stiftung.

Additional Supporting Information may be found in the online version of this article.

Correspondence to: Gunnar H. Heine, Department of Internal Medicine IV, Saarland University Medical Center, Homburg, Germany. E-mail: Gunnar.heine@uks.eu

Conflict of Interest: LZH has received personal fees for consultancy outside this work from Five Prime Therapeutics, San Francisco.

This article incorporates data from a poster presentation at the 20th Zytomik Leipziger Workshop on Translational Cytoomics.

[†]These authors contributed equally

Published online 9 June 2015 in Wiley Online Library (wileyonlinelibrary.com)

DOI: 10.1002/cyto.a.22703

© 2015 International Society for Advancement of Cytometry

• Abstract

Monocytes are heterogeneous cells consisting of (at least) three subsets: classical, intermediate, and nonclassical monocytes. Correct enumeration of cell counts necessitates well-defined gating strategies, which are essentially based upon CD14 and CD16 expression. For the delineation of intermediate from nonclassical monocytes, a “rectangular gating (RG) strategy” and a “trapezoid gating (TG) strategy” have been proposed. We compared the two gating strategies in a well-defined clinical cohort of patients with chronic kidney disease (CKD). Within the ongoing CARE FOR HOME study, monocyte subsets were reanalyzed in 416 CKD patients, who were followed 3.6 ± 1.6 years for the occurrence of a cardiovascular event. Gating was performed by either RG or TG. We analyzed the expression of surface markers, and compared the predictive role of cell counts of monocyte subsets, as defined by RG and TG, respectively. With both gating strategies, higher intermediate monocyte counts predicted the cardiovascular endpoint in Kaplan-Meier analyses ($P < 0.001$ with RG; $P < 0.001$ with TG). After correction for confounders, intermediate monocyte counts remained independent predictors in Cox-Regression analyses (HR = 1.013 [95% CI: 1.006–1.020; $P < 0.001$] with RG; HR = 1.015 [95% CI: 1.006–1.024; $P = 0.001$] with TG). NRI was 3.9% when reclassifying patients from quartiles of intermediate monocyte counts with RG strategy toward quartiles of intermediate monocytes counts with TG strategy. In expression analysis, those monocytes which are defined as intermediate monocytes by the RG strategy and as nonclassical monocytes by the TG strategy share characteristics of both subsets. In conclusion, intermediate monocytes were independent predictors of cardiovascular outcome irrespective of the applied gating strategy. Future studies should aim to identify markers that allow for an unequivocal definition of intermediate monocytes, which may further improve their power to predict cardiovascular events. © 2015 International Society for Advancement of Cytometry

• Key terms

cd14; cd16; monocytes; gating strategy; cardiovascular disease; chronic kidney disease

MONOCYTE heterogeneity was first described in 1989 based on the differential expression of the lipopolysaccharide coreceptor CD14 and the FcγRIII receptor CD16 (1). Initially two monocyte subpopulations have been distinguished by flow-cytometry: a population, which expresses high levels of CD14 and no CD16, and a population which coexpresses both markers (CD16+ monocytes).

Subsequent research characterized CD16+ monocytes as proinflammatory cells, as they were found to express high levels of TNFα and IL12p40/IL12p70 (2,3) and as their cell counts were found to be elevated in many inflammatory conditions [reviewed in (4,5)].

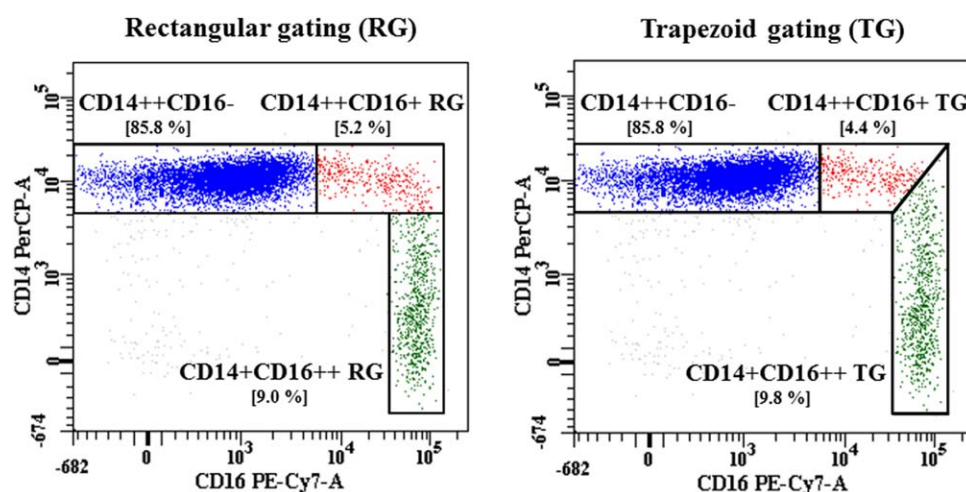


Figure 1. Two suggested gating strategies for monocyte subsets. The delineation of intermediate and nonclassical monocytes can be performed by two different gating strategies: the RG strategy or the TG strategy. [Color figure can be viewed in the online issue which is available at wileyonlinelibrary.com]

More than ten years ago, first evidence emerged that CD16⁺ monocytes consist of two phenotypical different subpopulations (6,7). Since then varying definitions and gating strategies for monocyte subsets coexisted in the literature impeding the comparison of study results from different groups. To solve this problem, an official nomenclature for circulating monocytes was proposed by an expert consensus committee, which was subsequently approved by the Nomenclature Committee of the International Union of Immunological Societies (8). This consensus acknowledges the existence of three different monocyte subsets: classical CD14⁺⁺CD16[−] monocytes, intermediate CD14⁺⁺CD16⁺ monocytes and nonclassical CD14⁺CD16⁺⁺ monocytes.

Prior to the introduction of this official nomenclature, intermediate monocytes have mostly been neglected or analyzed in common with nonclassical monocytes. However, despite being a cell population in transition from classical to nonclassical monocytes (9), intermediate monocytes are a phenotypical unique cell population with distinct tasks in the immune system (10,11): they were identified as major producers of reactive oxygen species and of proinflammatory cytokines (TNF α and IL1 β) in response to lipopolysaccharide, as highly proangiogenic cells and as cells with the highest capacity for antigen processing and presentation. In comparison, classical monocytes harbor the highest antimicrobial and phagocytic capacity, while nonclassical monocytes produce proinflammatory cytokines (TNF α , IL1 β , and CCL3) in response to viruses and nucleic acid containing immune complexes and patrol the endothelium of blood vessels (11,12). Moreover, in contrast to classical and nonclassical monocytes, intermediate monocytes were identified as independent predictors of cardiovascular outcome in several prospective cohort studies among patients with different stages of chronic kidney disease (CKD; (13–15)), and among patients undergoing coronary angiography (16).

Despite these essential advancements in monocyte nomenclature, the comparability of study results between different scientific groups is still limited. One major problem in

monocyte subset analyses is the delineation of intermediate from nonclassical monocytes. In general, two different gating strategies exist (17): the “rectangular gating (RG) strategy” and the “trapezoid gating (TG) strategy” (Fig. 1). Up to now no clinical data exist which compare both gating strategies.

A uniform definition for monocyte subset gating strategies is the basis for the initiation of large-scale multicenter studies on monocyte heterogeneity. To compare the two gating strategies, we now reanalyzed monocyte subsets among patients with CKD recruited in the large-scale prospective CARE FOR HOME study. Our data show that the two strategies give similar results with respect to prediction of cardiovascular outcome.

MATERIALS AND METHODS

Study Population

The present study is a reanalysis of the CARE FOR HOME (Cardiovascular and Renal Outcome in CKD 2–4 Patients - The Fourth Homburg evaluation) study. The ongoing CARE FOR HOME study recruits patients with CKD for identification of risk factors for CKD progression and cardiovascular complications in CKD. Short-term outcome data from CARE FOR HOME have been published before (15). The study was approved by the local Ethics Committee and all participants gave their written informed consent.

Patients were included in the CARE FOR HOME study if they had CKD GFR category G 2–G 4, which corresponds to an eGFR (estimated glomerular filtration rate) between 90 and 15 mL/min/1.73 m² according to the MDRD (Modification of Diet in Renal Disease) equation. Exclusion criteria were defined as concomitant human immunodeficiency virus infection, active cancer disease, malignant hematological disorders, acute renal failure (increase of plasma creatinine > 50% within four weeks), previous kidney transplantation, and age < 18 years. Furthermore, patients were excluded when they presented with systemic immunosuppressive medication, clinical apparent infections (with plasma CRP \geq 50 mg/l, and/or requiring systemic antibiotic therapy) and pregnancy.

History of cardiovascular comorbidity, smoking, diabetes mellitus, and current drug intake was assessed by a standardized questionnaire and by thorough chart review. Prevalent cardiovascular disease (CVD) was defined as previous myocardial infarction, coronary artery angioplasty/stenting/bypass grafting, major stroke, carotid endarterectomy/stenting, non-traumatic lower extremity amputation, or lower limb artery bypass surgery/angioplasty/stenting. Active smokers were defined as those individuals who were current smokers or had stopped smoking < 1 month before study enrolment. Prevalent diabetes mellitus was defined as self- or physician-reported diabetes mellitus, a fasting glucose > 126 mg/dL or intake of glucose-lowering medication. Body mass index was calculated as weight (kg)/[height (m)]².

Measurement of blood pressure was performed after five minutes of rest with an automated blood pressure recording apparatus (GE Carescope DINAMAP V100; GE Healthcare).

444 patients entered CARE FOR HOME between September 2008 and November 2012. Among these 444 patients, six patients had no baseline monocyte subset data (no total monocyte counts due to missing of differential hemogram), and reanalysis of monocyte subsets was not possible in 22 patients because data files could not be imported into the software for technical reasons. Thus, this analysis includes 416 patients with available differential hemograms and flow-cytometrical data (recorded monocyte count: 7000).

Laboratory Analyses

Blood samples were obtained under standardized conditions. Standard laboratory parameters were analyzed at the Central Laboratory of the Saarland University Medical Center. Estimated glomerular filtration rate at study enrolment was calculated using the MDRD 4 variable equation.

Leukocyte and monocyte counts were measured with automated cell counters using standard techniques. Monocyte subpopulations were analyzed by flow-cytometry in a whole-blood assay using 100 µl of whole blood according to our validated standard protocol (11). EDTA anticoagulated whole blood was stained with antibodies against CD86 (CD86-PE, HA5.2B7, Beckman-Coulter, Krefeld, Germany), CD14 (CD14-PerCP, MØP9, BD Biosciences, Heidelberg, Germany) and CD16 (CD16-PeCy7, 3G8, BD Biosciences) and analyzed flow-cytometrically using the FACS Canto II with FACSDiva Software Version 6.1.2 (BD Biosciences).

Monocytes were first gated in a SSC/CD86 dot plot, identifying monocytes as CD86+ cells, followed by a SSC/FSC dot plot to further gate cells with monocyte scatter properties (see Supporting Information Fig. S1 for monocyte gating). Next, in a CD14/CD16 dot plot, the three monocytes subsets were defined via the two different gating strategies: the “RG strategy” and the “TG strategy” (Fig. 1). For quantifying monocyte subset cell counts, we multiplied the relative percentage of each subset with the total monocyte numbers.

In addition, we aimed to phenotype those monocytes that are labeled intermediate monocytes by RG strategy and as nonclassical monocytes by TG strategy (defined as “indeterminate monocytes” hereafter) in a subgroup of 14

CARE FOR HOME participants. We measured expression of CCR2 (CD192), CCR5 (CD195), CX₃CR1, ACE (CD143), TLR2 (CD282), and TLR4 (CD284) on these indeterminate cells, as well as on those cells which are defined as intermediate monocytes and nonclassical monocytes by both gating strategies. Protein expression was quantified flow-cytometrically as median fluorescence intensity (MFI) and standardized against coated fluorescent particles (SPHEROTM; BD Biosciences). The following antibodies were used: CD192-Alexa Fluor® 647 (48607), CD195-APC (2D7/CCR5), and CD282-Alexa Fluor® 647 (11G7) from BD Biosciences, CX₃CR1-FITC (2A9-1) and CD143-FITC (9B9) from Biozol (Eching, Germany) and CD284-FITC (HTA125) from AMS Biotechnology (Abingdon, UK).

All flow-cytometry analyses were performed by technicians blinded to clinical baseline characteristics.

Outcome Analysis

All study participants were invited to our nephrological outpatient clinic for annual follow-up visits. Patients who were either unable or unwilling to follow this invitation, or who have reached end-stage renal disease during follow-up and became dialysis dependent, were contacted via telephone. In this case, medical records from the treating physicians were obtained to verify all events reported by study participants or their next of kin.

The composite cardiovascular end-point was defined as the first occurrence of an acute myocardial infarction, surgical or interventional coronary/cerebrovascular/peripheral-arterial revascularization, stroke with symptoms ≥ 24 h, amputation above the ankle and/or death of any cause. Two physicians blinded to monocyte data adjudicated all events. In the case of disagreement, a third physician made a final decision.

Patients not reaching an end point were censored at the time of the last annual follow-up visit (for patients who were contacted via telephone, at the time of the last examination by their treating physician). The present analysis is based upon follow-up data gathered until December 2014. Vital status was known for all patients at this time-point.

Statistics

Data management and statistical analysis were performed using SPSS Statistics 20 (SPSS, Inc., Chicago, IL) and GraphPad Prism4 (GraphPad, San Diego, CA). The level of significance was predefined as $P < 0.05$.

Categorical variables are presented as percentages of patients and compared using χ^2 or Fisher's exact tests, as appropriate. Continuous data are expressed as means ± standard deviation and compared using Student's *t* test (for two independent samples) or one-way analysis of variances (ANOVA) with Dunnett's post hoc test (for more than two independent samples). Median values [interquartile range] are given in case of skewed distributions.

Associations between continuous variables were tested using Pearson correlation testing. Comparison of correlation coefficients was performed with “Simple Stat Tests.”

Subjects were divided into 4 equally sized groups (quartiles) according to their levels of monocyte (subset) counts.

Kaplan-Meier survival curves were used to compare event-free survival (i.e., time until first occurrence of the cardiovascular endpoint) between groups. The Breslow test was used to test the hypothesis that at least one of the survival curves differs from the others. Cox proportional hazard models were calculated to analyze the relationship of monocyte (subset) cell counts with event-free survival after adjustment for age, gender, prevalent CVD, eGFR, HDL cholesterol, LDL cholesterol, mean blood pressure, C-reactive protein, and diabetes mellitus.

In order to compare the role of cell counts of intermediate monocytes, as defined by RG strategy and by TG strategy, respectively, for predicting three year cardiovascular outcome, we performed receiver operator characteristic (ROC) curve analyses among those patients who had complete information on three year event rate ($n = 353$).

Reclassification Analysis

To further compare the two gating strategies in the context of cardiovascular outcome prediction, we reclassified patients from quartiles of intermediate monocyte counts when applying the RG strategy to quartiles of intermediate monocyte counts when applying the TG strategy.

The net reclassification improvement for patients with events (NRI_{events}) was defined as the difference between the proportion of patients experiencing an event who moved to higher quartiles of intermediate monocyte counts with the TG strategy, and the proportion of patients experiencing an event who moved to lower quartiles of intermediate monocytes with the TG strategy (18). Similarly, the difference between the proportion of patients without an event who moved to lower quartiles of intermediate monocytes and the proportion of patients without an event who moved to higher quartiles of intermediate monocytes with the TG strategy was defined as $NRI_{non-events}$. The total net reclassification improvement (NRI_{total}) was calculated as $NRI_{events} + NRI_{non-events}$.

RESULTS

Patients' Characteristics

Monocyte subsets analysis based on the two different gating strategies was performed in 416 CARE FOR HOME participants. Patients were followed for the occurrence of a cardiovascular event (CVE) for a mean of 3.6 ± 1.6 years. The predefined CVE occurred in 106 patients (26%).

The baseline characteristics of the total cohort and of the cohort stratified by the subsequent occurrence of a CVE are depicted in Table 1. As expected, patients who suffered a CVE during follow-up were older and had lower eGFR; additionally, prevalent CVD and diabetes mellitus were more frequent in these patients.

Cross-Sectional Analysis

We first analyzed the association of monocyte subset counts with cardiovascular risk factors. Intermediate and nonclassical monocyte counts both correlated with higher age, lower mean blood pressure, higher CRP, and lower HDL cholesterol (Table 2 and Supporting Information Table S1). More-

over, male patients had higher cell counts of intermediate and nonclassical monocytes (Supporting Information Table S2). Intermediate monocyte counts correlated with kidney function, whereas nonclassical monocytes correlated with BMI as well as with hip and waist circumference (Table 2 and Supporting Information Table S1). No significant differences in correlation coefficients between monocyte subset cell counts and cardiovascular risk factors were observed when comparing both gating strategies.

Monocyte Subsets as Predictors of Cardiovascular Outcome

Patients who suffered a CVE had higher cell counts of total and classical as well as of intermediate and nonclassical monocytes with both gating strategies (RG and TG; Table 1).

We stratified the study cohort by cell counts of total monocytes and monocyte subsets—based on either gating strategy—into quartiles and performed univariate Kaplan-Meier survival analyses (Fig. 2 and Supporting Information Fig. S2). With both gating strategies, patients in higher quartiles of intermediate monocyte counts (RG: $P < 0.001$; TG: $P < 0.001$) had shorter event-free survival. By visual inspection, the survival curves seemingly separate to a slightly higher degree with the TG strategy, but the clinical relevance of such small differences is questionable at best. Quartiles of nonclassical monocytes by RG were not associated with event-free survival ($P = 0.113$) whereas quartiles of nonclassical monocytes by TG reached statistical significance ($P = 0.042$).

In multivariate Cox regression analysis, intermediate monocyte counts based on both gating strategies remained significantly associated with event-free survival after adjustment for age, gender, prevalent CVD, eGFR, diabetes mellitus, CRP, HDL-C, LDL-C and mean blood pressure (RG: HR = 1.013 [95% CI: 1.006–1.020; $P < 0.001$]; TG: HR = 1.015 [95% CI: 1.006–1.024; $P = 0.001$]). Nonclassical monocytes by both gating strategies were not independently associated with event-free survival (RG: HR = 1.003 [95% CI: 0.997–1.009; $P = 0.289$]; TG: HR = 1.004 [95% CI: 0.999–1.009; $P = 0.157$]). Cox regression analyses for monocyte subsets and for total monocytes are given in Supporting Information Table S3–S8.

Given that intermediate monocytes by both gating strategies were identified as independent predictors of CVE, we next compared the performance of intermediate monocytes based on RG and on TG strategy for CVE prediction in ROC curve analysis among those patients who had complete information on three year event rate ($n = 353$). Both, intermediate monocytes by RG and by TG, showed virtually identical AUC values (RG: AUC = 0.620 [0.548–0.693], $P = 0.001$; TG: AUC = 0.625 [0.554–0.695], $P = 0.001$; Fig. 3).

Finally, we performed reclassification analysis for intermediate monocytes based on RG and TG among the same 353 patients; 79 of these 353 patients reached the CVE within three years. Among those patients who suffered an event, three patients were reclassified to higher and two patients to lower quartiles of intermediate monocytes when applying the TG instead of the RG, yielding an NRI_{events} of 1.3%. Of the 274

Table 1. Patients' characteristics stratified by the subsequent occurrence of a cardiovascular event

	TOTAL COHORT (N = 416)	NO CVE (N = 310)	CVE (N = 106)	P
Gender (men)	248 (60%)	175 (57%)	73 (69%)	0.029
Prevalent CVD (yes)	129 (31%)	63 (20%)	66 (62%)	<0.001
Smoking (yes)	41 (10%)	29 (9%)	12 (11%)	0.338
Diabetes mellitus (yes)	161 (39%)	104 (34%)	57 (54%)	<0.001
Age (years)	65.1 ± 12.6	63.3 ± 13.0	70.5 ± 9.4	<0.001
BMI (kg/m ²)	30.2 ± 5.5	30.3 ± 5.5	29.8 ± 5.5	0.438
Systolic BP (mm Hg)	154 ± 25	154 ± 24	154 ± 27	0.908
Diastolic BP (mm Hg)	87 ± 13	88 ± 12	82 ± 13	<0.001
Mean BP (mm Hg)	109 ± 15	110 ± 14	106 ± 16	0.021
eGFR (ml/min/1.73 m ²)	45.2 ± 15.9	47.7 ± 15.6	37.7 ± 14.3	<0.001
K/DOQI stage 2 (%)	80 (19%)	71 (23%)	9 (9%)	<0.001
K/DOQI stage 3a (%)	140 (34%)	120 (39%)	20 (19%)	
K/DOQI stage 3b (%)	115 (28%)	72 (23%)	43 (41%)	
K/DOQI stage 4 (%)	81 (20%)	47 (15%)	34 (32%)	
UAE (mg/g creatinine)	36 (8 – 190)	27 (7 – 156)	71 (24 – 316)	0.125
Total cholesterol (mg/dl)	193 ± 43	198 ± 42	177 ± 41	<0.001
HDL cholesterol (mg/dl)	47 (39 – 61)	49 (41 – 63)	44 (36 – 55)	0.009
LDL cholesterol (mg/dl)	115 ± 36	118 ± 36	106 ± 33	<0.001
Triglycerides (mg/dl)	135 (97 – 192)	136 (97 – 207)	132 (96 – 164)	0.270
Apo A-I (mg/dl)	161 (142 – 184)	166 (146 – 188)	148 (134 – 167)	<0.001
hsCRP (mg/l)	2.7 (1.2 – 5.4)	2.4 (1.1 – 4.6)	4.1 (1.7 – 9.7)	0.001
Hemoglobin (g/dl)	13.4 ± 1.7	13.6 ± 1.6	13.0 ± 1.7	0.001
Leukocytes (cells/μl)	6874 ± 2005	6689 ± 2024	7414 ± 1856	0.001
Total monocytes (cells/μl)	562 ± 204	536 ± 193	638 ± 218	<0.001
Classical monocytes (cells/μl)	464 ± 175	444 ± 166	521 ± 186	<0.001
Intermediate RG monocytes (cells/μl)	35 ± 22	31 ± 17	45 ± 28	<0.001
Intermediate TG monocytes (cells/μl)	27 ± 17	24 ± 15	36 ± 21	<0.001
Nonclassical RG monocytes (cells/μl)	64 ± 32	61 ± 30	71 ± 38	0.014
Nonclassical TG monocytes (cells/μl)	70 ± 36	66 ± 32	79 ± 44	0.006

Values are mean ± SD, median (interquartile range), or *n* (%). Statistical analysis for the comparison of “No CVE” vs. “CVE” was performed with the Student's *t* test or Fisher's exact test, as appropriate. Significant *P* values are given in bold.

Apo A-I: apolipoprotein A-I; BMI: body mass index; BP: blood pressure; CVD: cardiovascular disease; CVE: cardiovascular event; eGFR: estimated glomerular filtration rate; HDL: high-density lipoprotein; hsCRP: high-sensitivity C-reactive protein; K/DOQI: kidney disease outcomes quality initiative; LDL: low-density lipoprotein; RG: rectangular gating; TG: trapezoid gating; UAE: urinary albumin excretion.

patients who did not experience an event, 20 patients moved to higher quartiles and 27 patients to lower quartiles of intermediate monocytes by TG (in line with the slightly better separation of the Kaplan Meier curves in Fig. 2), resulting in a $NRI_{\text{non-events}}$ of 2.6%. The NRI_{total} by TG is thus 3.9%.

Characterization of Surface Antigens

Finally, we analyzed whether those monocytes that are labeled as intermediate monocytes by RG, and at the same time as nonclassical monocytes by TG (“indeterminate monocytes”, see Fig. 4) rather resemble cells which are defined as intermediate monocytes by both gating strategies, or cells defined as nonclassical monocytes by both gating strategies. Therefore, we measured the expression of predefined surface proteins (CCR5, ACE, TLR2, TLR4, CCR2, and CX₃CR1) in a subgroup of 14 CARE FOR HOME participants. For markers, which are characteristically expressed by classical (CCR2) or nonclassical monocytes (CX₃CR1), respectively, indeterminate

monocytes showed an intermediate phenotype. Characteristic markers of intermediate monocytes (CCR5, ACE, TLR2, and TLR4) are highly expressed on these indeterminate monocytes. Interestingly, for CCR5 indeterminate monocytes showed the highest expression among monocyte subsets.

DISCUSSION

In this study, we compared in a well-defined clinical cohort the performance of two frequently applied gating strategies: the “RG strategy” vs. the “TG strategy.” By reanalyzing data from the CARE FOR HOME study, we found intermediate monocytes to be independent predictors of CVE among CKD patients irrespective of the applied gating strategy.

Monocyte heterogeneity has gained strong interest in the last decade, as distinct monocyte subsets have been implicated in the pathogenesis of CVD (19). Since the discovery of monocyte heterogeneity in 1989 (1) substantial work has been investigated in the characterization of monocyte subsets.

Table 2. Correlation coefficients of intermediate and nonclassical monocyte counts with cardiovascular risk factors

VARIABLE	INTERMEDIATE MONOCYTES					NONCLASSICAL MONOCYTES				
	RG		TG		RG VS. TG	RG		TG		RG VS. TG
	R	P	R	P		R	P	R	P	
Age	0.124	0.012	0.125	0.011	0.988	0.102	0.037	0.107	0.030	0.942
BMI	0.053	0.279	0.043	0.379	0.886	0.153	0.002	0.149	0.002	0.953
Hip circumference	0.001	0.980	−0.010	0.835	0.875	0.104	0.035	0.100	0.041	0.954
Waist circumference	0.009	0.860	−0.002	0.971	0.875	0.173	<0.001	0.162	0.001	0.871
Systolic BP	−0.082	0.095	−0.085	0.084	0.965	−0.065	0.189	−0.065	0.183	1.000
Diastolic BP	−0.144	0.003	−0.147	0.003	0.965	−0.109	0.026	−0.112	0.022	0.965
Mean BP	−0.129	0.009	−0.132	0.007	0.965	−0.099	0.045	−0.101	0.040	0.977
Creatinine	0.157	0.001	0.152	0.002	0.941	0.053	0.282	0.067	0.174	0.840
log UAE	0.097	0.049	0.102	0.038	0.942	0.000	0.993	0.008	0.876	0.909
eGFR	−0.147	0.003	−0.144	0.003	0.965	−0.044	0.373	−0.057	0.247	0.851
log hsCRP	0.257	<0.001	0.232	<0.001	0.703	0.223	<0.001	0.242	<0.001	0.773
Total cholesterol	−0.035	0.483	−0.040	0.420	0.943	−0.036	0.463	−0.033	0.503	0.966
LDL cholesterol	0.025	0.618	0.019	0.693	0.931	−0.010	0.842	−0.002	0.960	0.909
HDL cholesterol	−0.155	0.002	−0.155	0.002	1.000	−0.125	0.011	−0.130	0.008	0.942
Triglycerides	0.018	0.710	0.016	0.747	0.977	0.032	0.510	0.032	0.512	1.000
Leukocytes	0.323	<0.001	0.319	<0.001	0.949	0.304	<0.001	0.307	<0.001	0.962

Correlation analysis was performed with the Pearson test. Comparison of correlation coefficients was done with “Simple Stat Tests”. Significant correlations are given in bold.

BMI: body mass index; BP: blood pressure; eGFR: estimated glomerular filtration rate; HDL: high-density lipoprotein; hsCRP: high-sensitivity C-reactive protein; LDL: low-density lipoprotein; RG: rectangular gating; TG: trapezoid gating; UAE: urinary albumin excretion.

However, it was not until 2010 when an official nomenclature for circulating monocytes was published, acknowledging the existence of the three different monocyte subsets (8). Up to then, most studies on monocyte heterogeneity exclusively focused on classical and nonclassical monocytes, thereby either ignoring intermediate monocytes or lumping them together with classical or nonclassical monocytes. This hindered an earlier definite characterization of intermediate monocytes, which were only recently acknowledged as a separate cell population harboring a unique proinflammatory potential (6,11,12). At the same time, clinical studies demonstrated that patients with high counts of intermediate monocytes have an increased risk to suffer CVE (13–16). Congruously, immunomodulation of a distinct monocyte

subset is currently discussed as a promising therapeutic option in atherosclerosis (20).

Until now, most clinical data on monocyte heterogeneity come from single-center studies and multi-center studies are impeded by the absence of standardized procedures for monocyte subset analyses. Such protocols will be considered as mandatory prerequisites at the latest when intermediate monocytes become targets for novel cardiovascular treatment strategies.

However, even today, the lack of standardization of monocyte subset analyses may account for seemingly contradictory study results on monocyte heterogeneity between different laboratories (16,21). Presently, monocyte analysis deals with at least two major challenges: first, the correct identification of total monocytes in the FSC/SSC dot plot and second,

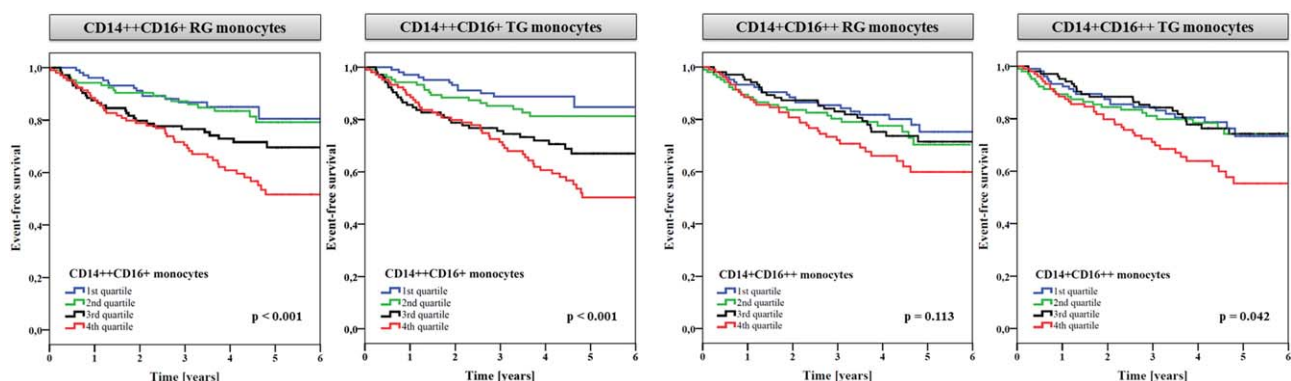


Figure 2. Kaplan-Meier survival curves. Relationship between quartiles of intermediate and nonclassical monocytes by both gating strategies and event-free survival in 416 CKD patients (Kaplan-Meier analysis with Breslow test). [Color figure can be viewed in the online issue which is available at wileyonlinelibrary.com]

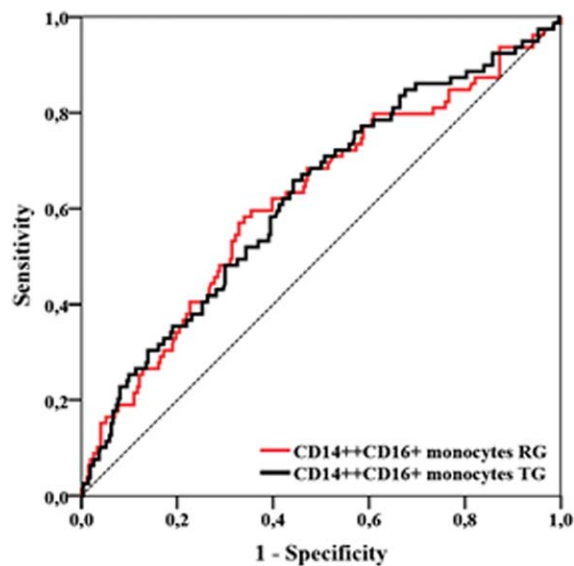


Figure 3. ROC curve analysis for intermediate monocytes by both gating strategies. ROC curve analysis was performed with those CKD patients who had information on three year event rate ($n = 353$). [Color figure can be viewed in the online issue which is available at wileyonlinelibrary.com]

the standardized delineation of the three monocyte subsets in the CD14/CD16 dot plot.

First, complete and specific identification of monocytes in the FSC/SSC dot plot is fundamental for precise monocyte enumeration [reviewed in (4)], which requires the application of a pan-monocytic marker for the correct delineation of monocytes from other leukocytes. Two different pan-monocytic markers are established for monocyte subset analysis, CD86 and HLA-DR, which both yield identical results (11,22). Moreover, only recently a novel strategy for monocyte gating has been suggested which uses LRP1 (low-density lipoprotein receptor-related protein 1; CD91) and which has been validated against the HLA-DR-based gating strategy (23). Monocyte subset analysis without a pan-monocytic marker can result in inaccurate cell counts particularly of nonclassical monocytes, as they may overlap with lymphocytes. In this study, we applied the CD86-based gating strategy for the identification of total monocytes.

Second, the gating of monocyte subsets in the CD14/CD16 dot plot has not been standardized before and thus virtually each scientific group has its own strategy to draw the gates for classical, intermediate, and nonclassical monocytes. The delineation between classical and intermediate monocytes can be achieved in a straightforward way by using an isotype control (17). In contrast, the delineation of intermediate and nonclassical monocytes is more arbitrary, and two different strategies have been proposed: the RG strategy, in which a horizontal line is drawn as an extension of the gate of classical monocytes, and the TG strategy, in which an oblique line for delineating intermediate from nonclassical monocytes is drawn. The latter inevitably labels more cells as nonclassical monocytes than the former.

When applying either gating strategy among CARE FOR HOME patients, we found similar associations of intermediate monocyte counts with cardiovascular risk factors in cross-

sectional analyses, and with adverse cardiovascular outcome in longitudinal analyses, which points toward robustness of this biomarker. In contrast, different results were observed for nonclassical monocytes in univariate (albeit not in multivariate) analyses, as nonclassical monocytes were predictors of CVE by TG, but not by RG. This results from the designation of indeterminate monocytes as nonclassical monocytes with the TG (but not with RG) strategy. Compared with cells, which are defined as nonclassical monocytes by both gating strategies, these indeterminate cells have a higher expression of chemokine receptors and may be considered more proinflammatory monocytes.

The three monocyte subsets display a unique molecular fingerprint (11,12,24). Genome-wide gene expression analyses identified subset-specific markers and characterized intermediate monocytes as proinflammatory mediators of immune response (11,12,24). Notably, all three studies on genome-wide characterization isolated monocyte subsets in accordance with the RG strategy.

In this study, we now tested predefined markers in different regions of monocyte subsets. By analyzing the expression of CCR5, ACE, TLR2, TLR4, CCR2, and CX₃CR1, proteins, which are centrally involved in inflammation and/or atherogenesis, we found that indeterminate monocytes have a specific expression pattern, which comprises characteristic markers of both CD16⁺ monocyte subsets. Notably, indeterminate monocytes showed the highest expression of CCR5, which has been associated with atherosclerosis in animal studies and which is considered a potential therapeutic option for patients at high cardiovascular risk (25). Admittedly, this unique expression pattern of surface protein on indeterminate monocytes suggests that any labeling of these cells as either intermediate or nonclassical monocytes is at least partly arbitrary, and that these cells should be considered to be in transition between intermediate and nonclassical monocytes (9). However, it is beyond the scope of the present manuscript to propose a novel classification of monocyte subsets with four or even more subsets. Instead, we are positive that the introduction of the consensus nomenclature in 2010 (8) was a substantial step forward for allowing better comparison of monocyte heterogeneity analyses between different research groups.

Further studies are needed in order to identify markers, which allow a definite delineation of intermediate and nonclassical monocytes. A first strategy has been proposed based on CCR2, which however has not been compared with other gating strategies (26). Thus, additional studies on the identification of markers for the delineation of intermediate and nonclassical monocytes are eagerly awaited.

For the time being, we propose to use the RG strategy for monocyte subset analyses due to several reasons. First, substitution of the TG strategy for the RG strategy will yield no substantial gain in outcome prediction. Second, most clinical studies applied the RG strategy and the comparability of future study results will be facilitated when the same gating strategy will be applied. Third, established protocols for isolation of monocyte subsets (i.e., intermediate and nonclassical monocytes) with magnetic beads or cell sorters yield cell populations, which are identical to monocyte

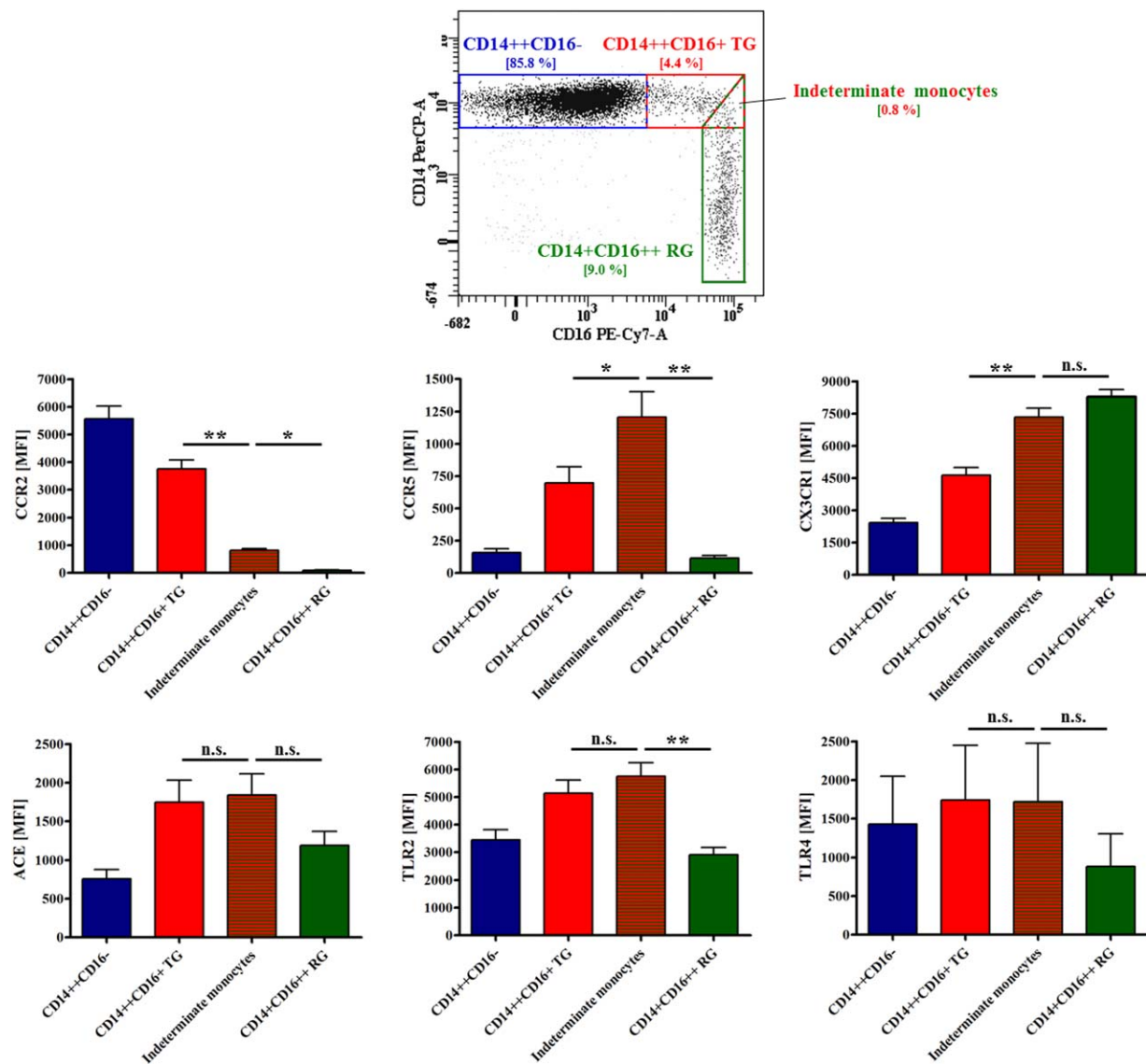


Figure 4. Protein expression analysis on monocyte subsets. Those monocytes that are labeled intermediate monocytes by RG and nonclassical monocytes by TG are denoted indeterminate monocytes. Expression of CCR2, CCR5, CX₃CR1, ACE, TLR2, and TLR4 was measured on classical monocytes (CD14++CD16-), intermediate monocytes by TG (CD14++CD16+ TG), indeterminate monocytes and nonclassical monocytes by RG (CD14+CD16++ RG) in 14 patients with CKD. Flow-cytometrical data were measured as median fluorescence intensity (MFI) and presented as means \pm SEM. Statistical analysis was performed with one-way ANOVA with Dunnett's post hoc test for the comparison of CD14++CD16+ TG, indeterminate and CD14+CD16++ RG monocytes. [Color figure can be viewed in the online issue which is available at wileyonlinelibrary.com]

subsets defined with RG strategy. Therefore, application RG rather than TG strategy will allow better comparison between experimental and clinical data. Comparison of future studies in isolated monocyte subsets will thus be facilitated when a RG strategy is applied. This is of particular importance as these isolation protocols have also been applied in recent genome-wide gene expression analyses, which have substantially sharpened our understanding of subset-specific monocyte biology in men. Forth, surface proteins which are characteristic of intermediate monocytes and which are implicated in CVD are highly expressed on indeterminate monocytes. Fifth, the RG strategy allows a more specific

delineation of those monocytes that are associated with future cardiovascular outcome—intermediate monocytes—from other monocytes with no implications for adverse cardiovascular outcome—nonclassical monocytes.

In summary, the RG strategy for monocyte subset analysis should be preferred over the TG strategy, until novel markers will hopefully allow a more straightforward delineation of intermediate and nonclassical monocytes.

ACKNOWLEDGMENTS

The authors thank Martina Wagner and Marie-Theres Blinn for their excellent technical assistance.

LITERATURE CITED

1. Passlick B, Flieger D, Ziegler-Heitbrock HW. Identification and characterization of a novel monocyte subpopulation in human peripheral blood. *Blood* 1989;74:2527–2534.
2. Belge kU, Dayyani F, Horelt A, Siedlar M, Frankenberger M, Frankenberger B, Espevik T, Ziegler-Heitbrock L. The proinflammatory cd14+cd16+DR++ monocytes are a major source of TNE. *J Immunol* 2002;168:3536–3542.
3. Szaflarska A, Baj-Krzyworzeka M, Siedlar M, Weglarczyk K, Ruggiero I, Hajto B, Zembala M. Antitumor response of cd14+/cd16+ monocyte subpopulation. *Exp Hematol* 2004;32:748–755.
4. Zawada AM, Rogacev KS, Schirmer SH, Sester M, Bohm M, Fliser D, Heine GH. Monocyte heterogeneity in human cardiovascular disease. *Immunobiology* 2012; 217:1273–1284.
5. Ziegler-Heitbrock L. The cd14+ cd16+ blood monocytes: their role in infection and inflammation. *J Leukoc Biol* 2007;81:584–592.
6. Ancuta P, Rao R, Moses A, Mehle A, Shaw SK, Luscinskas FW, Gabuzda D. Fractalkine preferentially mediates arrest and migration of cd16+ monocytes. *J Exp Med* 2003;197:1701–1707.
7. Grage-Griebenow E, Zawatzky R, Kahlert H, Brade L, Flad H, Ernst M. Identification of a novel dendritic cell-like subset of cd64(+)/cd16(+) blood monocytes. *Eur J Immunol* 2001;31:48–56.
8. Ziegler-Heitbrock L, Ancuta P, Crowe S, Dalod M, Grau V, Hart DN, Leenen PJ, Liu YJ, MacPherson G, Randolph GJ, et al. Nomenclature of monocytes and dendritic cells in blood. *Blood* 2010;116:e74–e80.
9. Rogacev KS, Zawada AM, Hundsdorfer J, Achenbach M, Held G, Fliser D, Heine GH. Immunosuppression and monocyte subsets. *Nephrol Dial Transplant* 2015;30: 143–153.
10. Qu C, Edwards EW, Tacke F, Angeli V, Llodra J, Sanchez-Schmitz G, Garin A, Haque NS, Peters W, van Rooijen N, et al. Role of CCR8 and other chemokine pathways in the migration of monocyte-derived dendritic cells to lymph nodes. *J Exp Med* 2004; 200:1231–1241.
11. Zawada AM, Rogacev KS, Rotter B, Winter P, Marell RR, Fliser D, Heine GH. SuperSAGE evidence for cd14++cd16+ monocytes as a third monocyte subset. *Blood* 2011;118:e50–e61.
12. Cros J, Cagnard N, Woollard K, Patey N, Zhang SY, Senechal B, Puel A, Biswas SK, Moshous D, Picard C, et al. Human CD14dim monocytes patrol and sense nucleic acids and viruses via TLR7 and TLR8 receptors. *Immunity* 2010;33:375–386.
13. Heine GH, Ulrich C, Seibert E, Seiler S, Marell J, Reichart B, Krause M, Schlitt A, Kohler H, Girndt M. Cd14(++)cd16+ monocytes but not total monocyte numbers predict cardiovascular events in dialysis patients. *Kidney Int* 2008;73:622–629.
14. Rogacev KS, Seiler S, Zawada AM, Reichart B, Herath E, Roth D, Ulrich C, Fliser D, Heine GH. Cd14++cd16+ monocytes and cardiovascular outcome in patients with chronic kidney disease. *Eur Heart J* 2011;32:84–92.
15. Rogacev KS, Zawada AM, Emrich I, Seiler S, Bohm M, Fliser D, Woollard KJ, Heine GH. Lower apo a-I and lower HDL-C levels are associated with higher intermediate cd14++cd16+ monocyte counts that predict cardiovascular events in chronic kidney disease. *Arterioscler Thromb Vasc Biol* 2014;34:2120–2127.
16. Rogacev KS, Cremers B, Zawada AM, Seiler S, Binder N, Ege P, Grosse-Dunker G, Heisel I, Hornof F, Jeken J, et al. CD14++CD16+ monocytes independently predict cardiovascular events: A cohort study of 951 patients referred for elective coronary angiography. *J Am Coll Cardiol* 2012;60:1512–1520.
17. Ziegler-Heitbrock L, Hofer TP. Toward a refined definition of monocyte subsets. *Front Immunol* 2013;4:23.
18. Pencina MJ, D'Agostino RB Sr., D'Agostino RB Jr., Vasan RS. Evaluating the added predictive ability of a new marker: From area under the ROC curve to reclassification and beyond. *Stat Med* 2008;27:157–172.
19. Ghattas A, Griffiths HR, Devitt A, Lip GY, Shantsila E. Monocytes in coronary artery disease and atherosclerosis: Where are we now?. *J Am Coll Cardiol* 2013;62:1541–1551.
20. Hristov M, Weber C. Differential role of monocyte subsets in atherosclerosis. *Thromb Haemost* 2011;106:757–762.
21. Berg KE, Ljungcrantz I, Andersson L, Bryngelsson C, Hedblad B, Fredrikson GN Nilsson J, Bjorkbacka H. Elevated cd14++cd16- monocytes predict cardiovascular events. *Circ Cardiovasc Genet* 2012;5:122–131.
22. Heimbeck I, Hofer TP, Eder C, Wright AK, Frankenberger M, Marei A, Boghdadi G, Scherberich J, Ziegler-Heitbrock L. Standardized single-platform assay for human monocyte subpopulations: Lower cd14+cd16++ monocytes in females. *Cytometry Part A* 2010;77A:823–830.
23. Ferrer DG, Jaldin-Fincati JR, Amigone JL, Capra RH, Collino CJ, Albertini RA, Chiabrando GA. Standardized flow cytometry assay for identification of human monocytic heterogeneity and lrp1 expression in monocyte subpopulations: decreased expression of this receptor in nonclassical monocytes. *Cytometry Part A* 2014;85A:601–610.
24. Wong KL, Tai JJ, Wong WC, Han H, Sem X, Yeap WH, Kourilsky P, Wong SC. Gene expression profiling reveals the defining features of the classical, intermediate, and nonclassical human monocyte subsets. *Blood* 2011;118:e16–31.
25. Combadière C1, Potteaux S, Rodero M, Simon T, Pezard A, Esposito B, Merval R, Proudfoot A, Tedgui A, Mallat Z. Combined inhibition of CCL2, CX3CR1, and CCR5 abrogates Ly6C(hi) and Ly6C(lo) monocytoysis and almost abolishes atherosclerosis in hypercholesterolemic mice. *Circulation* 2008;117:1649–1657.
26. Wrigley BJ, Shantsila E, Tapp LD, Lip GY. Cd14++cd16+ monocytes in patients with acute ischaemic heart failure. *Eur J Clin Invest* 2013;43:121–130.

Beitrag der Mitautoren für die Arbeit:

Sarah Seiler*, Gaetano Lucisano*, Philipp Ege, Lisa H. Fell, Kyrill S. Rogacev, Anne Lerner-Gräber, Matthias Klingele, Matthias Ziegler, Danilo Fliser, Gunnar H. Heine (2013) Single FGF-23 Measurement and Time-Averaged Plasma Phosphate Levels in Hemodialysis Patients. Clin J Am Soc Nephrol 8(10):1764-72. (*geteilte Erstautorenschaft)

Diese Studie wurde von Frau PD Dr. Sarah Seiler und Herrn Dr. Gaetano Lucisano in Zusammenarbeit mit Herrn Prof. Dr. Danilo Fliser und Herrn Prof. Dr. Gunnar Heine entworfen und geplant. Die Daten wurden durch Frau PD Dr. Sarah Seiler, Herrn Dr. Gaetano Lucisano, Herrn Dr. Philipp Ege, Frau Lisa Fell sowie durch Frau Dr. Anne Lerner-Gräber, und Herrn Dr. Matthias Klingele erhoben und von Frau PD Dr. Sarah Seiler, Herrn Dr. Gaetano Lucisano, Frau Lisa Fell sowie Herrn Prof. Dr. Matthias Ziegler und Herrn Prof. Dr. Gunnar Heine ausgewertet. Das Manuskript wurde von Frau PD Dr. Sarah Seiler, Herrn Dr. Gaetano Lucisano und von Herrn Prof. Dr. Gunnar Heine geschrieben.

Die oben aufgeführten Autoren haben die finale Version des Manuskripts gelesen, kritisch überarbeitet und ihr zugestimmt.

Single FGF-23 Measurement and Time-Averaged Plasma Phosphate Levels in Hemodialysis Patients

Sarah Seiler,* Gaetano Lucisano,* Philipp Ege,* Lisa H. Fell,* Kyrill S. Rogacev,* Anne Lerner-Gräber,* Matthias Klingele,* Matthias Ziegler,[†] Danilo Fliser,* and Gunnar H. Heine*

Summary

Background and objectives Plasma phosphate levels display considerable intraindividual variability. The phosphatonin fibroblast growth factor 23 is a central regulator of plasma phosphate levels, and it has been postulated to be a more stable marker than conventional CKD–mineral and bone disorder parameters. Thus, fibroblast growth factor 23 has been hypothesized to reflect time-averaged plasma phosphate levels in CKD patients.

Design, setting, participants, & measurements Among 40 patients from the outpatient dialysis center, serial measurements of plasma calcium and phosphate (before every dialysis session) as well as C-terminal fibroblast growth factor 23, parathyroid hormone, and alkaline phosphatase (one time weekly) were performed over a study period of 4 weeks in November and December of 2011. Intraindividual variability of repeated plasma fibroblast growth factor 23 measurements compared with other CKD–mineral and bone disorder markers was tested, and the association of a single plasma fibroblast growth factor 23 measurement with time-averaged plasma phosphate levels was analyzed.

Results Against expectations, intraindividual variability of fibroblast growth factor 23 (median coefficient of variation=27%; interquartile range=20–35) was not lower than variability of plasma phosphate (median coefficient of variation=15%; interquartile range=10–20), parathyroid hormone (median coefficient of variation=24%; interquartile range=15–39), plasma calcium (median coefficient of variation=3%; interquartile range=2–4), or alkaline phosphatase (median coefficient of variation=5%; interquartile range=3–10). Moreover, the correlation between the last fibroblast growth factor 23 measurement after 4 weeks and time-averaged plasma phosphate did not surpass the correlation between the last fibroblast growth factor 23 measurement and a single plasma phosphate value ($r=0.67$, $P<0.001$; $r=0.76$, $P<0.001$, respectively).

Conclusions Surprisingly, fibroblast growth factor 23 was not more closely associated to time-averaged plasma phosphate levels than a single plasma phosphate value, and it did not show a lower intraindividual variability than other tested markers of CKD–mineral and bone disorder. Thus, fibroblast growth factor 23 should not be used in clinical practice as a reflector of time-averaged plasma phosphate levels.

Clin J Am Soc Nephrol 8: 1764–1772, 2013. doi: 10.2215/CJN.13021212

Introduction

Elevated phosphate burden is considered to be an important driver of excess cardiovascular morbidity and mortality in CKD (1). Evidence from epidemiologic studies associated hyperphosphatemia with adverse outcome in dialysis (CKD 5D) patients (2–5), and experimental data revealed pathophysiological pathways for phosphate-induced vascular calcification (6). Subsequently, hyperphosphatemia has been acknowledged as a central therapeutic target in CKD, and recent Kidney Disease Improving Global Outcomes (KDIGO) guidelines on CKD–mineral and bone disorder (CKD-MBD) recommended prescription of oral phosphate binders to patients with elevated plasma phosphate, aiming to lower plasma phosphate to physiologic levels (7).

Of note, large intraindividual variability in plasma phosphate levels exists in hemodialysis patients:

plasma phosphate levels follow a circadian rhythm (8), and high biologic variability persists even when drawing blood samples at the same time of day in CKD 5D patients (9).

Therefore, a single monthly plasma phosphate measurement (as suggested by current KDIGO guidelines) may be suboptimal for assessing time-averaged plasma phosphate levels in individual dialysis patients, and a more reliable marker is eagerly awaited.

Fibroblast growth factor 23 (FGF-23) is a central regulator of plasma phosphate levels. FGF-23 is secreted from osteoblasts and osteocytes on stimulation by calcitriol (10), parathyroid hormone (11), and (yet incompletely identified) other mechanisms. FGF-23 increases urinary phosphate excretion by reducing expression of sodium phosphate cotransporters in the proximal tubules (12) and lowers circulating calcitriol

*Department for Internal Medicine IV —Nephrology and Hypertension, Saarland University Medical Center, Homburg, Germany; and [†]Psychological Institute, Humboldt-Universität zu Berlin, Berlin, Germany

Correspondence: Dr. Gunnar H. Heine, Department of Internal Medicine IV —Nephrology and Hypertension, Saarland University Medical Center, Homburg, Germany. Email: Gunnar.Heine@uks.eu

levels by decreasing renal expression of 1α hydroxylase, thus decreasing intestinal phosphate absorption (13,14).

Because of the central role of FGF-23 in keeping phosphate levels within physiologic boundaries, FGF-23 has been hypothesized to serve as a marker for time-averaged plasma phosphate levels (15), although no study has ever proven this idea.

Against this background, we initiated our Dialysis in Homburg evaluation (DIAL HOME) study and measured CKD-MBD parameters repeatedly over a period of 28 days. Our aim was twofold: first, compare intraindividual variability of distinct parameters of CKD-MBD and second, analyze whether a single FGF-23 measurement drawn at the end of this study period (day 28) adequately reflects averaged plasma phosphate levels during the preceding 4 weeks.

Materials and Methods

The DIAL HOME study was conducted over a 4-week period between November 28, 2011 and December 24, 2011. The local ethics committee approved the study design, and all participants gave their written informed consent before beginning of the study. The authors adhered to the Declaration of Helsinki.

We included CKD 5D patients who underwent three times weekly hemodialysis treatment at our outpatient dialysis center (Saarland University Medical Center, Homburg, Germany) if they had 3 months or more of dialysis vintage. Patients who were hospitalized and/or suffered from acute systemic infection at the time point of study initiation were excluded.

Forty-two adult hemodialysis patients met the inclusion criteria and gave their informed consent. One patient died during the study period, and another one patient withdrew his informed consent 1 week after beginning of the study. Thus, 40 participants completed the study, and their main baseline characteristics are shown in Table 1.

No modifications in any therapeutic factors affecting calcium-phosphate homeostasis during the 4-week study phase (namely dialysate calcium content, prescription of oral phosphate binders, active vitamin D, cholecalciferol, and calcimimetics) were allowed unless vitally indicated. Moreover, no changes in iron substitution, hemodialysis dose and/or frequency, anticoagulation, type, and surface of the dialyzer membrane, and dialysate flow rate were allowed throughout the study period.

The 4-week study comprised a total of 12 consecutive dialysis sessions; plasma samples were obtained from arteriovenous fistula needles or central venous catheters for dialysis immediately before each dialysis session. We measured predialysis plasma phosphate and calcium at each dialysis session. Plasma levels of C-terminal FGF-23, parathyroid hormone (PTH), and alkaline phosphatase (AP) were quantified one time weekly before each week's third dialysis session. Finally, we assessed 25-OH-vitamin D levels 6 weeks before study initiation and 1 week after study finalization, and these two values were averaged to yield an individual's 25-OH-vitamin D level.

Plasma samples were processed within 15 minutes, with the samples being centrifuged at 4,000 rpm for 5 minutes at room temperature. Supernatants were stored in aliquots

Table 1. Baseline characteristics of Dialysis in Homburg evaluation (DIAL HOME) study participants

Variable	Value
Calcium (mg/dl)	9.2 \pm 0.8
Phosphate (mg/dl)	5.2 \pm 1.7
Alkaline phosphatase (U/ml)	93.7 \pm 50.4
Parathyroid hormone (pg/ml)	127 (66–267)
C-terminal FGF-23 (rU/ml)	2785 (1386–9715)
25-OH-vitamin D (ng/ml)	32.0 \pm 10.1
Glucose (mg/dl)	128.7 \pm 44.9
Plasma protein (g/L)	70.0 \pm 5.1
Hemoglobin (g/dl)	11.3 \pm 1.5
Ferritin (ng/ml)	557 (346–744)
C-reactive protein (mg/L)	4.4 (2.2–13.4)
Systolic BP (mmHg)	137 \pm 25
Diastolic BP (mmHg)	70 \pm 13
Body mass index (kg/m ²)	28.4 \pm 6.2
Coronary artery disease (%)	14 (35)
Cerebrovascular disease (%)	8 (20)
Diabetes mellitus (%)	20 (50)
Active smoking (%)	6 (15)
Iron supplements (%)	21 (53)
Phosphate binder intake (%)	33 (83)
Cinacalcet intake (%)	6 (15)
Active vitamin D intake (%)	24 (60)
Self-reported diuresis >500 ml/24 h (%)	24 (60)

Continuous data are shown as mean \pm SD or median (interquartile range) as appropriate; categorical variables are depicted as number of patients (percentage). FGF-23, fibroblast growth factor 23.

at -80°C until further use. C-terminal FGF-23 levels were determined by ELISA (low cutoff value=1.5 rU/ml, high cutoff value=1500 rU/ml [samples with FGF-23>1500 rU/ml were measured after dilution]; Immotopics, San Clemente, CA). Levels of AP, calcium, and phosphate were determined by standard laboratory methods. PTH levels were measured by a second generation electrochemiluminescent immunoassay (normal range=15–65 pg/ml; Hoffmann-La Roche, Bale, Switzerland).

To minimize the influence of diurnal variation, time of blood collection was standardized for individual study participants, and patients were asked not to switch from morning to afternoon dialysis sessions or *vice versa* (in fact, only one patient temporarily changed from morning to afternoon dialysis sessions for logistic reasons).

After completion of the DIAL HOME study period, we additionally aimed to assess variation of FGF-23 levels during a single week. Therefore, we recruited 11 of the original 40 DIAL HOME participants in March of 2013, and we measured C-terminal FGF-23 before each of the three dialysis sessions (*e.g.*, Monday, Wednesday, and Friday or Tuesday, Thursday, and Saturday as appropriate).

History of smoking, current drug intake, and cardiovascular comorbidity were assessed by standardized questionnaires and verified by chart review. Cardiovascular

risk factors and comorbidity were defined as described previously (16,17). Echocardiography data on systolic left ventricular function were available in all patients.

Liver disease was defined by elevated liver enzymes (alanine/aspartate aminotransferase ≥ 100 U/L), laboratory cholestasis (direct bilirubin ≥ 1.0 mg/dL), prevalent chronic hepatitis B/ C, and/or histologic evidence of liver damage. Body weight and resting BP were recorded before and after each hemodialysis session.

In addition, we assessed information on food composition in 35 of 40 study participants by interview during the study period. Daily caloric and phosphate intakes were estimated using the German Bundeslebensmittelschlüssel provided by the Max-Rubner-Institute, Karlsruhe, Germany (www.mri.bund.de), which provides detailed information on nutritional compositions of a wide range of German foods.

Statistical analyses were performed with PASW Statistics 18, and the level of significance was set at P value < 0.05 . Categorical variables are presented as percentage of patients and compared by chi-squared test. Continuous data are expressed as mean \pm SD or median (interquartile range [IQR]) as appropriate based on distribution properties and were compared by Mann-Whitney test, t test, or ANOVA for trend.

To evaluate the intraindividual stability of FGF-23, calcium, phosphate, AP, and PTH, we calculated percentage coefficients of variation (CVs; SD divided by the mean $\times 100$) (10) from the four measurements taken at the last dialysis day of each week.

Correlation coefficients between continuous variables were calculated according to Pearson.

Results

Population Characteristics

Forty patients, of whom 16 (40%) patients were women, completed the 4-week study period. Mean age of our patients was 69 ± 14 years, and mean dialysis vintage was 3.1 (IQR=1.7–6.1) years. Two patients had undergone parathyroidectomy before study initiation. All participants underwent dialysis three times per week. Mean dialysis session length was 246 ± 26 minutes; 30 patients were treated in

the morning shift, and 10 patients were treated in the afternoon shift.

Mean daily phosphate intake was 2362 ± 1292 mg, and mean daily caloric intake was 1438 ± 525 kcal; phosphate intake was strongly correlated with caloric intake ($r=0.87$, $P<0.001$) but not mean plasma phosphate levels ($r=0.15$, $P=0.40$). Of note, there was no correlation between FGF-23 at week 4 and daily oral phosphate intake ($r=0.21$, $P=0.23$).

Comedication targeting CKD-MBD parameters comprised active vitamin D (24 patients), cinacalcet (6 patients), and various classes of phosphate binders (lanthanum carbonate [18 patients], calcium acetate [16 patients], sevelamer [15 patients], aluminum hydroxide [2 patients], and magnesium carbonate [2 patients]), and no changes in this medication occurred during the study period. Other main baseline characteristics are shown in Table 1.

Dialysis filter and dialysis dose were kept constant during the study period for all patients, with the exception of a single patient, in whom session time was reduced from 5 to 4 hours in the last 2 study weeks. Dialysate calcium concentration was kept stable at 3.0 mEq/L throughout the study period in all but one patient.

Intraindividual Variability of Calcium-Phosphate Metabolism Markers

Baseline measurements of CKD-MBD parameters are depicted in Table 1. During the 4-week study period, we observed infradian rhythms in plasma phosphate levels, with peak values before the first dialysis session of each week, followed by a progressive decrease before the second and third sessions of each week (Figure 1).

In contrast, no infradian rhythms were observed in C-terminal FGF-23 levels among a subgroup of 11 study participants recruited after our original DIAL HOME study period (Supplemental Figure 1).

For evaluating the stability of CKD-MBD parameters during the 4-week study period, we first examined the intraindividual median and range of variation for plasma phosphate, calcium, PTH, and FGF-23 measured at the end of the first, second, third, and fourth study weeks (Figure 2; patients rank ordered by individual participants' mean and FGF-23 depicted on both linear [Figure 2E] and

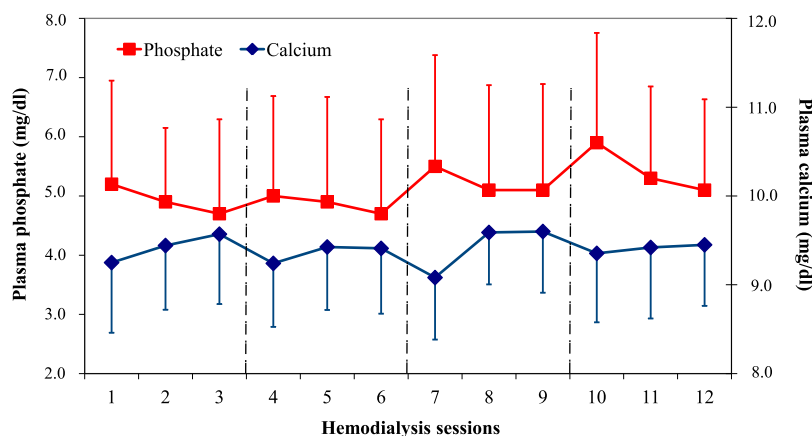


Figure 1. | Plasma phosphate and calcium levels throughout the study period. Note that measurements 1, 4, 7, and 10 refer to the first measurements of each week; the 4 study weeks are separated by dashed lines. Phosphate and calcium levels are depicted as means and SDs.

logarithmic scales [Figure 2F]). By visual inspection, the overall range of intraindividual variation seems less pronounced for FGF-23 compared with PTH and phosphate. Nonetheless, when calculating the CV for each CKD-MBD parameter from the same four measurements, FGF-23 (median CV=27% [IQR=20–35]) and PTH (median CV=24% [IQR=15–39]) showed the highest CV values followed by phosphate (median CV=15% [IQR=10–20]), AP (median CV=5% [IQR=3–10]), and calcium (median CV=3% [IQR=2–4]) (Figure 3). If log-transferred FGF-23

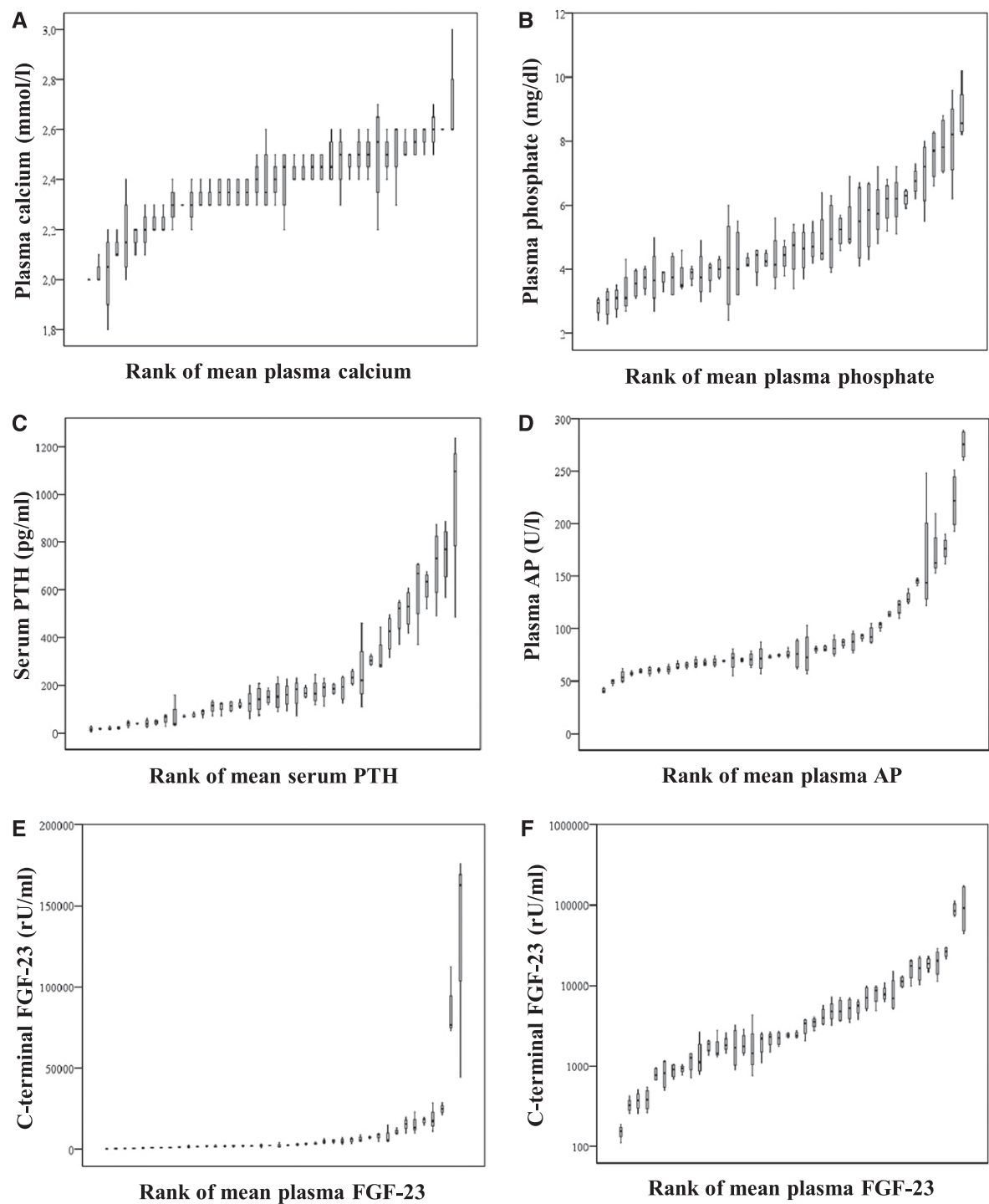


Figure 2. | Range of variation in CKD-MBD parameters. Depicted are medians, interquartile ranges, and minimum and maximum blood values of (A) calcium, (B) phosphate, (C) parathyroid hormone, (D) alkaline phosphatase, (E) C-terminal FGF-23 on a linear scale, and (F) C-terminal FGF-23 on a logarithmic scale. Values for each individual patient are plotted in rank order of their individual means. AP, alkaline phosphatase; CKD-MBD, CKD–mineral and bone disorder; FGF-23, fibroblast growth factor 23; PTH, parathyroid hormone.

levels were used for calculating CV, then FGF-23 becomes a seemingly more stable CKD-MBD parameter than plasma phosphate (median CV=4% [IQR=3–5]).

Of note, calculating CVs from all 12 phosphate measurements (*e.g.*, on different days of the weeks; CV=14% [IQR=11–18]) or the first dialysis day of each week (*e.g.*, Monday or Tuesday; CV=13% [IQR=8–19]) rather than from four measurements on Fridays or Saturdays, respectively, yielded virtually identical findings.

Correlations between a Single FGF-23 Measurement and Plasma Phosphate Levels

To further analyze how far a single FGF-23 measurement reliably indicates average plasma phosphate levels within the preceding weeks, we compared the correlation of the FGF-23 levels at study end with either a single plasma phosphate measurement obtained at the same day or time-averaged plasma phosphate levels over the 4-week study period.

Table 2 depicts correlation coefficients between CKD-MBD parameters measured at the end of the 4-week study period; expectedly, a significant correlation between FGF-23 and plasma phosphate was found (Figure 4A).

Notably, a correlation analysis between FGF-23 at study end and time-averaged plasma phosphate levels (Figure 4B) yielded a numerically lower correlation coefficient than the correlation analysis between FGF-23 and a single phosphate measurement (Figure 4A). In a linear regression analysis, a single phosphate measurement even outperformed time-averaged plasma phosphate levels as a predictor for log-transformed FGF-23 at study end (coefficient

of regression [B], 95% confidence interval [95% CI], and level of significance [P] for a single phosphate measurement and time-averaged plasma phosphate, respectively: B=0.27, 95% CI=0.08 to 0.46, $P=0.007$; B=0.08, 95% CI=−0.11 to 0.27, $P=0.41$).

Moreover, despite the seemingly high correlation coefficient between FGF-23 and both single and time-averaged plasma phosphate levels, individuals with very similar FGF-23 measurement may have widely differing plasma phosphate levels (as depicted in Figure 4 for a plasma FGF-23 of ~8,000 rU/ml), further arguing against the use of FGF-23 as a reliable indicator of plasma phosphate levels.

We aimed to better characterize those patients with high FGF-23 levels (arbitrarily defined as ≥ 2000 rU/ml at week 4) and normophosphatemia during the 4-week study (time-averaged plasma phosphate ≤ 4.5 mg/dl). Five patients fulfilled these criteria; they did not significantly differ in daily dietary phosphate (2312 ± 529 mg) or caloric intake (1571 ± 262 kcal) from the remaining patients (daily dietary phosphate intake = 2370 ± 1385 mg, daily caloric intake = 1416 ± 557 kcal; $P=0.93$ and $P=0.55$, respectively). Moreover, we excluded a significant difference in dialysis vintage (FGF-23 ≥ 2000 rU/ml and normophosphatemia = 4.4 ± 2.4 years; remaining patients = 3.7 ± 2.4 years; $P=0.87$). Finally, compared with the remaining 35 patients, 5 patients with plasma phosphate levels within the normal range and FGF-23 levels ≥ 2000 rU/ml did not differ in the prevalence of heart failure ($P=0.69$), diabetes mellitus ($P=0.63$), liver disease ($P=0.26$), or residual renal function (defined as self-reported diuresis ≥ 500 ml/24 hours).

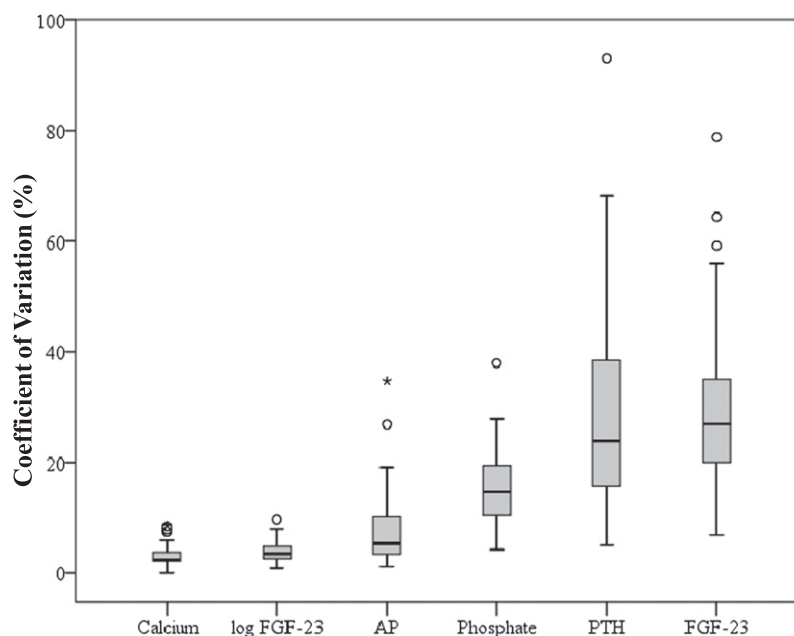


Figure 3. | Intraindividual variation of CKD-MBD parameters. For each individual patient, coefficients of variation were calculated from four measurements (at the end of the first, second, third, and fourth weeks). Depicted are medians, interquartile ranges, and outliers from individual coefficients of variation across the study cohort of 40 hemodialysis patients. AP, alkaline phosphatase; CKD-MBD, CKD-mineral and bone disorder; FGF-23, fibroblast growth factor 23; PTH, parathyroid hormone.

Table 2. Correlation coefficients between CKD–mineral and bone disorder parameters

CKD-MBD Parameter	Phosphate	AP	Log PTH	Log FGF-23	Time-Averaged Phosphate
Calcium	$r=-0.17$, $P=0.31$	$r=0.17$, $P=0.29$	$r=-0.06$, $P=0.71$	$r=0.05$, $P=0.77$	$r=-0.35$, $P=0.03$
Phosphate		$r=0.13$, $P=0.42$	$r=0.45$, $P=0.004$	$r=0.76$, $P<0.001$	$r=0.87$, $P<0.001$
AP			$r=0.40$, $P=0.01$	$r=0.25$, $P=0.12$	$r=0.08$, $P=0.61$
Log PTH				$r=0.41$, $P=0.009$	$r=0.34$, $P=0.03$
Log FGF-23					$r=0.67$, $P<0.001$

Because of non-normal distribution, FGF-23 and PTH were log-transformed for this analysis. AP, alkaline phosphatase; PTH, parathyroid hormone; FGF-23, fibroblast growth factor 23; r , Pearson correlation coefficient; P , level of significance.

Discussion

In our DIAL HOME study, we set out to test the use of FGF-23 as a stable reflector of time-averaged plasma phosphate levels during the preceding 4 weeks. Such use of FGF-23 was suggested earlier (15) on the basis of the central physiologic role of FGF-23 in phosphate regulation (18).

We *a priori* postulated that any stable marker of time-averaged plasma phosphate levels should fulfill two requirements. First, such a marker should have a lower intraindividual variability than plasma phosphate itself. Second, in a given individual, a single measurement of this marker should be more closely associated with mean plasma phosphate levels averaged from repeated measurements than a random single phosphate value.

Intraindividual Variation of CKD-MBD Parameters

First, we could confirm that plasma phosphate levels undergo substantial infradian rhythm, with highest levels after the long interdialytic interval at the beginning of the week on Mondays/Tuesdays. In contrast, we found no such infradian rhythm for FGF-23 levels.

Because circadian rhythms in plasma phosphate levels have been described earlier (9,19,20), we deliberately set out a study protocol, in which patients were not considered to change from morning to afternoon dialysis sessions and *vice versa*.

Respecting these infradian rhythms of plasma phosphate, we decided to calculate CVs on the basis of a single weekly phosphate measurement (on the same days on which FGF-23, AP, and PTH were measured; *i.e.*, Fridays or Saturdays) rather than all 12 phosphate values for comparing intraindividual stability of CKD-MBD parameters. In line with clinical practice, most dialysis units perform routine laboratory tests on the same days of the week. Notably, calculating CVs from all 12 measurements or the first dialysis day of each week rather than 4 measurements on Fridays or Saturdays, respectively, yielded virtually identical findings.

Against our expectations, we found that repeatedly measured FGF-23 displayed higher rather than lower CVs compared with plasma phosphate measurements. After log transformation, FGF-23 values seemingly become more stable.

Notably, the only other epidemiologic study that assessed stability of FGF-23 in CKD patients revealed similar

findings: among 44 peritoneal dialysis patients who underwent three monthly FGF-23 measurements, FGF-23 became a seemingly stable parameter only after log transformation (21).

Admittedly, high stability after log transfer of a biologic variable is of limited clinical relevance, because nephrologists will be confronted with crude FGF-23 values rather than log-transferred values in their clinical practice.

Association between FGF-23 and Time-Averaged Plasma Phosphate

As expected, we found a strong correlation between FGF-23 levels and plasma phosphate levels at any given time point, which was shown before among individuals with intact renal function (22,23) and in multiple cohort studies across the spectrum of CKD (24–28).

This close association between FGF-23 and plasma phosphate levels and the high intraindividual variability of plasma phosphate measurements fueled the idea that FGF-23 might mirror time-averaged plasma phosphate levels, similar to glycosylated hemoglobin in glucose metabolism (29). Interestingly, the idea of using FGF-23 as such a marker for time-averaged plasma phosphate levels has never been proven by adequate clinical data.

We now found that the correlation between FGF-23 levels and time-averaged phosphate did not surpass the correlation between FGF-23 levels and a single phosphate measurement. Moreover, we exemplarily illustrate that CKD patients with similar FGF-23 levels may have dramatically different plasma phosphate levels: patients who are in KDIGO target ranges for plasma phosphate and patients with massively elevated plasma phosphate levels may share virtually identical FGF-23 levels. Although various factors beyond CKD-MBD parameters may affect FGF-23 (30–32), we did not identify single factors explaining the coexistence of very high FGF-23 levels and normophosphatemia in individual patients, which may result from the limited patient size of our cohort.

In summary, on the basis of our data, no single FGF-23 level can reliably separate patients with adequate plasma phosphate values from patients with poor plasma phosphate control.

Limitations

We cannot rule out that FGF-23 measurement may reveal information on phosphate balance that is not reflected by

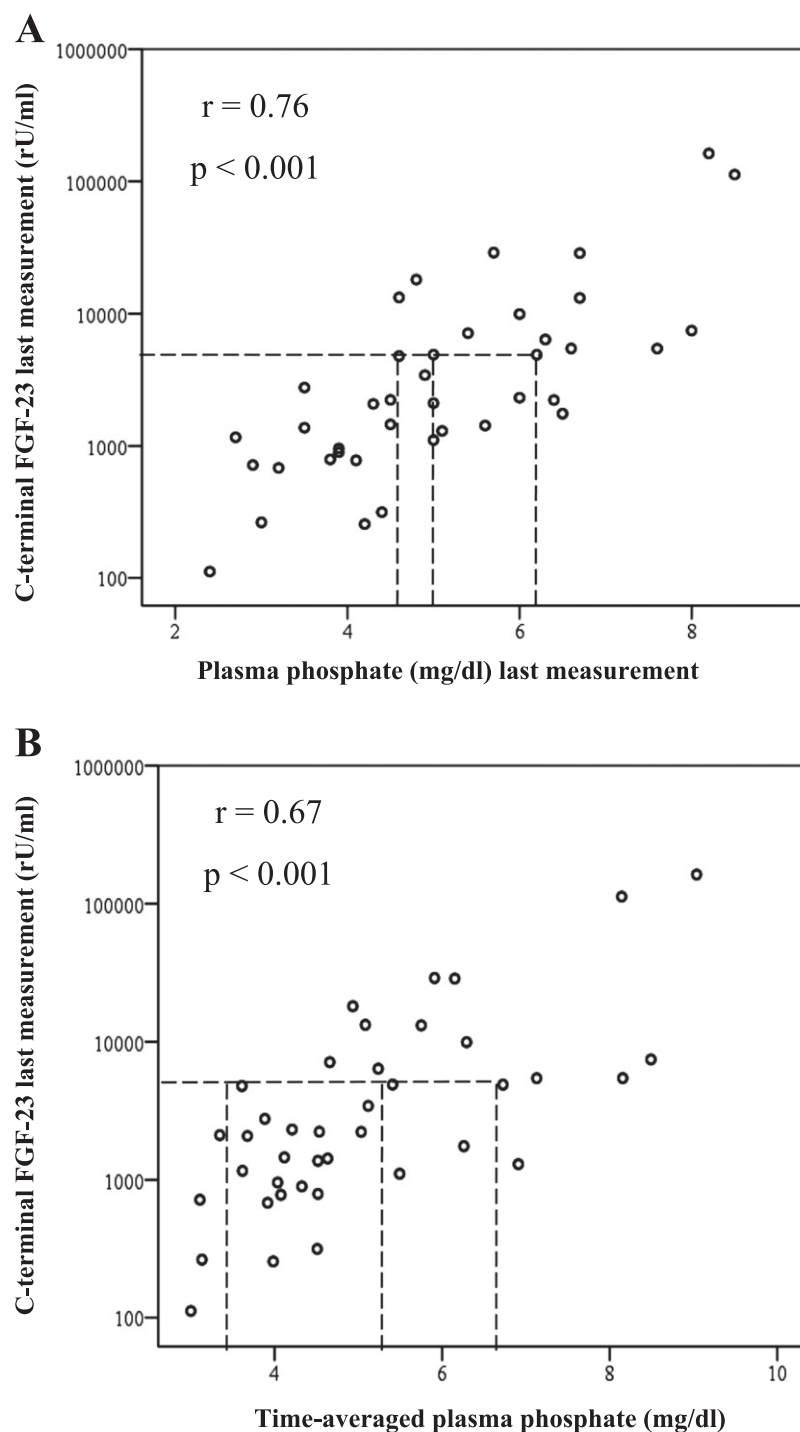


Figure 4. | Correlation of FGF-23 measured at study end with (A) a single plasma phosphate measurement obtained at study end or (B) plasma phosphate measurements averaged across the 4-week study period. As a representative example illustrating wide ranges of individual plasma phosphate measurements in patients with similar FGF-23 levels, lines are drawn for patients with FGF-23 of ~8,000 rU/ml. Note that FGF-23 levels are depicted on a logarithmic scale. FGF-23, fibroblast growth factor 23.

immediate changes in plasma phosphate levels. Of note, the largest amount of phosphate exists in other compartments outside the intravascular space, and harmful extraosseous phosphate deposition with vascular calcification may occur even before plasma phosphate levels are overtly elevated. Nonetheless, epidemiologic data on the association

between FGF-23 levels and vascular calcification revealed discrepant findings (14,33).

Moreover, we arbitrarily defined a study period of 4 weeks for assessing average plasma phosphate levels, and it may be argued that an even longer observation period would have yielded discrepant results.

Additionally, in CKD 5 patients who have very high FGF-23 levels, serial dilutions are necessary for measuring C-terminal FGF-23 levels. These dilutions could increase analytic variability and hence, CVs in our sample. Of note, CVs did not differ between patients with the lowest (CV=26% [IQR=20–39]) and highest (CV=27% [IQR=19–35]) FGF-23 levels.

As another limitation, we focused our cohort study on C-terminal FGF-23 levels, because many nephrologists use C-terminal FGF-23 rather than intact FGF-23 measurements in clinical practice for logistic and economical reasons. Moreover, because of higher instability of intact FGF-23 in the preanalytic phase, the measurement of C-terminal FGF-23 is recommended, especially for samples from CKD patients (34).

In our DIAL HOME study, we investigated two aspects: first, the intraindividual stability of FGF-23 in case of repeated measurements and second, its value as a marker for time-averaged plasma phosphate levels over 4 weeks. Against our expectations, plasma FGF-23 had a higher intraindividual variation than plasma phosphate, and plasma FGF-23 failed to provide specific information on time-averaged plasma phosphate levels during the preceding weeks.

Acknowledgments.

We thank Marie-Theres Blinn and Martina Wagner for their excellent assistance work.

Disclosures.

S.S. and K.S.R. have received speaker fees from Sanofi. G.L., P.E., L.H.F., A.L.-G., and M.Z. have no conflict of interest to declare. M.K. has received speaker fees from Baxter, Abbot, and Fresenius. D.F. has been a board member and additionally, received speaker fees from Shire, Amgen, Sanofi-Genzyme, and FMC. G.H.H. has received travel grants and speaker fees from Shire.

References

- Ketteler M, Wolf M, Hahn K, Ritz E: Phosphate: A novel cardiovascular risk factor. *Eur Heart J* 34: 1099–1101, 2013
- Block GA, Hulbert-Shearon TE, Levin NW, Port FK: Association of serum phosphorus and calcium x phosphate product with mortality risk in chronic hemodialysis patients: A national study. *Am J Kidney Dis* 31: 607–617, 1998
- Block GA, Klassen PS, Lazarus JM, Ofsthun N, Lowrie EG, Chertow GM: Mineral metabolism, mortality, and morbidity in maintenance hemodialysis. *J Am Soc Nephrol* 15: 2208–2218, 2004
- Tentori F, Blayney MJ, Albert JM, Gillespie BW, Kerr PG, Bommer J, Young EW, Akizawa T, Akiba T, Pisoni RL, Robinson BM, Port FK: Mortality risk for dialysis patients with different levels of serum calcium, phosphorus, and PTH: The Dialysis Outcomes and Practice Patterns Study (DOPPS). *Am J Kidney Dis* 52: 519–530, 2008
- Wald R, Sarnak MJ, Tighiouart H, Cheung AK, Levey AS, Eknoyan G, Miskulin DC: Disordered mineral metabolism in hemodialysis patients: An analysis of cumulative effects in the Hemodialysis (HEMO) Study. *Am J Kidney Dis* 52: 531–540, 2008
- Shroff R, Long DA, Shanahan C: Mechanistic insights into vascular calcification in CKD. *J Am Soc Nephrol* 24: 179–189, 2013
- Kidney Disease: Improving Global Outcomes (KDIGO) CKD-MBD Work Group: KDIGO clinical practice guideline for the diagnosis, evaluation, prevention, and treatment of Chronic Kidney Disease-Mineral and Bone Disorder (CKD-MBD). *Kidney Int Suppl* 113: S1–S130, 2009
- Ring T, Sanden AK, Hansen HH, Halkier P, Nielsen C, Fog L: Ultradian variation in serum phosphate concentration in patients on haemodialysis. *Nephrol Dial Transplant* 10: 59–63, 1995
- Levitt H, Smith KG, Rosner MH: Variability in calcium, phosphorus, and parathyroid hormone in patients on hemodialysis. *Hemodial Int* 13: 518–525, 2009
- Liu S, Tang W, Zhou J, Stubbs JR, Luo Q, Pi M, Quarles LD: Fibroblast growth factor 23 is a counter-regulatory phosphaturic hormone for vitamin D. *J Am Soc Nephrol* 17: 1305–1315, 2006
- Kawata T, Imanishi Y, Kobayashi K, Miki T, Arnold A, Inaba M, Nishizawa Y: Parathyroid hormone regulates fibroblast growth factor-23 in a mouse model of primary hyperparathyroidism. *J Am Soc Nephrol* 18: 2683–2688, 2007
- Baum M, Schiavi S, Dwarakanath V, Quigley R: Effect of fibroblast growth factor-23 on phosphate transport in proximal tubules. *Kidney Int* 68: 1148–1153, 2005
- Seiler S, Heine GH, Fliser D: Clinical relevance of FGF-23 in chronic kidney disease. *Kidney Int Suppl* 114: S34–S42, 2009
- Heine GH, Seiler S, Fliser D: FGF-23: The rise of a novel cardiovascular risk marker in CKD. *Nephrol Dial Transplant* 27: 3072–3081, 2012
- Parker BD, Schurgers LJ, Brandenburg VM, Christenson RH, Vermeer C, Ketteler M, Shlipak MG, Whooley MA, Ix JH: The associations of fibroblast growth factor 23 and uncarboxylated matrix Gla protein with mortality in coronary artery disease: The Heart and Soul Study. *Ann Intern Med* 152: 640–648, 2010
- Rogacev KS, Seiler S, Zawada AM, Reichart B, Herath E, Roth D, Ulrich C, Fliser D, Heine GH: CD14++CD16+ monocytes and cardiovascular outcome in patients with chronic kidney disease. *Eur Heart J* 32: 84–92, 2011
- Rogacev KS, Cremers B, Zawada AM, Seiler S, Binder N, Ege P, Große-Dunker G, Heisel I, Hornof F, Jeken J, Rebling NM, Ulrich C, Scheller B, Böhm M, Fliser D, Heine GH: CD14++CD16+ monocytes independently predict cardiovascular events: A cohort study of 951 patients referred for elective coronary angiography. *J Am Coll Cardiol* 60: 1512–1520, 2012
- Ketteler M, Petermann AT: Phosphate and FGF23 in early CKD: On how to tackle an invisible foe. *Nephrol Dial Transplant* 26: 2430–2432, 2011
- Perry HM 3rd, Province MA, Droke DM, Kim GS, Shaheb S, Avioli LV: Diurnal variation of serum calcium and phosphorus in postmenopausal women. *Calcif Tissue Int* 38: 115–118, 1986
- Ishida M, Seino Y, Yamaoka K, Tanaka Y, Satomura K, Kurose Y, Yabuchi H: The circadian rhythms of blood ionized calcium in humans. *Scand J Clin Lab Invest Suppl* 165: 83–86, 1983
- Isakova T, Xie H, Barchi-Chung A, Vargas G, Sowden N, Houston J, Wahl P, Lundquist A, Epstein M, Smith K, Contreras G, Ortega L, Lenz O, Briones P, Egbert P, Ikizler TA, Jueppner H, Wolf M: Fibroblast growth factor 23 in patients undergoing peritoneal dialysis. *Clin J Am Soc Nephrol* 6: 2688–2695, 2011
- Taylor EN, Rimm EB, Stampfer MJ, Curhan GC: Plasma fibroblast growth factor 23, parathyroid hormone, phosphorus, and risk of coronary heart disease. *Am Heart J* 161: 956–962, 2011
- Semba RD, Fink JC, Sun K, Cappola AR, Dalal M, Crasto C, Ferrucci L, Fried LP: Serum fibroblast growth factor-23 and risk of incident chronic kidney disease in older community-dwelling women. *Clin J Am Soc Nephrol* 7: 85–91, 2012
- Seiler S, Reichart B, Roth D, Seibert E, Fliser D, Heine GH: FGF-23 and future cardiovascular events in patients with chronic kidney disease before initiation of dialysis treatment. *Nephrol Dial Transplant* 25: 3983–3989, 2010
- Isakova T, Xie H, Yang W, Xie D, Anderson AH, Scialla J, Wahl P, Gutiérrez OM, Steigerwalt S, He J, Schwartz S, Lo J, Ojo A, Sondheim J, Hsu CY, Lash J, Leonard M, Kusek JW, Feldman HI, Wolf M: Chronic Renal Insufficiency Cohort (CRIC) Study Group: Fibroblast growth factor 23 and risks of mortality and end-stage renal disease in patients with chronic kidney disease. *JAMA* 305: 2432–2439, 2011
- Kendrick J, Cheung AK, Kaufman JS, Greene T, Roberts WL, Smits G, Chonchol M; HOST Investigators: FGF-23 associates with death, cardiovascular events, and initiation of chronic dialysis. *J Am Soc Nephrol* 22: 1913–1922, 2011
- Gutiérrez OM, Mannstadt M, Isakova T, Rauh-Hain JA, Tamez H, Shah A, Smith K, Lee H, Thadhani R, Jüppner H, Wolf M: Fibroblast growth factor 23 and mortality among patients undergoing hemodialysis. *N Engl J Med* 359: 584–592, 2008
- Jean G, Terrat JC, Vanel T, Huot JM, Lorrain C, Mayor B, Chazot C: High levels of serum fibroblast growth factor (FGF)-23 are

- associated with increased mortality in long haemodialysis patients. *Nephrol Dial Transplant* 24: 2792–2796, 2009
29. American Diabetes Association: Standards of medical care in diabetes—2009. *Diabetes Care* 32[Suppl 1]: S13–S61, 2009
 30. Hryszko T, Rydzewska-Rosolowska A, Brzosko S, Koc-Zorawska E, Mysliwiec M: Low molecular weight iron dextran increases fibroblast growth factor-23 concentration, together with parathyroid hormone decrease in hemodialyzed patients. *Ther Apher Dial* 16: 146–151, 2012
 31. Munoz Mendoza J, Isakova T, Ricardo AC, Xie H, Navaneethan SD, Anderson AH, Bazzano LA, Xie D, Kretzler M, Nessel L, Hamm LL, Negrea L, Leonard MB, Raj D, Wolf M; Chronic Renal Insufficiency Cohort: Fibroblast growth factor 23 and inflammation in CKD. *Clin J Am Soc Nephrol* 7: 1155–1162, 2012
 32. Seiler S, Cremers B, Rebling NM, Hornof F, Jeken J, Kersting S, Steimle C, Ege P, Fehrenz M, Rogacev KS, Scheller B, Böhm M, Fliser D, Heine GH: The phosphatonin fibroblast growth factor 23 links calcium-phosphate metabolism with left-ventricular dysfunction and atrial fibrillation. *Eur Heart J* 32: 2688–2696, 2011
 33. Wolf M: Update on fibroblast growth factor 23 in chronic kidney disease. *Kidney Int* 82: 737–747, 2012
 34. Fassbender WJ, Brandenburg V, Schmitz S, Sandig D, Simon SA, Windolf J, Stumpf UC: Evaluation of human fibroblast growth factor 23 (FGF-23) C-terminal and intact enzyme-linked immunosorbent-assays in end-stage renal disease patients. *Clin Lab* 55: 144–152, 2009

Received: December 23, 2012 **Accepted:** June 7, 2012

S.S. and G.L. contributed equally to this work.

Published online ahead of print. Publication date available at www.cjasn.org.

This article contains supplemental material online at <http://cjasn.asnjournals.org/lookup/suppl/doi:10.2215/CJN.13021212/-/DCSupplemental>.

Beitrag der Mitautoren für die Arbeit:

Lisa H. Fell, Adam M. Zawada, Kyrill S. Rogacev, Sarah Seiler, Danilo Fliser, Gunnar H. Heine (2014) Distinct immunologic effects of different intravenous iron preparations on monocytes. Nephrol Dial Transplant 29(4):809-22

Diese Studie wurde von Frau Lisa Fell, Herrn PD Dr. Kyrill Rogacev, Herrn Dr. Adam Zawada sowie von Herrn Prof. Dr. Danilo Fliser und Herrn Prof. Dr. Gunnar Heine entworfen und geplant. Die Patienten wurden durch Frau PD Dr. Sarah Seiler und Herrn Prof. Dr. Gunnar Heine rekrutiert und die anschließende Laborarbeit von Frau Lisa Fell und Herrn Dr. Adam Zawada durchgeführt. Alle Autoren haben an der statistischen Auswertung der Daten und deren Interpretation mitgewirkt. Das Manuskript wurde von Frau Lisa Fell, Herrn Dr. Adam Zawada sowie von Herrn Prof. Dr. Gunnar Heine geschrieben.

Die oben aufgeführten Autoren haben die finale Version des Manuskripts gelesen, kritisch überarbeitet und ihr zugestimmt.

Distinct immunologic effects of different intravenous iron preparations on monocytes

Lisa H. Fell, Adam M. Zawada, Kyrill S. Rogacev, Sarah Seiler, Danilo Fliser and Gunnar H. Heine

Department of Internal Medicine IV – Nephrology and Hypertension, Saarland University Medical Center, Homburg, Germany

Correspondence and offprint requests to: Gunnar H. Heine; E-mail: gunnar.heine@uks.eu

ABSTRACT

Background. Iron deficiency contributes to anaemia in patients with chronic kidney disease. *I.v.* iron is therefore widely used for anaemia treatment, although it may induce oxidative stress and activate monocytes. Different *i.v.* iron preparations are available, but interestingly their substance-specific immunologic effects are poorly studied.

Methods. We analysed the effect of iron sucrose, ferric carboxymaltose, iron isomaltoside 1000, low-molecular-weight iron dextran and ferumoxytol on classical, intermediate and nonclassical monocyte biology. We therefore stimulated *in vitro* mature monocytes and haematopoietic CD34⁺ stem cells during their differentiation into monocytes with different concentrations (0.133, 0.266, 0.533 mg/mL) of *i.v.* iron preparations. Alterations of monocyte subset distribution, expression of surface markers (CD86, CCR5, CX₃CR1), as well as production of pro-inflammatory cytokines (TNF- α , IL-1 β) and reactive oxygen species were measured using flow cytometry. Additionally, we analysed phagocytosis and antigen presentation capacity.

Results. We found specific immunologic effects after stimulation with iron sucrose which were not induced by the other iron preparations. Iron sucrose activated monocyte subsets leading to significantly increased CD86 expression. Simultaneously CD16 and CX₃CR1 expression and monocytic phagocytosis capacity were decreased. Additionally, differentiation of monocytes from haematopoietic CD34⁺ stem cells was almost completely abolished after stimulation with iron sucrose.

Conclusions. Our findings demonstrate that specific immunologic effects of distinct *i.v.* iron preparations exist. The clinical relevance of these findings requires further investigation.

Keywords: CD14, CD16, immune deficiency, iron therapy, monocyte subsets

INTRODUCTION

Iron deficiency is highly prevalent in chronic kidney disease (CKD) patients [1]. After erythropoiesis-stimulating agents failed to improve cardiovascular disease burden among CKD patients in several recent large-scale randomized clinical trials [2–4], the idea of iron supplementation for anaemia treatment has re-gained interest in nephrology in recent years [5].

Iron supplementation may be provided either orally or intravenously. However, oral absorption of iron is poor in many CKD patients due to their chronic micro-inflammatory status with commensurately high hepcidin levels [6]. Hepcidin itself impairs intestinal iron absorption and transport from the enterocytes to the plasma [7].

Therefore the use of intravenous (*i.v.*) iron preparations has been recommended [8, 9]. Several *i.v.* iron preparations have been developed, most of which (like iron sucrose, ferric carboxymaltose, low-molecular-weight iron dextran and ferumoxytol) consist of a ferritin-like polynuclear, non-ionic ferric-oxyhydroxide core and a carbohydrate shell. Another *i.v.* iron preparation, iron isomaltoside 1000, differs in structure from these molecules, since it has been described as a matrix-like structure with interchanging layers of linear isomaltoside 1000 oligomers and iron atoms placed in cavities between, and within, the oligosaccharide molecules [10]. *I.v.* iron preparations vary in their carbohydrate ligands as well as in the chemistry of the coupling process and thus in physiochemical and pharmacokinetic parameters such as molecular weight, reactivity as well as thermodynamic stability [11]. These differences result in a substance-specific kinetic of non-transferrin-bound iron (NTBI; 'free iron') release from iron complexes after their *i.v.* administration [12]. Within the cell, NTBI can induce the formation of reactive oxygen species (ROS) [13, 14]. Oxidative stress, in turn, results in endothelial damage and dysfunction and triggers inflammation [15, 16]. Moreover, recent reports suggest that *i.v.* iron administration may impair the function of circulating leukocytes with subsequently increased susceptibility

to bacterial infections [17]. Of note, most scientific work has focused on implications of 'free iron' on neutrophils [18], and only few reports have been published on interaction of 'free iron' with monocytes [19], despite the central role of monocytes in iron metabolism and host defence [20].

Moreover, previous research on iron toxicity has completely neglected the existence of monocyte heterogeneity, constituting a knowledge gap regarding the effects of *i.v.* iron preparations on different monocyte subsets. Three distinct monocyte subsets, namely, classical CD14⁺⁺CD16⁻ monocytes, intermediate CD14⁺⁺CD16⁺ monocytes and nonclassical CD14⁺CD16⁺⁺ monocytes have been acknowledged by the recent consensus statement [21]. Intermediate monocytes are characterized as inflammatory and potentially proatherogenic cells; high cell counts of intermediate monocytes predict adverse cardiovascular outcome in CKD patients [22, 23].

Against this background, the purpose of this study was to investigate the immunoactivation of different monocyte subsets by five *i.v.* iron preparations which are commonly used in clinical nephrology, namely iron sucrose, ferric carboxymaltose, iron isomaltoside 1000, low-molecular-weight iron dextran and ferumoxytol [24].

SUBJECTS AND METHODS

Subjects

For our *in vitro* analysis, we recruited two groups of study participants:

- (1) control subjects without overt CKD (depending on the analyses, three to seven subjects per experiment, as indicated below; all subjects had serum creatinine <1.5 mg/dL), and
- (2) patients with severe CKD [four patients with CKD stage G 4 - 5 (GFR < 30 mL/min/1.73 m²) not yet on renal replacement therapy, and four haemodialysis patients].

All participants gave informed consent. The study protocol was approved by the local Ethics Committee and was conducted in accordance with the Declaration of Helsinki.

Flow cytometric analysis

Monocyte subsets were flow cytometrically identified in cell culture or in whole-blood assays according to our standardized and validated gating strategy using FACS Canto II with FACS-Diva Software (BD Biosciences, Heidelberg, Germany) [22]. In brief, using a side scatter/CD86 dot plot, monocytes were detected as CD86-positive cells with monocytic scatter properties. Subsequently the three monocyte subsets classical, intermediate and nonclassical monocytes were gated based on their surface expression pattern of CD14 (LPS receptor) and CD16 (FcγIII receptor).

In the whole-blood assays we stimulated 150 µL blood with different *i.v.* iron preparations: iron sucrose (Venofer®), ferric carboxymaltose (ferinject®) (both from Vifor Pharma AG, Glattbrugg, Switzerland), iron isomaltoside 1000

(MonoFer®), low-molecular-weight iron dextran (CosmoFer®) (both from Pharmacosmos, Holbæk, Denmark) and ferumoxytol (Feraheme®, from AMAG Pharmaceuticals, Lexington, MA, USA).

All stimulations were done at 37°C and 5% CO₂, and three iron concentrations were used: 0.133, 0.266 and 0.533 mg/mL.

Protein surface expression and intracellular cytokine production were quantified as mean fluorescence intensity (MFI). The following antibodies were used: anti-CD14 PerCP (Mφ9), anti-CD16 PeCy7 (3G8) and anti-CD195 APC (2D7/CCR5) and anti-TNF FITC (MAb11) (BD Biosciences, Heidelberg, Germany), anti-CD86 PE (HA5.2B7) (Beckman-Coulter, Krefeld, Germany), anti-CX₃CR1 FITC (2A9-1) (Biozol, Eching, Germany), and anti-IL-1β Alexa Fluor® 647 (JK1B-1) (Biolegend, Fell, Germany).

Surface expression of CD14, CD16, CD86, CCR5 and CX₃CR1 was determined after incubating 150 µL EDTA anticoagulated blood with iron preparations for 5 h.

For intracellular measurement of TNF-α and IL-1β, 150 µL Li-hep anticoagulated blood was incubated with iron preparations for 2 h before and for 1 h after addition of 350 µM of brefeldin A (Sigma-Aldrich, Taufkirchen, Germany). After staining for CD14, CD16 and CD86 and lysis, cells were fixed with paraformaldehyde (4%), washed with a saponin-containing buffer, stained with antibodies against TNF-α and IL-1β, washed and fixed with paraformaldehyde (1%).

In vitro generation of monocytes from haematopoietic CD34⁺ stem cells

For *in vitro* generation of monocytes, haematopoietic CD34⁺ stem cells were isolated and monocytes generated according to our standardized protocol (manuscript in preparation). Briefly, peripheral blood mononuclear cells (PBMCs) were isolated from EDTA anticoagulated blood by Ficoll-Paque (Lymphocyte Separation Medium; PAA, Cölbe, Germany) gradient density centrifugation. CD34⁺ cells were isolated using the CD34 MicroBead Kit (Miltenyi Biotec, Bergisch Gladbach, Germany). For determining quality of isolation, CD34⁺ cells were stained with anti-CD34 APC (581; BD Biosciences) and anti-CD45 PE (HI30; BD Biosciences) antibodies. Mean purity assessed by flow cytometry was 85.3 ± 4.8%.

Isolated CD34⁺ haematopoietic stem cells were expanded in 6-well plates (1 × 10⁴ cells/mL) for 13 days in the Haematopoietic Progenitor Cell Expansion Medium DXF, enriched with Cytokine Mix E (PromoCell GmbH, Heidelberg, Germany). After expansion, cells were seeded in 12-well plates for differentiation to monocytes in the Haematopoietic Progenitor Medium (PromoCell GmbH) supplemented with iron preparations. Daily progress was flow cytometrically monitored after anti-CD14, anti-CD16 and anti-CD86 staining, subdividing cells into monocyte subsets. At Day 7 of differentiation, surface expression of CCR5 and CX₃CR1 was additionally measured.

Measurement of ROS

For measurement of ROS, PBMCs were isolated from EDTA anticoagulated blood and stimulated with iron preparations for 3 h. Afterwards cells were incubated with 10 µM

of the cell-permanent carboxy-H₂DFFDA (Life technologies, Darmstadt, Germany) for 15 min at 37°C and 5% CO₂. Samples were stained with CD14, CD16 and CD86 and the amount of ROS (MFI of H₂DFFDA) was flow cytometrically determined as described above.

In analogy, for ROS determination of *in vitro* generated monocytes at Day 7 of differentiation, 200 µL of cell suspension was incubated with carboxy-H₂DFFDA. Afterwards samples were stained and MFI-values were flow cytometrically calculated.

Phagocytosis assay

For measurement of monocytic phagocytosis capacity Fluores-brite Yellow Green (YG) Carboxylate Microspheres (0.75 µm, Polysciences, Eppelheim, Germany) were opsonized with heterologous serum (mixed with Krebs Ringers PBS), adjusted to 10⁸ particles/mL and shaken gently for 30 min at 37°C. After stimulation of 150 µL of citrate anticoagulated blood with iron preparations for 4.5 h, 50 µL of opsonized particles were added and incubated for additional 30 min at 37°C with mild shaking. Samples were stained as described above, and counts of FITC-positive cells were determined flow cytometrically in each monocyte subset.

Within *in vitro* generated monocytes, phagocytosis capacity was measured at Day 7 of differentiation. Therefore, 90 µL of cell suspension was incubated with opsonized particles as described before.

Proliferation assay

Monocyte subset-specific ability to induce T-cell proliferation was measured using the cytoplasmic dilution of CFDA-SE (Vybrant CFDA-SE Cell Tracer Kit; Life technologies). In detail, PBMCs were isolated from EDTA anticoagulated blood and labelled with 5 µM CFDA-SE for 10 min at 37°C. Cells were cultivated in 96-well plates at a density of 6 × 10⁵ cells and stimulated with iron preparations in the presence of 2.5 µg/mL staphylococcal enterotoxin B (SEB; Sigma-Aldrich). After 3 days, counts of proliferating T-cells were analysed flow cytometrically by measuring CFDA-SE dilution, identifying T-cells by anti-CD3 APC staining (SK7; Biolegend).

Measurement of iron uptake

For measurement of monocytic iron uptake, 150 µL of Li-hep anticoagulated blood was stimulated with iron preparations for 1 h. Samples were stained with antibodies against CD14, CD16 and CD86 as well as with calcein acetoxymethyl ester (Biomol, Hamburg, Germany) in a final concentration of 0.2 µM. Iron uptake was determined based on the ability of iron to bind calcein and to quench its fluorescence.

Determination of viability

For measurement of cellular viability, PBMCs were isolated from EDTA anticoagulated blood and stimulated with iron preparations for 3 h. Subsequently, samples were stained with Annexin V and 7-AAD in Annexin V Binding Buffer (FITC Annexin V Apoptosis Detection Kit with 7-AAD, Biolegend). Flow cytometrically, monocyte subsets were identified as

Table 1. Expression of CD14, CD16 and CD86 on circulating mature classical, intermediate and nonclassical monocytes from control subjects

Monocyte subset	Control	Iron sucrose			Ferric carboxymaltose			Iron isomaltoside 1000		
		0.133 mg/mL	0.266 mg/mL	0.533 mg/mL	0.133 mg/mL	0.266 mg/mL	0.533 mg/mL	0.133 mg/mL	0.266 mg/mL	0.533 mg/mL
CD14	Classical monocytes	5453 ± 302	4766 ± 258	5202 ± 265	5166 ± 360	5324 ± 419	5147 ± 345	5194 ± 318	5116 ± 310	5094 ± 363
	Intermediate monocytes	4842 ± 349	4258 ± 380	4385 ± 338	3960 ± 276	4503 ± 275	4554 ± 415	4620 ± 423	4512 ± 367	4530 ± 384
	Nonclassical monocytes	292 ± 25	320 ± 37	356 ± 23	335 ± 23	307 ± 31	296 ± 27	280 ± 24	318 ± 35	313 ± 31
CD16	Classical monocytes	892 ± 119	233 ± 43**	201 ± 43**	116 ± 24**	847 ± 70	808 ± 90	839 ± 81	820 ± 74	836 ± 84
	Intermediate monocytes	6608 ± 1256	9159 ± 1598	7841 ± 1596	7348 ± 1530	8364 ± 2273	7353 ± 1593	8186 ± 2300	8157 ± 1994	7425 ± 1697
	Nonclassical monocytes	34 563 ± 1021	29 593 ± 1772	29 186 ± 1904	22 271 ± 2376**	31 979 ± 1680	31 873 ± 1637	33 687 ± 1982	31 530 ± 2027	33 258 ± 1785
CD86	Classical monocytes	553 ± 51	582 ± 36	809 ± 49*	1291 ± 63**	551 ± 56	540 ± 53	551 ± 53	535 ± 53	541 ± 60
	Intermediate monocytes	1100 ± 128	1564 ± 117	1881 ± 192**	2207 ± 154**	1202 ± 186	1200 ± 143	1222 ± 146	1262 ± 154	1202 ± 154
	Nonclassical monocytes	1419 ± 148	1551 ± 122	2047 ± 241	2204 ± 249*	1376 ± 138	1397 ± 131	1388 ± 146	1355 ± 122	1386 ± 131

Indicated are mean fluorescence intensity [MFI] ± SEM; n = 7

*P < 0.05, **P < 0.01

described above, and viable cells were defined as 7-AAD-negative monocytes.

Statistics

Statistical analysis was performed for each iron preparation using one-way analysis of variance (ANOVA), followed by Dunnett's multiple comparison test as *post hoc* test. Data were presented as percentages or MFI \pm SEM (standard error of the mean).

RESULTS

Impact of iron preparations on human monocyte subsets

We first aimed to analyse the impact of the three iron preparations iron sucrose, ferric carboxymaltose and iron isomaltoside 1000 on human monocyte subsets collected from control subjects without overt CKD. Therefore, we stimulated whole blood with the different iron preparations and analysed their

effect on the expression of CD14, CD16 and CD86 on classical, intermediate and nonclassical monocytes. We found iron sucrose dose-dependently to increase CD86 surface expression on all monocyte subsets. In addition, we observed a significant reduction of CD16 expression on classical monocytes, and on nonclassical monocytes (Table 1). Despite this down-regulation of CD16 expression, no significant changes in monocyte subset distribution occurred (Figure 1), and CD14 expression did not change (Table 1). Ferric carboxymaltose and iron isomaltoside 1000 did not affect the expression of CD14, CD16 or CD86 (Table 1).

Effect of iron preparations on monocytic chemokine receptor expression, inflammation response and functional characteristics

We analysed the effect of the three different iron preparations iron sucrose, ferric carboxymaltose and iron isomaltoside 1000 on subset-specific expression of chemokine receptors CCR5 and CX₃CR1, on production of pro-inflammatory

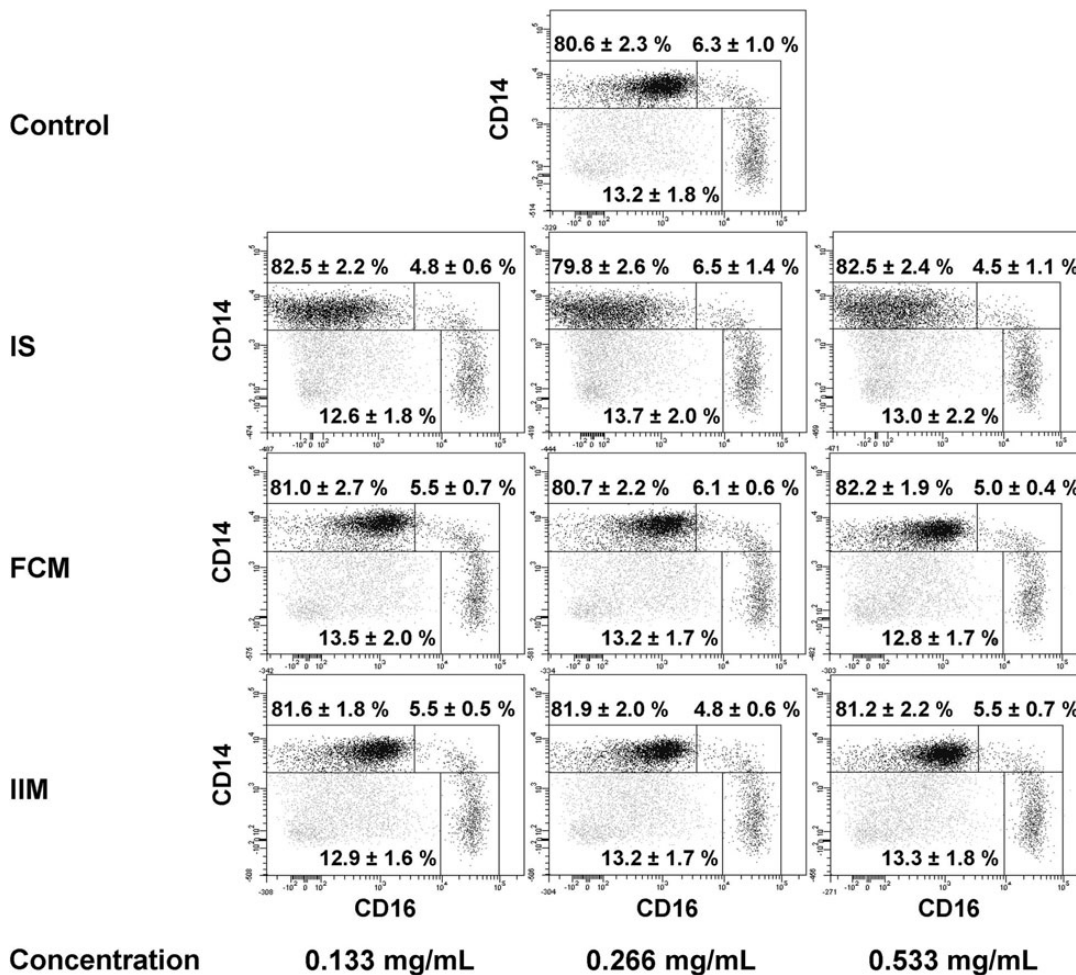


FIGURE 1: Representative example of monocyte subset distribution after stimulation with iron sucrose (IS), ferric carboxymaltose (FCM) or iron isomaltoside 1000 (ISM) (0.133, 0.266 and 0.533 mg/mL). Blood was collected from control subjects. Classical monocytes are shown in the upper left gate, intermediate monocytes in the upper right gate and nonclassical monocytes in the lower right gate of each dot plot. Statistical analysis was performed for each iron preparation using ANOVA, followed by Dunnett's multiple comparison test as *post hoc* test; data of seven independent experiments are presented as mean \pm SEM.

Table 2. Expression of CCR5 and CX₃CR1 as well as production of TNF- α , IL-1 β and ROS in circulating mature classical, intermediate and nonclassical monocytes from control subjects

Monocyte subset	Control	Iron sucrose			Ferric carboxymaltose			Iron isomaltoside 1000		
		0.133 mg/mL	0.266 mg/mL	0.533 mg/mL	0.133 mg/mL	0.266 mg/mL	0.533 mg/mL	0.133 mg/mL	0.266 mg/mL	0.533 mg/mL
CCR5	Classical monocytes	76 \pm 10	115 \pm 16	102 \pm 18	82 \pm 25	73 \pm 10	77 \pm 9	76 \pm 9	76 \pm 9	75 \pm 8
	Intermediate monocytes	297 \pm 86	369 \pm 121	340 \pm 118	277 \pm 126	303 \pm 100	284 \pm 82	300 \pm 91	311 \pm 93	290 \pm 91
	Nonclassical monocytes	99 \pm 19	115 \pm 24	99 \pm 23	63 \pm 28	94 \pm 20	96 \pm 12	95 \pm 19	80 \pm 11	95 \pm 16
CX ₃ CR1	Classical monocytes	1138 \pm 73	845 \pm 57**	660 \pm 50**	496 \pm 35**	1156 \pm 87	1158 \pm 75	1164 \pm 80	1242 \pm 73	1202 \pm 86
	Intermediate monocytes	2180 \pm 209	1755 \pm 198	1505 \pm 189*	1130 \pm 120**	2221 \pm 206	2160 \pm 229	2310 \pm 254	2341 \pm 275	2708 \pm 467
	Nonclassical monocytes	4860 \pm 231	4141 \pm 293	3368 \pm 303**	2697 \pm 223**	4922 \pm 266	4863 \pm 252	4904 \pm 189	4946 \pm 182	4827 \pm 348
TNF- α	Classical monocytes	168 \pm 30	140 \pm 20	123 \pm 14	119 \pm 14	185 \pm 32	191 \pm 36	183 \pm 40	182 \pm 36	182 \pm 32
	Intermediate monocytes	183 \pm 29	216 \pm 44	181 \pm 26	177 \pm 27	207 \pm 34	228 \pm 47	220 \pm 36	189 \pm 39	187 \pm 20
	Nonclassical monocytes	125 \pm 18	162 \pm 19	141 \pm 16	131 \pm 15	148 \pm 21	148 \pm 23	155 \pm 23	142 \pm 23	145 \pm 17
IL-1 β	Classical monocytes	73 \pm 19	133 \pm 38	128 \pm 35	148 \pm 40	85 \pm 12	84 \pm 12	95 \pm 19	93 \pm 23	92 \pm 31
	Intermediate monocytes	122 \pm 26	173 \pm 46	168 \pm 28	169 \pm 28	137 \pm 28	160 \pm 32	162 \pm 39	136 \pm 30	123 \pm 24
	Nonclassical monocytes	90 \pm 15	112 \pm 23	89 \pm 12	89 \pm 14	108 \pm 14	104 \pm 11	110 \pm 15	104 \pm 15	103 \pm 17
ROS	Classical monocytes	2899 \pm 684	3403 \pm 767	3503 \pm 781	3449 \pm 769	3043 \pm 691	3260 \pm 706	3201 \pm 822	3403 \pm 873	3613 \pm 937
	Intermediate monocytes	3760 \pm 898	4758 \pm 1266	4400 \pm 893	4687 \pm 989	3973 \pm 987	4173 \pm 948	4184 \pm 1158	4351 \pm 1141	4768 \pm 1321
	Nonclassical monocytes	3179 \pm 806	3795 \pm 1026	4011 \pm 1105	3784 \pm 1027	3248 \pm 878	3503 \pm 922	3531 \pm 1103	3686 \pm 1152	3972 \pm 1233

Indicated are mean fluorescence intensity [MFI] \pm SEM; $n = 7$ for analysis of CCR5 and CX₃CR1 expression, $n = 4$ for analysis of TNF- α and IL-1 β production, $n = 6$ for analysis of ROS production* $P < 0.05$, ** $P < 0.01$

cytokines (TNF- α and IL-1 β) and on ROS production. CX₃CR1 expression was specifically and dose-dependently reduced by iron sucrose, while CCR5 expression was not. Moreover, iron sucrose tended to increase IL-1 β and ROS production, but not TNF- α production. Ferric carboxymaltose and iron isomaltoside 1000 affected neither cytokine production, chemokine receptor expression nor ROS production significantly (Table 2).

Next, we tested the effect of iron preparations on the main functional characteristics of monocytes, namely phagocytosis capacity and antigen presentation (via analysis of T-cell proliferation). In contrast to ferric carboxymaltose and iron isomaltoside 1000, iron sucrose significantly reduced the capacity of classical monocytes to phagocyte microspheres (Figure 2A). T-cell proliferation tended to be decreased after stimulation with the highest dosage of iron sucrose, but tended to be increased after stimulation with lower dosages of iron sucrose, ferric carboxymaltose and iron isomaltoside 1000 (Figure 2B). To prove biological plausibility of these results, we first excluded that the effects of iron sucrose are caused by increased apoptosis of monocytes (Figure 3A), and next showed that iron sucrose is more avidly taken up by monocytes than ferric carboxymaltose or iron isomaltoside 1000 (Figure 3B), which may account for the preparation-specific effects of iron sucrose on monocyte function.

Impact of iron preparations on monocyte differentiation

In order to test whether specific iron preparations (iron sucrose, ferric carboxymaltose and iron isomaltoside 1000) differently affect development of monocytes, we analysed *in vitro* differentiation of isolated CD34⁺ haematopoietic stem cells into classical and intermediate monocytes. Iron sucrose significantly reduced *in vitro* differentiation into intermediate monocytes even at the lowest dose (Figure 4), which is mirrored by a strongly decreased CD14 and CD16 expression on these cells (Table 3). Simultaneously it significantly increased CD86 expression on *in vitro* differentiated monocytes, which is in line with its effect on circulating mature monocytes. Although a significant reduction of CD14 on classical monocytes was observed after stimulation with ferric carboxymaltose and iron isomaltoside 1000, these iron preparations affected neither *in vitro* differentiation of monocyte subsets nor their expression of CD16 and CD86.

Implication of iron preparations on characteristics of *in vitro*-differentiated monocytes

We then determined the expression of CCR5 and CX₃CR1, as well as ROS production, by *in vitro* differentiated monocyte subsets (Table 4). CX₃CR1 expression was increased after treatment with iron sucrose and ferric carboxymaltose, whereas CCR5 expression and ROS production were not significantly altered.

Finally, *in vitro* differentiated classical and intermediate monocytes displayed a dose-dependent reduction in their phagocytosis capacity after iron sucrose treatment, even though the level of significance was not reached (data not shown).

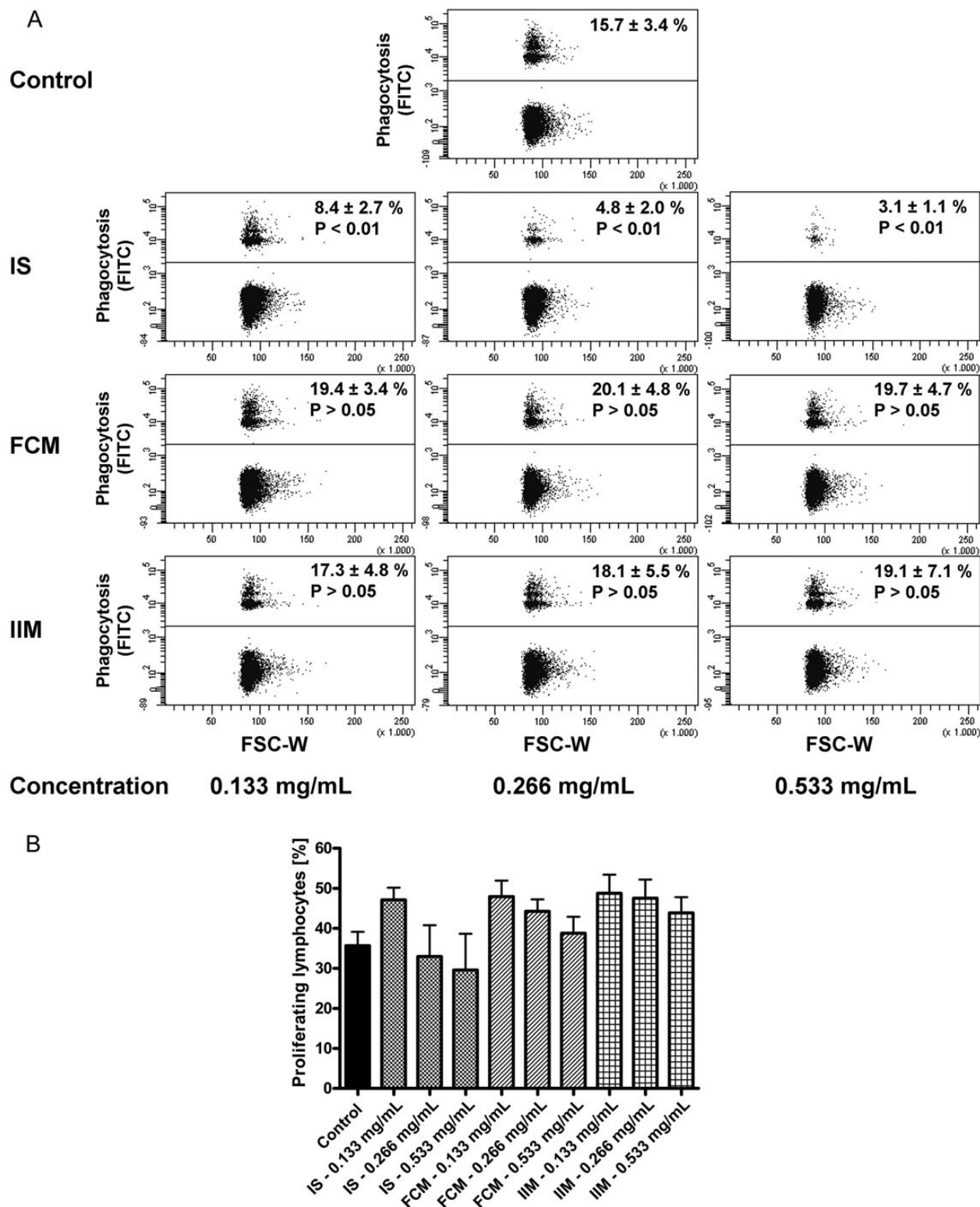


FIGURE 2: (A). Representative example of classical monocytes to phagocyte opsonized carboxylate microspheres (0.75 μ m, Yellow Green) within 30 min after stimulation with iron sucrose (IS), ferric carboxymaltose (FCM) or iron isomaltoside 1000 (IIM) (0.133, 0.266 and 0.533 mg/mL). Blood was collected from control subjects. Counts of FITC-positive cells (upper population) were determined flow cytometrically and statistical analysis was performed for each iron preparation by using ANOVA followed by Dunnett's multiple comparison test as *post hoc* test; data of six independent experiments are presented as mean \pm SEM. **(B).** Flow cytometric analysis of T-cell proliferation after stimulation with staphylococcal enterotoxin B (SEB) (2.5 μ g/mL) and the different iron preparations iron sucrose (IS), ferric carboxymaltose (FCM) and iron isomaltoside 1000 (IIM) (0.133, 0.266 and 0.533 mg/mL) for 3 days. Blood was collected from control subjects. Statistical analysis was performed for each iron preparation by using ANOVA followed by Dunnett's multiple comparison test as *post hoc* test; data of seven independent experiments are presented as mean \pm SEM.

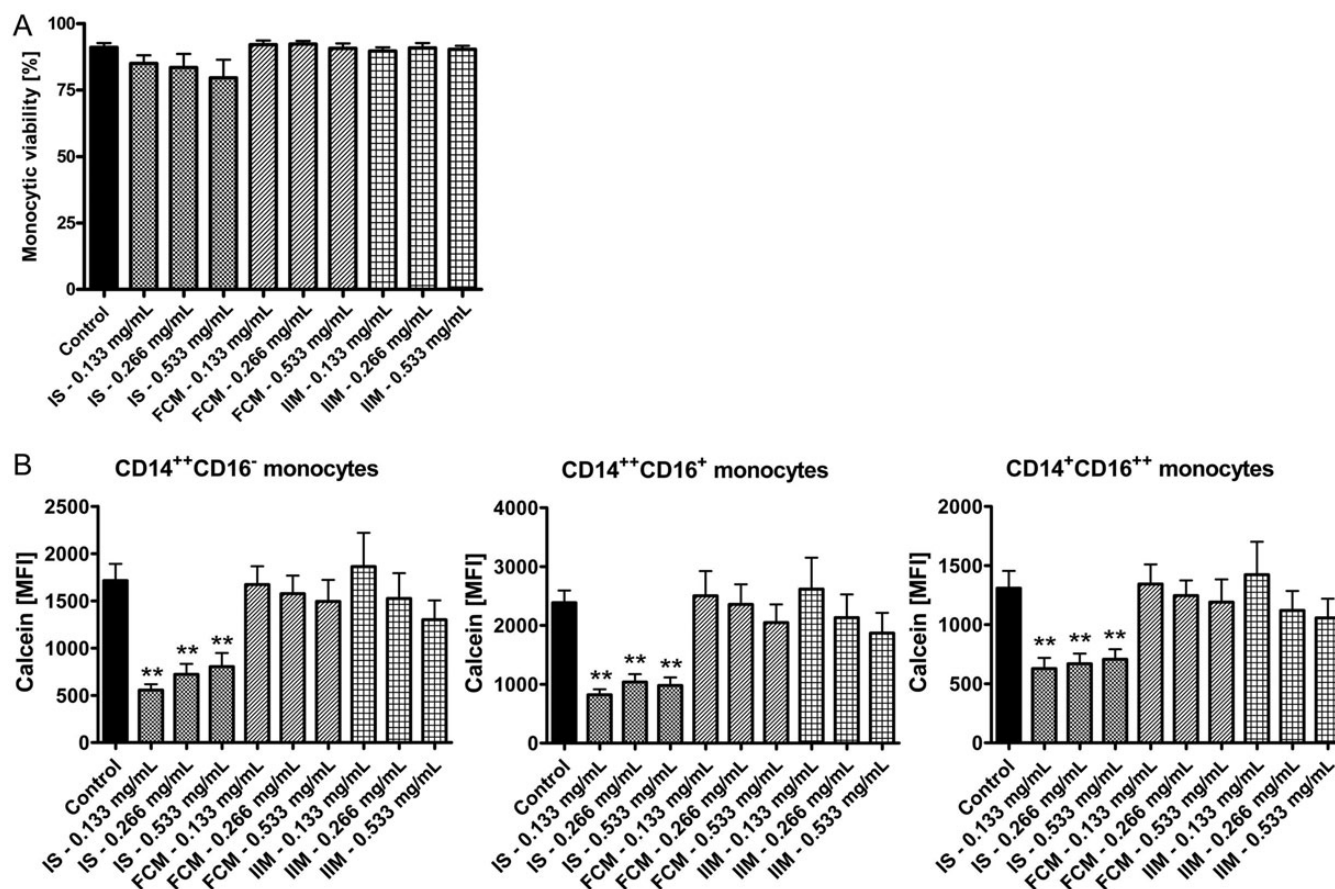


FIGURE 3: (A) Flow cytometric analysis of monocytic viability after stimulation with iron sucrose (IS), ferric carboxymaltose (FCM) or iron isomaltoside 1000 (IIM) (0.133, 0.266 and 0.533 mg/mL) by 7-AAD staining. Blood was collected from control subjects. Statistical analysis was performed for each iron preparation by using ANOVA and the Dunnett's multiple comparison test as *post hoc* test; data of five independent experiments are presented as mean \pm SEM. **(B).** Flow cytometric calcein assay for the analysis of the iron content in classical, intermediate and nonclassical monocytes after stimulation of whole blood for 1 h with iron sucrose (IS), ferric carboxymaltose (FCM) or iron isomaltoside 1000 (IIM) (0.133, 0.266 and 0.533 mg/mL). As iron intracellularly binds calcein and quenches its fluorescence, lower fluorescence intensity represents higher intracellular iron content. Blood was collected from control subjects. Data were measured as mean fluorescence intensity (MFI). Statistical analysis was performed using ANOVA and the Dunnett's multiple comparison test as *post hoc* test; data of six independent experiments are presented as mean \pm SEM; ** $P < 0.01$.

Impact of iron preparations on human monocyte subsets from CKD patients

We next analysed (i) whether these observed effects of iron sucrose can be transferred from control subjects without overt CKD to patients with severe CKD and (ii) whether two other iron preparations, namely low-molecular-weight iron dextran and ferumoxytol, induce monocyte activation similar to iron sucrose.

We first found iron sucrose to dose-dependently increase CD86 surface expression on classical and intermediate monocytes and to significantly reduce CD16 expression on classical monocytes, whereas monocyte subset distribution and CD14 expression were not changed (Figure 5, Supplementary Table S1). Ferric carboxymaltose, iron isomaltoside 1000, low-molecular-weight iron dextran and ferumoxytol affected neither monocyte subset distribution nor expression of CD14, CD16 or CD86 on monocyte subsets (Supplementary Table S1).

Effect of iron preparations on monocytic chemokine receptor expression and functional characteristics on monocytes from CKD patients

CX₃CR1 expression was dose-dependently reduced by iron sucrose, while CCR5 expression and ROS production were not significantly altered. Ferric carboxymaltose, iron isomaltoside 1000, low-molecular-weight iron dextran and ferumoxytol affected neither chemokine receptor expression nor ROS production (Supplementary Table S1).

Next, we found a significant reduction of the phagocytosis capacity of classical monocytes after stimulation with iron sucrose (Figure 6A). Moreover, T-cell proliferation was heterogeneously affected by different iron preparations in different dosages (Figure 6B). Finally, compared with the other four iron preparations, iron sucrose is more avidly taken up by monocytes as found in the calcein assay (Supplementary Figure S1).

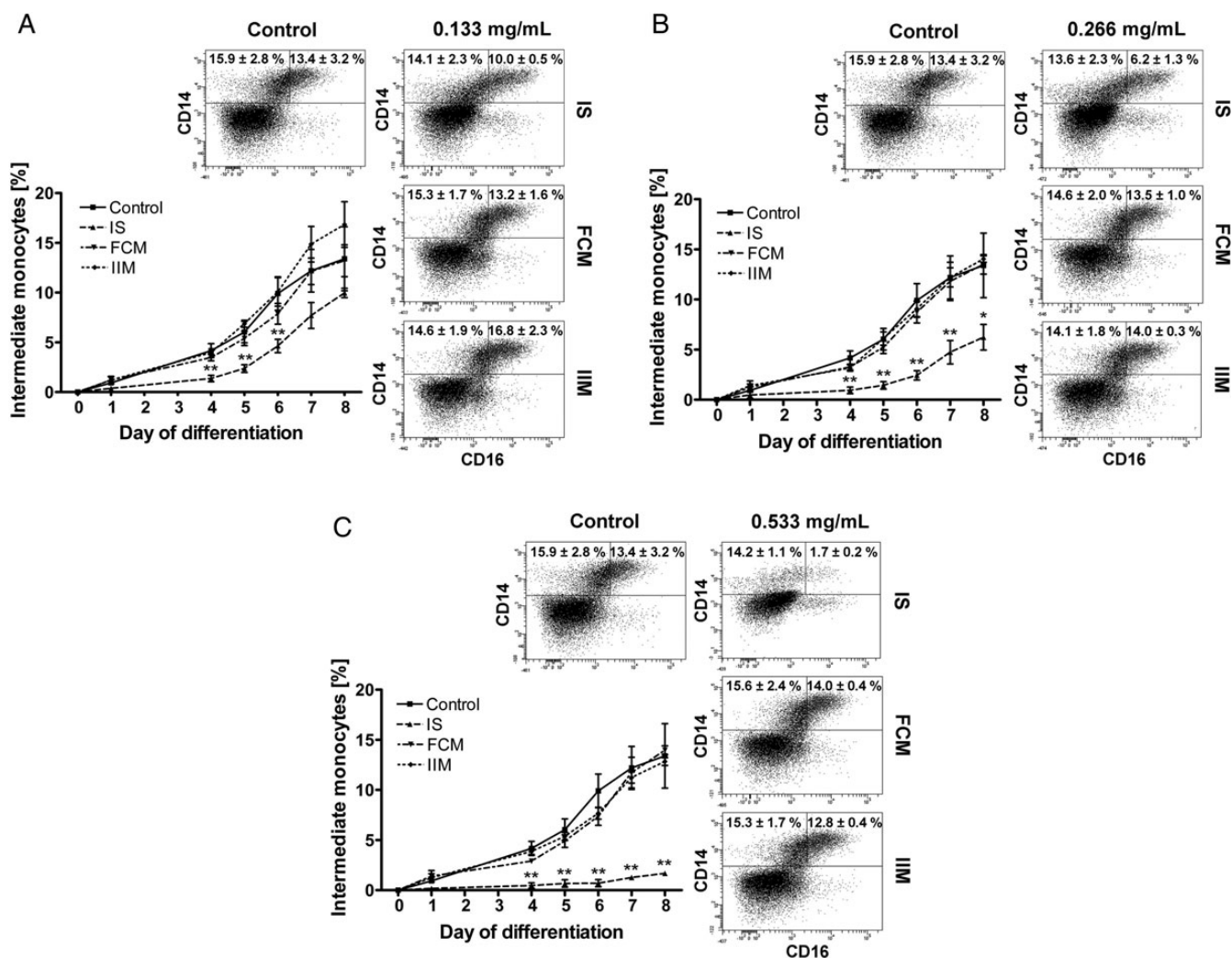


FIGURE 4: *In vitro* differentiation of haematopoietic CD34⁺ stem cells into classical and intermediate monocytes after stimulation with iron sucrose (IS), ferric carboxymaltose (FCM) or iron isomaltoside 1000 (IIM) [0.133 mg/mL (A), 0.266 mg/mL (B) and 0.533 mg/mL (C)]. Iron preparations were added at Day 0. Blood was collected from control subjects. Statistical analysis was performed using ANOVA and the Dunnett's multiple comparison test as *post hoc* test; data of three independent experiments are presented as mean ± SEM; *P < 0.05, **P < 0.01.

In summary, effects of iron sucrose on monocytes from patients with severe CKD were in line with effects observed in monocytes from subjects without overt CKD. For technical reasons we did not analyse *in vitro* differentiation of monocytes from haematopoietic CD34⁺ stem cells and monocytic viability.

DISCUSSION

Use of *i.v.* iron preparations for anaemia treatment has attracted substantial interest in recent years. Despite an inverse association between haemoglobin levels and cardiovascular event rate [25, 26] and mortality [27] in observational studies, large intervention trials that used erythropoietin or other erythropoietin-stimulating agents (ESA) for normalizing haemoglobin levels in CKD patients failed to reduce cardiovascular events and death. Therefore, recent KDIGO consensus

guidelines advocate the use of iron supplements with the aim both to increase haemoglobin and to reduce ESA doses [1]. Moreover KDIGO guidelines acknowledge the need for *i.v.* iron supplements in dialysis patients, in whom gastrointestinal absorption of oral iron supplements is generally poor [1].

The increasing use of *i.v.* iron preparations necessitates a critical analysis of their side effects [28, 29], which are mainly attributed to the abruptly increasing amount of NTBI ('free iron') after *i.v.* iron infusion.

It has long been acknowledged that *i.v.* iron preparations impair leukocyte immune function and trigger bacterial infections [17]. Interestingly, previous experimental work focussed on the effect of *i.v.* iron preparations on neutrophil biology, whereas their impact on monocytes received little interest in the past.

Against this background, we now analysed the effect of the three different *i.v.* iron preparations, iron sucrose, ferric carboxymaltose and iron isomaltoside 1000, in both therapeutically

Table 3. Expression of CD14, CD16 and CD86 on classical and intermediate monocytes after differentiation from haematopoietic stem cells from control subjects

Monocyte subset		Control	Iron sucrose			Ferric carboxymaltose			Iron isomaltoside 1000		
			0.133 mg/mL	0.266 mg/mL	0.533 mg/mL	0.133 mg/mL	0.266 mg/mL	0.533 mg/mL	0.133 mg/mL	0.266 mg/mL	0.533 mg/mL
CD14	Classical monocytes	10 546 ± 394	6835 ± 702*	7027 ± 536	6088 ± 1474*	7329 ± 218**	7050 ± 264**	7842 ± 726**	8352 ± 469	7376 ± 430**	8528 ± 830
	Intermediate monocytes	25 929 ± 2713	19 929 ± 820	18 009 ± 348*	17 709 ± 1948*	19 417 ± 1022	19 272 ± 801	20 952 ± 1991	21 481 ± 1579	19 247 ± 1429	20 862 ± 2394
CD16	Classical monocytes	1147 ± 33	867 ± 32**	769 ± 60**	630 ± 35**	1335 ± 88	1342 ± 121	1316 ± 81	1232 ± 140	1272 ± 82	1177 ± 104
	Intermediate monocytes	5549 ± 638	6462 ± 103	5654 ± 445	4806 ± 475	5125 ± 355	5173 ± 225	5227 ± 86	7327 ± 1545	5801 ± 83	5364 ± 164
CD86	Classical monocytes	838 ± 106	945 ± 15	1259 ± 110*	1659 ± 91**	940 ± 118	964 ± 102	894 ± 60	707 ± 57	779 ± 54	762 ± 19
	Intermediate monocytes	3178 ± 550	3074 ± 462	3370 ± 380	3654 ± 816	3819 ± 563	3814 ± 555	3233 ± 285	2751 ± 42	3011 ± 199	2834 ± 170

Indicated are mean fluorescence intensity [MFI] ± SEM; *n* = 3**P* < 0.05, ***P* < 0.01**Table 4.** Expression of CCR5 and CX₃CR1 and ROS production by *in vitro* differentiated classical and intermediate monocytes from control subjects

Monocyte subset		Control	Iron sucrose			Ferric carboxymaltose			Iron isomaltoside 1000		
			0.133 mg/mL	0.266 mg/mL	0.533 mg/mL	0.133 mg/mL	0.266 mg/mL	0.533 mg/mL	0.133 mg/mL	0.266 mg/mL	0.533 mg/mL
CCR5	Classical monocytes	643 ± 154	433 ± 62	418 ± 44	337 ± 5	599 ± 112	547 ± 107	551 ± 110	508 ± 115	519 ± 97	524 ± 116
	Intermediate monocytes	1365 ± 195	1274 ± 103	1135 ± 133	862 ± 15	1326 ± 142	1291 ± 139	1285 ± 190	1246 ± 120	1247 ± 142	1278 ± 219
CX ₃ CR1	Classical monocytes	3982 ± 370	5936 ± 386	6057 ± 678	3308 ± 510	4980 ± 117	5481 ± 164*	5415 ± 326*	5304 ± 1085	5029 ± 588	4731 ± 463
	Intermediate monocytes	5602 ± 420	10 118 ± 491*	10 906 ± 957**	7885 ± 1148	6961 ± 183*	7612 ± 182**	7506 ± 395**	7869 ± 1943	7064 ± 718	6570 ± 483
ROS	Classical monocytes	2714 ± 919	7471 ± 2622	8710 ± 3032	10 715 ± 4186	5104 ± 1888	5550 ± 2158	5831 ± 2147	3697 ± 1160	4103 ± 1384	4959 ± 1724
	Intermediate monocytes	3628 ± 1141	10 642 ± 3877	12 392 ± 4802	11 998 ± 5096	7231 ± 2547	7635 ± 2820	8783 ± 3102	5347 ± 1580	5910 ± 1886	7044 ± 2453

Indicated are mean fluorescence intensity [MFI] ± SEM; *n* = 3**P* < 0.05, ***P* < 0.01

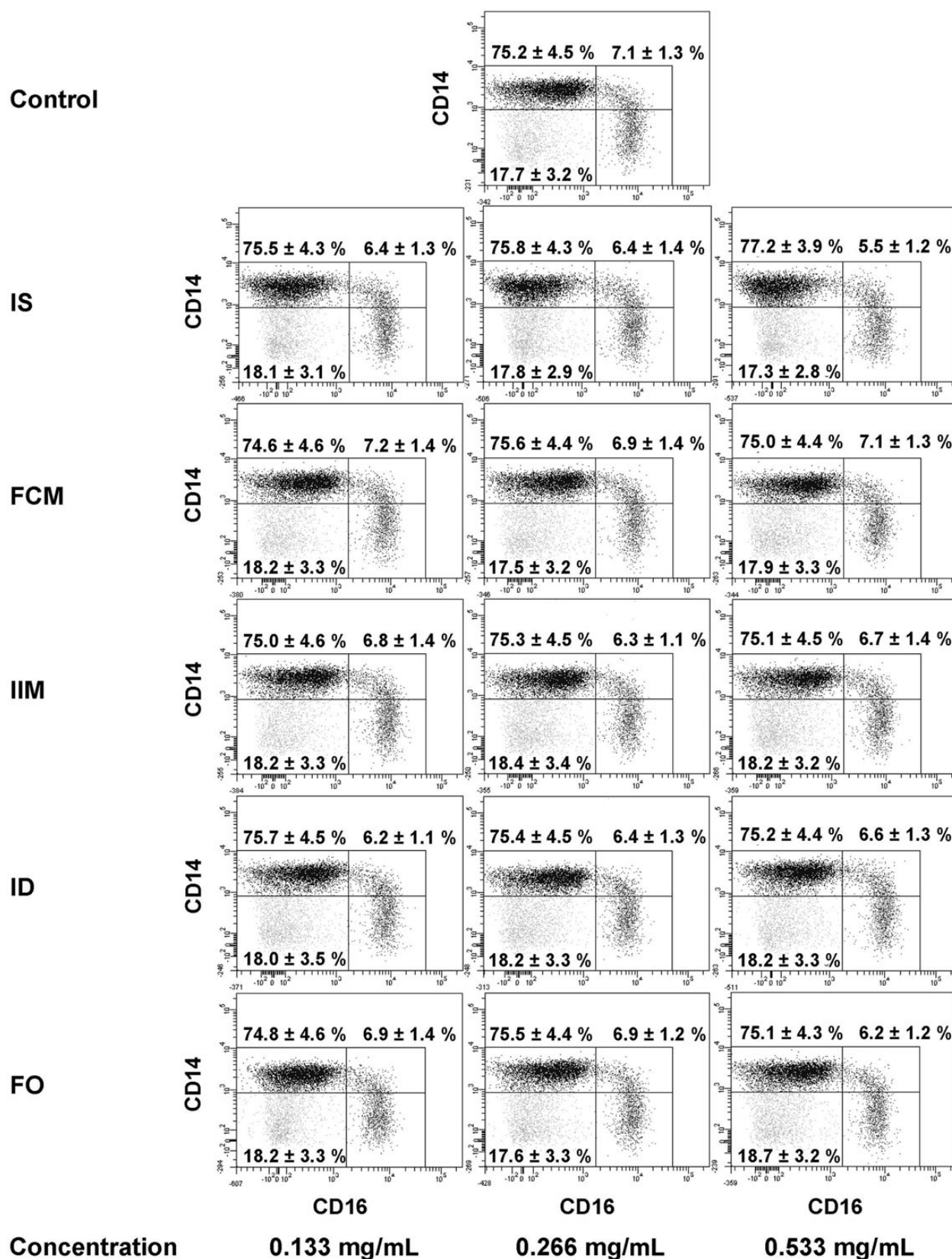


FIGURE 5: Representative example of monocyte subset distribution after stimulation with iron sucrose (IS), ferric carboxymaltose (FCM), iron isomaltoside 1000 (ISM), low-molecular-weight iron dextran (ID) and ferumoxytol (FO) (0.133, 0.266 and 0.533 mg/mL). Blood was collected from patients with severe CKD. Classical monocytes are shown in the upper left gate, intermediate monocytes in the upper right gate and nonclassical monocytes in the lower right gate of each dot plot. Statistical analysis was performed for each iron preparation using ANOVA, followed by Dunnett's multiple comparison test as *post hoc* test; data of eight independent experiments are presented as mean ± SEM.

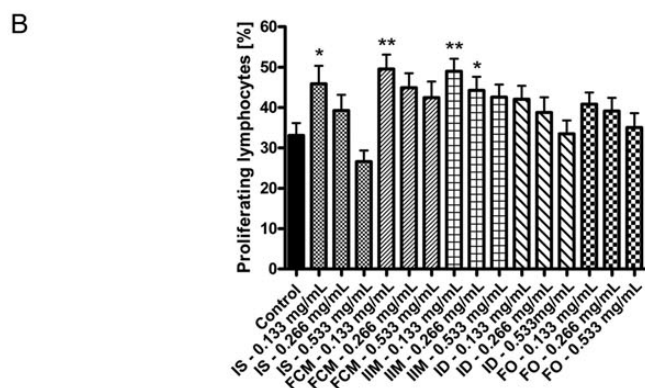
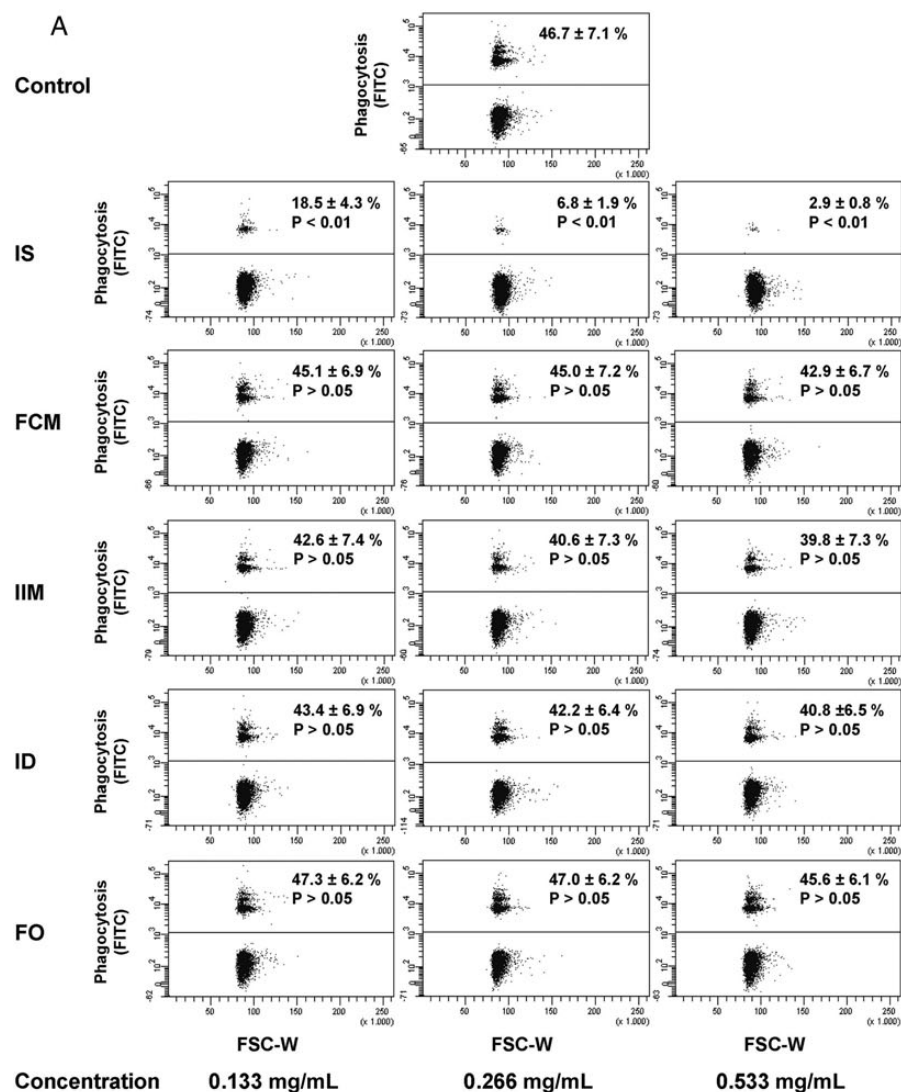


FIGURE 6: (A) Representative example of classical monocytes to phagocyte opsonized carboxylate microspheres (0.75 μ m, Yellow Green) within 30 min after stimulation with iron sucrose (IS), ferric carboxymaltose (FCM), iron isomaltoside 1000 (IIM), low-molecular-weight iron dextran (ID) and ferumoxytol (FO) (0.133, 0.266 and 0.533 mg/mL). Blood was collected from patients with severe CKD. Counts of FITC-positive cells (upper population) were determined flow cytometrically and statistical analysis was performed for each iron preparation by using ANOVA followed by Dunnett's multiple comparison test as *post hoc* test; data of eight independent experiments are presented as mean \pm SEM. **(B).** Flow cytometric analysis of T-cell proliferation after stimulation with staphylococcal enterotoxin B (SEB) (2.5 μ g/mL) and the different iron preparations iron sucrose (IS), ferric carboxymaltose (FCM) and iron isomaltoside 1000 (IIM), low-molecular-weight iron dextran (ID) and ferumoxytol (FO) (0.133, 0.266 and 0.533 mg/mL) for 3 days. Blood was collected from patients with severe CKD. Statistical analysis was performed for each iron preparation by using ANOVA followed by Dunnett's multiple comparison test as *post hoc* test; data of eight independent experiments are presented as mean \pm SEM; *P < 0.05, **P < 0.01.

recommended and suprathreshold dosages on monocytes from control subjects *in vitro*. To verify the relevance of these effects in clinical nephrology, we further tested the immunological *in vitro* effects of these three preparations on monocytes collected from patients with severe CKD; this additionally allowed us to test two further preparations, namely low-molecular-weight iron dextran and ferumoxytol. Iron sucrose induced significant changes in monocytic immune function, which occurred even at lower, therapeutically recommended dosages, whereas ferric carboxymaltose, iron isomaltoside 1000, low-molecular-weight iron dextran and ferumoxytol had no relevant effects at any dosage. We first found that iron sucrose changed expression of CD16, without affecting subset distribution of mature circulating monocytes. In differentiation experiments, the reduced CD16 expression after *i.v.* iron sucrose stimulation occurred in conjunction with a dose-dependent inhibition of stem cell differentiation into classical and intermediate monocytes.

We next assessed the effect of iron stimulation on specific characteristics of intermediate monocytes, namely cytokine and ROS production and chemokine receptor expression. We hereby firstly confirmed that intermediate monocytes have the highest capacity to produce pro-inflammatory cytokines [30] and ROS [22]. Next, we found that iron sucrose tended to increase IL-1 β and ROS production. Interestingly, Martin-Malo *et al.* reported that iron sucrose and ferric carboxymaltose increased percentages of ROS-producing cells and apoptotic cells both *in vitro*—in PBMCs from healthy donors and patients CKD stage 5—and *in vivo* during haemodialysis sessions [31].

While intermediate monocytes are prone to production of pro-inflammatory cytokines and ROS, and to antigen presentation, classical monocytes have the highest phagocytosis capacity [32], which is verified in the present analysis. Confirming our hypothesis of an impaired monocytic function after iron sucrose stimulation, we found a dose-dependent reduction of phagocytosis even at the lowest dose. This effect is in line with previous studies testing the effect of iron sucrose on phagocytosis capacity of polymorphonuclear leukocytes [17, 33].

Taken together, only iron sucrose impaired monocytic functions *in vitro*. This may result from pharmacokinetic differences between *i.v.* iron preparations, which differ in their carbohydrate ligands, consequently their structural build-up, distinct molecular weights (iron sucrose: 140 100 Da, ferric carboxymaltose: 233 100 Da, iron isomaltoside 1000: 150 000 Da, low-molecular-weight iron dextran: 165 000 Da, ferumoxytol: 275 700 Da) [10] and half-lives (iron sucrose: 5.3 h; ferric carboxymaltose: 7.4–9.4 h, iron isomaltoside 1000: 23.2 h, low-molecular-weight iron dextran: 27–30 h, ferumoxytol: 14.7 h) [34, 35]. Among those iron preparations, iron sucrose has the lowest molecular weight, the shortest half-life and the lowest stability, which in conjunction determine the amount and the kinetic of free iron release. Moreover, in relation to the size of the iron particles, iron sucrose has the highest content of labile iron when compared with the other iron preparations [10, 36]. It is proposed that stable *i.v.* iron preparations, like ferric carboxymaltose, iron isomaltoside 1000, low-molecular-weight iron dextran and ferumoxytol, release few NTBI and are mainly taken up as complex by phagocytosis [37]. In

contrast, less stable iron preparations, such as iron sucrose, release higher levels of NTBI. Even though most of this free iron is taken up by transferrin and other proteins, some amount of NTBI may directly be taken up in an unregulated way by different cell types or freely translocate across cell membranes [34, 38, 39]. Intracellularly, ‘free iron’ constitutes the labile iron pool, consisting of iron that is not linked to its storage protein ferritin [13, 38]. This labile iron pool may induce distinct toxic effects such as ROS production and subsequently DNA damage and lipid peroxidation [40, 41].

In our work, we were able to demonstrate a more rapid uptake of iron sucrose compared with ferric carboxymaltose, iron isomaltoside 1000, low-molecular-weight iron dextran and ferumoxytol in all three monocyte subsets, using the calcein assay. These results are in line with the findings of Sonnweber *et al.* [19], who had shown that *i.v.* injected iron sucrose is taken up by monocytes and increases circulating ferritin levels resulting in an impaired monocytic immune function, cytokine expression and activation of the NF- κ B pathway.

Our study has several limitations. In most experiments, we incubated whole blood or blood cells only for 5 h for technical reasons: previous experiments have shown that monocyte subsets change their surface marker expression after a longer incubation period *in vitro*. This particularly affects surface expression of CD16, which renders flow cytometric distinction of monocyte subsets impossible. This short incubation time might have biased our study results, as monocyte effects of ferric carboxymaltose, iron isomaltoside 1000, low-molecular-weight iron dextran and ferumoxytol may become evident only after longer incubation. Nonetheless, even those experiments that lasted several days, e.g. *in vitro* differentiation of haematopoietic stem cells into monocytes, pointed towards a particular effect of iron sucrose on monocyte biology.

As a further limitation, we cannot formally prove the biological relevance of our study results. We deliberately chose to focus our study on *in vitro* effects of iron on mature circulating monocytes and haematopoietic stem cells. *In vivo* monocytes might be exposed to lower iron concentrations than in our *in vitro* analysis, after iron complexes may rapidly be taken up *in vivo* by cells of the reticuloendothelial system via endocytosis [37].

Nonetheless, given that monocytes are the central regulators of the innate immune systems, and that CKD by itself negatively affects monocytic functions, we are confident that repetitive infusion of iron sucrose for treatment of anaemia in CKD may be considered as potentially immunoactivating. To further unravel the biological impact of different iron preparations, a randomized controlled trial with clinical endpoints comparing iron sucrose and other *i.v.* iron preparations would be informative. Nonetheless, until such a trial will be initiated, *in vitro* data will be necessary in order to better appreciate the risk of distinct iron preparations.

Taken together, when comparing the *i.v.* iron preparations iron sucrose, ferric carboxymaltose, iron isomaltoside 1000, low-molecular-weight iron dextran and ferumoxytol, we found strong and selective immunologic effects of iron sucrose on monocyte subsets even at pharmacological dosages. These findings underscore the notion that each specific *i.v.* iron

preparations may exert particular biological functions and may confer specific side effects.

SUPPLEMENTARY DATA

Supplementary data are available online at <http://ndt.oxfordjournals.org>.

ACKNOWLEDGEMENTS

The organizational skills of Marie-Theres Blinn and Martina Wagner are deeply appreciated. The study was supported by a grant from Pharmacosmos (Holbaek, Denmark).

CONFLICT OF INTEREST STATEMENT

Study design, laboratory work and data interpretation were performed only by the authors. In addition, the manuscript was solely written by the authors. They declare that the results presented in this paper have not been published previously in whole or part, except in abstract format.

REFERENCES

- Group KDIGOAW. KDIGO clinical practice guideline for anemia in chronic kidney disease. *Kidney Int Suppl* 2012; 2: 279–335
- Drueke TB, Locatelli F, Clyne N *et al*. Normalization of hemoglobin level in patients with chronic kidney disease and anemia. *N Engl J Med* 2006; 355: 2071–2084
- Singh AK, Szczech L, Tang KL *et al*. Correction of anemia with epoetin alfa in chronic kidney disease. *N Engl J Med* 2006; 355: 2085–2098
- Pfeffer MA, Burdmann EA, Chen CY *et al*. A trial of darbepoetin alfa in type 2 diabetes and chronic kidney disease. *N Engl J Med* 2009; 361: 2019–2032
- Joshi AD, Holdford DA, Brophy DF *et al*. Utilization patterns of IV iron and erythropoiesis stimulating agents in anemic chronic kidney disease patients: a multihospital study. *Anemia* 2012; 2012: 248430
- Kalantar-Zadeh K, Regidor DL, McAllister CJ *et al*. Time-dependent associations between iron and mortality in hemodialysis patients. *J Am Soc Nephrol* 2005; 16: 3070–3080
- Theurl I, Theurl M, Seifert M *et al*. Autocrine formation of hepcidin induces iron retention in human monocytes. *Blood* 2008; 111: 2392–2399
- Alleyne M, Horne MK, Miller JL. Individualized treatment for iron-deficiency anemia in adults. *Am J Med* 2008; 121: 943–948
- Coyne DW, Kapoian T, Suki W *et al*. Ferric gluconate is highly efficacious in anemic hemodialysis patients with high serum ferritin and low transferrin saturation: results of the Dialysis Patients' Response to IV Iron with Elevated Ferritin (DRIVE) Study. *J Am Soc Nephrol* 2007; 18: 975–984
- Jahn MR, Andreassen HB, Futterer S *et al*. A comparative study of the physicochemical properties of iron isomaltoside 1000 (Monofer), a new intravenous iron preparation and its clinical implications. *Eur J Pharm Biopharm* 2011; 78: 480–491
- Li H, Wang SX. Intravenous iron sucrose in peritoneal dialysis patients with renal anemia. *Perit Dial Int* 2008; 28: 149–154
- Kooistra MP, Kersting S, Gosriwatana I *et al*. Nontransferrin-bound iron in the plasma of haemodialysis patients after intravenous iron saccharate infusion. *Eur J Clin Invest* 2002; 32(Suppl 1): 36–41
- Brisot P, Ropert M, Le Lan C *et al*. Non-transferrin bound iron: a key role in iron overload and iron toxicity. *Biochim Biophys Acta* 2012; 1820: 403–410
- Pai AB, Conner T, McQuade CR *et al*. Non-transferrin bound iron, cytokine activation and intracellular reactive oxygen species generation in hemodialysis patients receiving intravenous iron dextran or iron sucrose. *Biomaterials* 2011; 24: 603–613
- Collard K, White D, Copplestone A. The effect of maximum storage on iron status, oxidative stress and antioxidant protection in paediatric packed cell units. *Blood Transfus* 2013; 11: 419–425
- Vaziri ND. Roles of oxidative stress and antioxidant therapy in chronic kidney disease and hypertension. *Curr Opin Nephrol Hypertens* 2004; 13: 93–99
- Ichii H, Masuda Y, Hassanzadeh T *et al*. Iron sucrose impairs phagocytic function and promotes apoptosis in polymorphonuclear leukocytes. *Am J Nephrol* 2012; 36: 50–57
- Patruta SI, Edlinger R, Sunder-Plassmann G *et al*. Neutrophil impairment associated with iron therapy in hemodialysis patients with functional iron deficiency. *J Am Soc Nephrol* 1998; 9: 655–663
- Sonnweber T, Theurl I, Seifert M *et al*. Impact of iron treatment on immune effector function and cellular iron status of circulating monocytes in dialysis patients. *Nephrol Dial Transplant* 2011; 26: 977–987
- Weiss G. Iron metabolism in the anemia of chronic disease. *Biochim Biophys Acta* 2009; 1790: 682–693
- Ziegler-Heitbrock L, Ancuta P, Crowe S *et al*. Nomenclature of monocytes and dendritic cells in blood. *Blood* 2010; 116: e74–e80
- Zawada AM, Rogacev KS, Rotter B *et al*. SuperSAGE evidence for CD14++CD16+ monocytes as a third monocyte subset. *Blood* 2011; 118: e50–e61
- Rogacev KS, Seiler S, Zawada AM *et al*. CD14++CD16+ monocytes and cardiovascular outcome in patients with chronic kidney disease. *Eur Heart J* 2011; 32: 84–92
- Bailie GR, Larkina M, Goodkin DA *et al*. Variation in intravenous iron use internationally and over time: the Dialysis Outcomes and Practice Patterns Study (DOPPS). *Nephrol Dial Transplant* 2013; 28: 2570–2579
- Foley RN, Parfrey PS, Harnett JD *et al*. The impact of anemia on cardiomyopathy, morbidity, and mortality in end-stage renal disease. *Am J Kidney Dis* 1996; 28: 53–61
- Harnett JD, Foley RN, Kent GM *et al*. Congestive heart failure in dialysis patients: prevalence, incidence, prognosis and risk factors. *Kidney Int* 1995; 47: 884–890
- Regidor DL, Kopple JD, Kovesdy CP *et al*. Associations between changes in hemoglobin and administered erythropoiesis-stimulating agent and survival in hemodialysis patients. *J Am Soc Nephrol* 2006; 17: 1181–1191
- Zager RA, Johnson AC, Hanson SY *et al*. Parenteral iron formulations: a comparative toxicologic analysis and mechanisms of cell injury. *Am J Kidney Dis* 2002; 40: 90–103
- Macdougall IC, Geisser P. Use of intravenous iron supplementation in chronic kidney disease: an update. *Iran J Kidney Dis* 2013; 7: 9–22
- Belge KU, Dayyani F, Horelt A *et al*. The proinflammatory CD14+CD16+DR++ monocytes are a major source of TNF. *J Immunol* 2002; 168: 3536–3542
- Martin-Malo A, Merino A, Carracedo J *et al*. Effects of intravenous iron on mononuclear cells during the haemodialysis session. *Nephrol Dial Transplant* 2012; 27: 2465–2471
- Zawada AM, Rogacev KS, Schirmer SH *et al*. Monocyte heterogeneity in human cardiovascular disease. *Immunobiology* 2012; 217: 1273–1284
- Deicher R, Ziai F, Cohen G *et al*. High-dose parenteral iron sucrose depresses neutrophil intracellular killing capacity. *Kidney Int* 2003; 64: 728–736
- Geisser P, Burckhardt S. The pharmacokinetics and pharmacodynamics of iron preparations. *Pharmaceutics* 2011; 3: 12–33
- Nordfeld K, Andreassen H, Thomsen LL. Pharmacokinetics of iron isomaltoside 1000 in patients with inflammatory bowel disease. *Drug Des Devel Ther* 2012; 6: 43–51

36. Futterer S, Andrusenko I, Kolb U *et al.* Structural characterization of iron oxide/hydroxide nanoparticles in nine different parenteral drugs for the treatment of iron deficiency anaemia by electron diffraction (ED) and X-ray powder diffraction (XRPD). *J Pharm Biomed Anal* 2013; 86: 151–160
37. Danielson BG. Structure, chemistry, and pharmacokinetics of intravenous iron agents. *J Am Soc Nephrol* 2004; 15(Suppl 2): S93–S98
38. Cabantchik ZI, Breuer W, Zanninelli G *et al.* LPI-labile plasma iron in iron overload. *Best Pract Res Clin Haematol* 2005; 18: 277–287
39. Pootrakul P, Breuer W, Sametband M *et al.* Labile plasma iron (LPI) as an indicator of chelatable plasma redox activity in iron-overloaded beta-thalassemia/HbE patients treated with an oral chelator. *Blood* 2004; 104: 1504–1510
40. Evans RW, Rafique R, Zarea A *et al.* Nature of non-transferrin-bound iron: studies on iron citrate complexes and thalassemic sera. *J Biol Inorg Chem* 2008; 13: 57–74
41. Chrichton RR, Danielson BG, Geisser P. *Iron Therapy with Special Emphasis on Intravenous Administration*. Bremen, Germany: UNI-MED Science, 2008

Received for publication: 25.7.2013; Accepted in revised form: 13.12.2013

Beitrag der Mitautoren für die Arbeit:

Lisa H. Fell, Sarah Seiler, Björn Rotter, Peter Winter, Martina Sester, Danilo Fliser, Gunnar H. Heine*, Adam M. Zawada* (2015) Impact of individual *i.v.* iron preparations on the differentiation of monocytes towards macrophages and dendritic cells, eingereicht (*geteilte Letztautorenschaft)

Diese Studie wurde von Frau Lisa Fell, Frau Prof. Dr. Martina Sester, Frau PD Dr. Sarah Seiler sowie von Herrn Prof. Dr. Gunnar Heine und Herrn Dr. Adam Zawada entworfen und geplant. Die Probandenrekrutierung und die Laborarbeit in Homburg erfolgte durch Frau Lisa Fell. Die microRNA Analyse und die statistische Auswertung dieser Daten führten Herr Dr. Björn Rotter und Herr Dr. Peter Winter durch. Frau Lisa Fell, Frau Prof. Dr. Martina Sester, Frau PD Dr. Sarah Seiler, Herr Prof. Dr. Danilo Fliser, sowie Herr Prof. Dr. Gunnar Heine und Herr Dr. Adam Zawada haben an der statistischen Auswertung der Daten und deren Interpretation mitgewirkt. Das Manuskript wurde von Frau Lisa Fell, Frau PD Dr. Sarah Seiler, Herrn Prof. Dr. Gunnar Heine und Herrn Dr. Adam Zawada geschrieben.

Die oben aufgeführten Autoren haben die finale Version des Manuskripts gelesen, kritisch überarbeitet und ihr zugestimmt.

Impact of individual intravenous iron preparations on the differentiation of monocytes towards macrophages and dendritic cells

Running title: Iron preparations and leukocytes

Lisa H. Fell¹, Sarah Seiler¹, Björn Rotter², Peter Winter², Martina Sester³, Danilo Fliser¹,
Gunnar H. Heine^{1,*}, Adam M. Zawada^{1,*}

*Both authors contributed equally

¹Department of Internal Medicine IV – Nephrology and Hypertension, Saarland University Medical Center, Homburg, Germany;

²GenXPro GmbH, Frankfurt am Main, Germany;

³Department of Transplant and Infection Immunology, Saarland University Medical Center, Homburg, Germany

Corresponding author:

Prof. Dr. Gunnar H. Heine

Department of Internal Medicine IV - Nephrology and Hypertension

Saarland University Medical Center, Homburg, Germany

Phone +49-6841-1623527

Fax +49-6841-1623545

Gunnar.Heine@uks.eu

Word count abstract: 229

Word count text: 3489

ABSTRACT

Background

Treatment of iron deficiency with intravenous (*i.v.*) iron is a first-line strategy to improve anaemia of chronic kidney disease. Previous *in vitro* experiments demonstrated that different *i.v.* iron preparations inhibit differentiation of hematopoietic stem cells to monocytes, but their effect on monocyte differentiation to macrophages and mature dendritic cells (mDCs) has not been assessed. We now investigated substance-specific effects of iron sucrose (IS), sodium ferric gluconate (SFG), ferric carboxymaltose (FCM), and iron isomaltoside 1000 (IIM) on monocytic differentiation to M1/M2 macrophages and mDCs.

Methods

Via flow-cytometry and miRNA expression analysis, we morphologically and functionally characterised monocyte differentiation to M1/M2 macrophages and mDCs after monocyte stimulation with IS, SFG, FCM and IIM (0.133 mg/mL, 0.266 mg/mL, 0.533 mg/mL, respectively).

Results

Phenotypically, IS and SFG dysregulated the expression of macrophage (e.g. CD40, CD163) and mDC (e.g. CD1c, CD141) surface markers. Functionally, IS and SFG impaired macrophage phagocytosis capacity and increased the ability of mDCs to stimulate T-cell proliferation. Phenotypic and functional alterations were less pronounced with FCM, and virtually absent with IIM. In miRNA expression analysis of mDCs, IS dysregulated miRNAs as miR-146b-5p and miR-155-5p which are linked to toll-like receptor and MAPK signalling pathways.

Conclusions

This *in vitro* study demonstrates that less stable *i.v.* iron preparations specifically affect monocyte differentiation towards macrophages and mDCs. The *in vivo* relevance of these findings should be delineated in future clinical trials.

KEYWORD

CKD, Dendritic cells, immune deficiency, infection, iron therapy, macrophages

SUMMARY

Treatment of iron deficiency with intravenous (*i.v.*) iron preparations can improve anaemia and quality of life in patients with chronic kidney disease (CKD). In this *in vitro* study, we investigated the substance-specific effects of iron sucrose, sodium ferric gluconate, ferric carboxymaltose, and iron isomaltoside 1000 on monocyte differentiation into macrophages and dendritic cells. We found that less stable *i.v.* iron preparations like iron sucrose and sodium ferric gluconate strongly change phenotype and function of M1 and M2 macrophages, and dendritic cells, whereas the other preparations had less or no relevant effects.

INTRODUCTION

Iron deficiency is a common contributor to anaemia of chronic kidney disease (CKD) [1]. Oral iron preparations often fail to replete iron stores at least in advanced CKD patients, who have chronic micro-inflammation with subsequently high plasma hepcidin levels. In enterocytes, hepcidin leads to internalisation and degradation of the central iron transport protein ferroportin, which impedes intestinal absorption of iron salts after oral intake [2, 3]. In contrast, intravenous (*i.v.*) iron preparations allow effective administration of high iron doses [4], which are generally considered to be well tolerated [5, 6].

In recent years, the clinical use of *i.v.* iron preparations has substantially increased [7]. In parallel, awareness of their potential systemic side effects rose, which may include renal, cardiovascular and immunologic reactions [8-10].

Several *i.v.* iron preparations are in clinical use, mostly as iron-carbohydrate-complexes; these iron preparations vary in their carbohydrate ligands and therefore differ in molecular weight, reactivity, thermodynamic stability and half-lives [11-13]. We and others have recently proposed that these various *i.v.* iron preparations may have different safety profiles [14, 15]. In a previous *in vitro* study, we found that less stable *i.v.* iron preparations, such as iron sucrose, induce phenotypical and functional monocytic alterations, which may directly be caused by their low stability and their consecutively accelerated uptake by monocytes [14].

Originating from myeloid precursors, monocytes play a central role physiologically in host defence [16] and pathophysiologically in numerous inflammatory diseases [17]. In both scenarios, *via* growth factor- and cytokine-induced adhesion and transendothelial migration, circulating monocytes are recruited into tissues, where they differentiate into macrophages and dendritic cells (DCs) [18].

Against this background, we now aimed to investigate the impact of different *i.v.* iron preparations on recruitment of monocytes from the bloodstream into tissues. We further characterised monocytic differentiation into macrophages and DCs by phenotypical and

functional assays. These findings were connected to gene regulation by analysing microRNA (miRNA) expression profiles in DCs.

SUBJECTS AND METHODS

Subjects

For *in vitro* experiments, we recruited control subjects (4 to 6 subjects per experiment). All participants gave informed consent. The study protocol was approved by the local Ethics Committee and was conducted in accordance with the Declaration of Helsinki.

Iron preparations

The following *i.v.* iron preparations were used in the present study: iron sucrose (Venofer[®]), ferric carboxymaltose (Ferinject[®]) (both from Vifor Pharma AG, Glattbrugg, Switzerland), sodium ferric gluconate (Ferrlecit[®]) (Aventis Pharma Deutschland GmbH) and iron isomaltoside 1000 (MonoFer[®]) (from Pharmacosmos, Holbæk, Denmark) in three concentrations: 0.133 mg/mL, 0.266 mg/mL and 0.533 mg/mL, which correspond in a 70 kg individual to a pharmacological application of ~ 400, ~ 800 and ~1600 mg iron.

Monocyte isolation

Peripheral blood mononuclear cells (PBMCs) were isolated from EDTA (Ethylenediaminetetraacetic acid) anticoagulated blood by Ficoll-Paque (Lymphocyte Separation Medium; PAA, Cölbe, Germany) gradient density centrifugation. For differentiation experiments, PBMCs (1×10^6 PBMCs/cm² for macrophages or 2.5×10^6 PBMCs/cm² for mDCs) were incubated in monocyte attachment medium (Promocell, Heidelberg, Germany) at 37°C. After 1 h non-adherent cells were washed away with RPMI 1640 (Sigma-Aldrich, Taufkirchen, Germany) and adherent monocytes were used for differentiation. For adhesion and transmigration assays, monocytes were isolated with the pan monocyte isolation kit (Miltenyi Biotec, Bergisch Gladbach, Germany) according to manufacturer's protocol.

Monocytic adhesion assay

To test monocytic adhesion on endothelial cells, isolated monocytes were stimulated with *i.v.* iron preparations for 3 h at 37°C (3×10^5 monocytes per condition) and then washed with RPMI 1640. Human umbilical vein endothelial cells (HUVECs) were cultured in endothelial cell media in fibronectin (both from PromoCell) coated 12-well plates. HUVEC monolayers were washed with RPMI 1640 before iron stimulated monocytes were added. After 30 min incubation, non-adherent monocytes were washed away with RPMI 1640 and the number of adherent monocytes was evaluated by phase contrast microscopy (Biozero BZ-8000, Keyence, Neu-Isenburg, Germany) in 10 microscopic fields per sample.

Monocyte transmigration assay

To analyse monocytic migration potential, isolated monocytes were stimulated with *i.v.* iron preparations for 3 h at 37°C (5×10^5 monocytes per condition), washed twice in RPMI 1640 and labelled with anti-CD45 antibody (**Table S1**) for 1 h at 37°C. Cells were seeded into the upper chamber of Millicell hanging inserts (8 µm pore size, Millipore, Schwalbach, Germany), which were placed in 24-well plates. Lower chambers were filled with RPMI 1640 enriched with 50 ng/mL MCP-1 (monocyte chemotactic protein-1, Biolegend, Fell, Germany). After 60 min at 37°C, the number of transmigrated cells was evaluated by fluorescence microscopy in 10 microscopic fields per sample.

***in vitro* differentiation of monocytes into mDCs**

For DC differentiation, monocytes were incubated in DC Generation Medium (PromoCell, provided with Cytokine Mix A/B), enriched with Cytokine Mix A and supplemented with *i.v.* iron preparations, at 37°C and 5% CO₂. Medium was changed after 3 days. On day 6 Cytokine Mix B was added to induce maturation of DCs; experiments were performed on day 8.

***in vitro* differentiation of monocytes into macrophages**

Macrophages were generated according to Martinez et al. (2006) [19]. Isolated monocytes were incubated in RPMI 1640, enriched with 100 ng/mL M-CSF and 20% FBS (fetal bovine serum, Life Technologies, Darmstadt, Germany) and supplemented with *i.v.* iron preparations for 7 days at 37°C and 5% CO₂. For polarisation into M1/M2 macrophages, cells were incubated for 18 h in RPMI 1640 with 5% FBS, supplemented with iron preparations and 100 ng/mL LPS and 20 ng/mL IFN-γ for M1 polarisation or with 20 ng/mL IL-4 for M2 polarisation (Biolegend). For experiments, macrophages were detached with macrophage detachment solution (Promocell).

Flow-cytometric analyses

Expression of mDC markers (CD1c, CD141, CD80, CD83, CD86, CD1a, CD40, HLA-DR) and of macrophage markers (CD14, CD16, CD32, CD40, CD64, CD80, CD86, CD163, CD206, CD68) were quantified flow-cytometrically (FACS Canto II with FACSDiva Software; BD Biosciences, Heidelberg, Germany) as median fluorescence intensity (MFI). Cells were stained with appropriate antibodies (**Table S1**) for 15 min at 4°C, washed and fixed with paraformaldehyde (1%) (Sigma-Aldrich). For intracellular measurement of CD68, macrophages were fixed with paraformaldehyde (4%), washed with buffer, containing 0.1% saponin (Sigma-Aldrich), stained with anti-CD68 PE for 45 min at room temperature, washed and fixed with paraformaldehyde (1%).

Phagocytosis assay

Phagocytosis capacity of macrophages was assessed using Fluoresbrite yellow green carboxylate microspheres (0.75 µm, Polysciences, Eppelheim, Germany). Microspheres were opsonised with heterologous serum (adjusted to 10⁸ particles/mL with Krebs-Ringer solution) and gentle shaking for 30 min at 37°C. 20 µL opsonized particles were added to 100 µL of

cells and incubated for 30 min at 37°C with mild shaking. Phagocytosis capacity was determined flow-cytometrically as counts of FITC-positive cells.

T-cell proliferation assay

CD4⁺ and CD8⁺ T-cells were purified from PBMCs by negative selection with the naïve pan T-cell isolation kit (Miltenyi Biotech) and labelled with 5 µM CFDA-SE (Vybrant CFDA-SE Cell Tracer Kit; Life Technologies) for 10 min at 37°C. Stained T-cells were cultured with autologous mDCs (ratio of 5:1) in the presence of 2.5 µg/mL staphylococcal enterotoxin B (SEB; Sigma-Aldrich). After 3 days, counts of proliferating CD4⁺ and CD8⁺ T-cells were analysed flow-cytometrically by measuring CFDA-SE dilution, identifying T-cells by their CD3, CD4, CD8 expression (**Table S1**).

miRNA isolation and miRNA expression analysis

Genome-wide miRNA expression analysis in mDCs was performed with smallRNA-seq at GenXPRO GmbH as described previously [20]. Briefly, RNA was isolated with the miRNeasy mini kit (Qiagen, Hilden, Germany) according to manufacturer's protocol. For each condition, samples of 3 different subjects were pooled. For quantification of miRNA expression, small RNA-Seq libraries were analysed with omiRas [21]. Data processing started with 3'adaptor clipping by local alignment of the adaptor sequence to each read. Illumina's marked quality region was removed and reads were summarized to UniTags. After singletons were removed, remaining tags were mapped to human genome (hg19) with bowtie [22] and annotated with various models of coding and non-coding RNAs retrieved from the UCSC table browser. Tags mapping to exonic regions of coding genes were excluded and non-coding RNAs were quantified in each library. For tags mapping to multiple genomic loci the number of reads corresponding to the tag was divided by the number of mapping loci. To account for differences in sequencing depth, tag counts were normalized (tags per million

[tpm]) and differential expression was detected with DEGseq bioconductor package [23]. A p-value of $< 10^{-10}$ was considered statistically significant.

Statistics

Categorical variables are presented as counts (percentages), and continuous variables as mean \pm SEM (standard error of the mean). Statistical analysis was performed for each iron preparation using one-way analysis of variance (ANOVA), followed by Dunnett's test as post-hoc test. A p-value of < 0.05 was considered statistically significant.

RESULTS

Impact of iron preparations on monocytic adhesion and transmigration

We first aimed to analyse the impact of various concentrations of the four *i.v.* iron preparations iron sucrose (IS), sodium ferric gluconate (SFG), ferric carboxymaltose (FCM) and iron isomaltoside 1000 (IIM) on monocyte adhesion and MCP-1 mediated transmigration. We found IS and SFG to increase monocytic adhesion on activated HUVECs even at the lowest dosage, although the level of significance was not reached. FCM and IIM had not effects on monocytic adhesion. Monocytic transmigration was not substantially affected by any of the iron preparations (**Figure 1, S1**).

Effect of iron preparations on monocyte differentiation into macrophages

In order to test whether iron preparations affect macrophage differentiation, we *in vitro* differentiated monocytes into M1 and M2 macrophages under iron stimulation. Macrophages were characterized phenotypically by their expression of specific surface markers (CD68 [M1/M2 marker]; CD40, CD64, CD80, CD86 [M1 markers]; CD14, CD16, CD32, CD163, CD206 [M2 markers]), and functionally by their phagocytosis capacity.

IS significantly down-regulated the expression of CD40, CD80 and CD86 on M1 macrophages. SFG reduced the expression of these markers as well, albeit to a lesser degree. Likewise, IS and SFG impaired expression of CD68, CD16 and CD206 on M2 macrophages. In contrast, FCM and IIM did not significantly affect expression of M1 and M2 markers (**Table 1**).

In functional analysis, we found IS, SFG and FCM to strongly reduce the phagocytosis capacity of M1 macrophages (**Figure 2**), and - to a lesser extent - in M2 macrophages (**Figure S2**). IIM had no effect on the phagocytosis capacity of either M1 or M2 macrophages.

Impact of iron preparations on monocyte differentiation into mDCs

Next, we tested the effects of *i.v.* iron preparations on DC differentiation *in vitro*. Therefore, we differentiated isolated monocytes into mature DCs (mDCs) under iron stimulation and analysed phenotypical (expression of CD1c, CD141, CD80, CD83, CD86, CD1a, CD40 and HLA-DR) and functional characteristics (induction of T-cell proliferation) of mDCs.

We found that IS and SFG strongly decreased surface expression of CD1c, CD80, CD86, CD1a, and CD40 on mDCs, while the expression of CD141 and HLA-DR was significantly increased (**Figure 3A-H**). FCM significantly decreased CD1c expression, whereas stimulation with IIM did not affect the expression of any mDC marker.

For functional characterisation, we stimulated mDCs with SEB and co-cultured them with isolated T-cells to analyse the capacity of mDCs to induce T-cell proliferation. With all iron preparations, proliferation of total T-cells was slightly – but not significantly – increased (**Figure 3I**), whereas proliferation of the CD8⁺ T-cell subset was significantly induced by IS, SFG and FCM (**Figure 3J**).

Impact of IS and IIM on miRNA expression in mDCs

Finally we aimed to analyse whether the iron-induced changes in phenotypical and functional characteristics of mDCs may be linked to changes in miRNA expression, as miRNAs are centrally involved in the regulation of immune processes *via* posttranscriptional gene regulation. Therefore we performed ultra-deep miRNA sequencing with pooled small RNAs from mDCs differentiated under control conditions, under stimulation with 0.266 mg/mL IS and with 0.266 mg/mL IIM, thus yielding three independent miRNA expression libraries (“control”, “iron sucrose (IS)”, “iron isomaltoside 1000 (IIM)”).

After eliminating low quality reads and tags which were detected only once, total number of reads was 21,165,607, which allowed us to analyse 631 different miRNAs across the three

libraries (**Table S2**). The most differentially expressed miRNAs are listed in **Table 2a** (control vs IS), **2b** (control vs IIM) and **Table S3** (IIM vs IS).

Compared to control, only 33 miRNAs were differentially expressed in IIM stimulated mDCs, of which 10 were up-regulated and 23 down-regulated. In contrast, IS stimulation dysregulated 108 miRNAs in mDCs, of which 32 miRNAs were up-regulated and 76 down-regulated (**Figure 4**). Of these 108 miRNAs, 25 miRNAs were similarly affected by IIM stimulation (up-regulation with both iron preparations, or down-regulation with both preparations), but the effect size was generally more pronounced after IS stimulation.

In a pathway analysis [24, 25], these 25 miRNAs could be linked to specific cellular pathways, such as the toll-like receptor signalling pathway, the MAPK signalling pathway and the regulation of cell cycle (e.g. miR-146b-5p, miR-155-5p, miR-26a-5p). *Vice versa*, miRNAs which were specifically dysregulated after IS stimulation, but not after IIM stimulation, could be linked to the chemokine signalling pathway or the Jak-STAT signalling pathway (e.g. miR-126-3p, miR-148b-3p, miR-26b-5p). Finally, we identified several miRNAs differentially expressed after IS stimulation (miR-34c, let-7c, miR-671, miR-137) which could be linked to appropriate changes in surface protein expression (CD141, HLA-DR, CD83) on IS stimulated mDCs.

DISCUSSION

Anaemia of chronic kidney disease (CKD) substantially contributes to extrarenal comorbidity in patients with impaired renal function [26, 27]. Since low haemoglobin predicts adverse outcome among CKD patients [28], anaemia treatment with erythropoiesis-stimulating agents (ESA) had been a cornerstone of nephrological care for two decades. However, after several randomised trials failed to demonstrate a prognostic benefit of ESA treatment in CKD [29-31], the safety of this treatment strategy came into question. This led to significantly reduced prescription rates for ESA since 2008 and a subsequent drop in mean haemoglobin levels among CKD patients [7], rendering alternative treatment strategies for anaemia of CKD mandatory.

Against this background, the use of iron preparations regained popularity in the last decade [7]. Since there is a broad consensus that oral iron preparations are poorly absorbed at least in patients with advanced CKD, current guidelines recommend early application of intravenous (*i.v.*) iron preparations [32]. With its increasing clinical use, potential toxicological side effects of *i.v.* iron preparations, which may comprise untoward renal, cardiovascular and immunological reactions [29, 33, 34], gained broad interest in recent years [8-10]. It is still uncertain whether these toxicological side effects are drug-class effects, or preparation-specific effects.

We recently investigated the impact of different *i.v.* iron preparations on monocyte development and biology *in vitro* and found substance-specific immunological effects. Less stable iron preparations such as iron sucrose were rapidly taken up by cells and dose-dependently impaired differentiation of hematopoietic stem cells towards monocytes. Moreover, they reduced phagocytosis capacity of mature monocytes [14].

Of note, innate immunity regulation requires a close interplay of monocytes with their macrophage and dendritic cell progeny. Monocytes circulate for few days in the peripheral blood; thereafter, *via* endothelial attachment and subsequent transendothelial migration, they

may be recruited into tissues where they differentiate into macrophages and mature dendritic cells (mDCs) [18].

Against this background, we aimed to compare the impact of less stable (iron sucrose [IS] and sodium ferric gluconate [SFG]) and more stable (ferric carboxymaltose [FCM] and iron isomaltoside 1000 [IIM]) *i.v.* iron preparations on this transition of monocytes into macrophages and mDCs.

In our experiments we first analysed the two initial steps of differentiation, i.e. monocyte endothelial adhesion and migration. In general, more stable *i.v.* iron preparation – FCM and IIM – neither affected adhesion nor migration substantially. Instead, less stable *i.v.* iron preparations – IS and SFG – numerically increased monocytic adhesion, which is in line with recent experimental data from others: Kuo *et al.* demonstrated that IS increased the expression of intracellular cell adhesion molecule-1 (ICAM-1) and vascular cell adhesion molecule-1 (VCAM-1) in a NF- κ B depending pathway. The authors underscored the biological impact of their findings by murine models, in which IS accelerated early atherogenesis [35]. Kartikasari *et al.* found that iron loading of endothelial cells and monocytes promotes firm adhesion of human monocytes to the endothelium [36].

In vivo, adhesion and transmigration of monocytes is followed by their differentiation into either macrophages or DCs. There is general consensus that defence against pathogens such as bacteria, protozoa and viruses are mediated by M1 macrophages, whereas M2 macrophages exert anti-inflammatory functions and regulate wound healing [37]. Therefore, we next differentiated monocytes towards classically activated (M1), alternatively activated (M2) macrophages, or mDCs, respectively, under stimulation with the different *i.v.* iron preparations. To characterize M1 and M2 phenotypically, we assessed the expression of central surface markers, such as CD40 and the costimulatory molecules CD80 and CD86 for M1 macrophages, as well as Fc γ receptors CD16 and CD32, scavenger receptor CD163 and mannose receptor CD206 for M2 macrophages. The expression of these surface proteins,

which have crucial roles in pathogen recognition, T-cell stimulation and/or phagocytosis [38-40], was reduced by IS and SFG. Likewise, in functional assays macrophage phagocytosis capacity was substantially reduced after stimulation with IS and SFG, but not with more stable *i.v.* iron preparations. Comparably, earlier *in vitro* studies reported a reduced phagocytosis capacity of polymorphonuclear leukocytes and monocytes after IS stimulation [14, 41].

Similarly, we found substance-specific effects of *i.v.* iron preparations on mDCs: again, less stable preparations – IS, SFG – affected the phenotype of mDCs, as they down-regulated the surface expression of CD1c, CD80, CD83, CD86, CD40 and CD1a, and *vice versa* up-regulated CD141 and HLA-DR expression. FCM has less pronounced effects, and IIM again was immunologically neutral. In functional analyses we determined the capacity of mDCs to activate T-cells and to induce proliferation of T-cells. In line with our previous results [14] all iron preparations numerically increased proliferation of total T-cells. When analysing T-cell subtypes, IS, SFG and FCM stimulation of mDCs increased CD8⁺ T-cell proliferation, whereas IIM did not.

While the existence of macrophage subtypes is generally acknowledged, definition of DCs – particularly of myeloid mDCs – is less straightforward. It has been suggested that two phenotypically and functionally distinct types of myeloid mDCs may exist in blood and tissues, which have been defined as CD1c⁺ and CD141⁺ DCs [42, 43]. These cells are differentiated by a particular pattern of surface proteins: CD80, CD83, CD86, CD40 and CD1a are highly expressed on CD1c⁺ DCs, but not on CD141⁺ DCs, which themselves overexpress HLA-DR [44, 45]. Functionally, CD141⁺ and CD1c⁺ mDCs differ in their capacity to cross-present antigens to naïve T-cells, as CD141⁺ DCs show an increased ability to stimulate CD8⁺ T-cells [44]. Based upon our expression analyses and functional assays, we hypothesize that IS and SFG stimulation may induce major shifts in myeloid DC subtype distribution towards CD141⁺ DCs, although we cannot provide firm proof for this hypothesis.

To analyse underlying pathophysiological pathways of the observed immunological effects, we performed genome-wide miRNA expression analysis. miRNAs regulate the expression of many genes implicated in iron uptake, -storage and -utilisation [46]. We now aimed to analyse whether iron uptake by mononuclear cells may *vice versa* induce miRNA dysregulation with subsequent phenotypical and functional alterations of DCs.

Interestingly, IS had larger effects on miRNAs than IIM. This firstly comprises dysregulation of miRNAs which are linked to surface protein expression [47]. Next, IS down-regulated miR-let-7d, which has central functions in iron absorption and utilization [48], and several miRNAs that are strongly involved in inflammation, comprising miR-32, which is crucial for viral defense [49], miR-132, miR-146 and miR-155, which regulate central inflammatory pathways such as the toll like receptor (TLR) pathway [50].

Of note, several other miRNAs linked to iron uptake and metabolism were dysregulated after stimulation with both IS and IIM, such as miR-320 [51] and miR-210 [52, 53].

Our observations underscore the notion that different *i.v.* iron preparations may substance-specifically affect functions of mononuclear cells and confer compound-specific side effects, since less stable *i.v.* iron preparations induced more pronounced immunologic effects. These findings are in line with our previous data on monocyte biology [14].

We assume that these effects result from pharmacokinetic differences between *i.v.* iron preparations, which differ in their carbohydrate ligands, their structural build-up, molecular weights and therefore in their half-lives and stability. Collectively, these factors determine ferrokinetics, with more pronounced free iron release from IS and SFG than from FCM and IIM [11, 13, 14].

As a limitation, we deliberately focussed our analysis on myeloid differentiation of monocytes towards M1/M2 macrophages and mDCs, and did not analyse further subtypes of DCs, or other leukocyte subpopulations. One intention of our *in vitro* study was to define assays for

iron toxicity which may be applied later in clinical studies; we therefore aimed to circumscribe the assays' complexity.

In conclusion, our *in vitro* studies demonstrate that less stable *i.v.* iron preparations such as IS and SFG have a higher potential to modulate monocytes, macrophages and mDCs than more stable preparations such as FCM and particularly IIM. These findings are of interest, as numerous CKD patients presently receive repeated infusions of less stable iron preparations, which have been associated with a high burden of infectious complications [54]. As a next major step, we feel an imminent need to initiate randomised clinical trials which compare the effects of different *i.v.* iron preparations on laboratory surrogates of immune regulation, and subsequently on manifest clinical events.

ACKNOWLEDGMENTS

Organisational skills of Marie-Theres Blinn and laboratory assistance of Kathrin Untersteller are deeply appreciated.

CONFLICT OF INTEREST STATEMENT

The study was supported by a grant from Pharmacosmos (Holbaek, Denmark) and HOMFOR (Saarland University Medical Center, Homburg, Germany). Study design, laboratory work and data presentation was only performed by the authors.

We declare that the results presented in this paper have not been published previously in whole or part, except in abstract format.

SUPPLEMENTARY DATA

Figure S1. Monocytic adhesion and transmigration potential after stimulation with 0.266 mg/mL and 0.533 mg/mL iron sucrose, sodium ferric gluconate, ferric carboxymaltose or iron isomaltoside 1000.

Figure S2. Phagocytosis capacity of M2 macrophages after stimulation with iron sucrose, sodium ferric gluconate, ferric carboxymaltose or iron isomaltoside 1000.

Table S1. Antibodies used in this study for flow-cytometric and microscopic analysis.

Table S2. Raw data of microRNA analysis of monocyte derived mature dendritic cells in the control approach and after stimulation with iron sucrose and iron isomaltoside 1000.

Table S3. Comparative microRNA analysis of monocyte derived mature dendritic cells after stimulation with iron sucrose and iron isomaltoside 1000.

Supplementary data are available online at <http://ndt.oxfordjournals.org>.

REFERENCES

1. Group KDIGO KAW. KDIGO Clinical Practice Guideline for Anemia in Chronic Kidney Disease. *Kidney inter., Suppl.* 2012; 2: 279-335
2. Macdougall IC, Bock AH, Carrera F, *et al.* FIND-CKD: a randomized trial of intravenous ferric carboxymaltose versus oral iron in patients with chronic kidney disease and iron deficiency anaemia. *Nephrol Dial Transplant* 2014; 29(11): 2075-2084
3. Andrews NC. Closing the iron gate. *N Engl J Med* 2012; 366(4): 376-377
4. Coyne DW, Kapoian T, Suki W, *et al.* Ferric gluconate is highly efficacious in anemic hemodialysis patients with high serum ferritin and low transferrin saturation: results of the Dialysis Patients' Response to IV Iron with Elevated Ferritin (DRIVE) Study. *J Am Soc Nephrol* 2007; 18(3): 975-984
5. Zitt E, Sturm G, Kronenberg F, *et al.* Iron supplementation and mortality in incident dialysis patients: an observational study. *PLoS One* 2014; 9(12): e114144
6. Agarwal R. Nonhematological benefits of iron. *Am J Nephrol* 2007; 27(6): 565-571
7. Winkelmayer WC, Mitani AA, Goldstein BA, *et al.* Trends in anemia care in older patients approaching end-stage renal disease in the United States (1995-2010). *JAMA Intern Med* 2014; 174(5): 699-707
8. Fishbane S, Mathew A, Vaziri ND. Iron toxicity: relevance for dialysis patients. *Nephrol Dial Transplant* 2014; 29(2): 255-259
9. Vaziri ND. Understanding iron: promoting its safe use in patients with chronic kidney failure treated by hemodialysis. *Am J Kidney Dis* 2013; 61(6): 992-1000
10. Macdougall IC, Geisser P. Use of intravenous iron supplementation in chronic kidney disease: an update. *Iran J Kidney Dis* 2013; 7(1): 9-22
11. Geisser P, Burckhardt S. The Pharmacokinetics and Pharmacodynamics of Iron Preparations. *Pharmaceutics* 2011; 3(1): 12-33
12. Nordfjeld K, Andreassen H, Thomsen LL. Pharmacokinetics of iron isomaltoside 1000 in patients with inflammatory bowel disease. *Drug Des Devel Ther* 2012; 6: 43-51
13. Jahn MR, Andreassen HB, Futterer S, *et al.* A comparative study of the physicochemical properties of iron isomaltoside 1000 (Monofer), a new intravenous iron preparation and its clinical implications. *Eur J Pharm Biopharm* 2011; 78(3): 480-491
14. Fell LH, Zawada AM, Rogacev KS, *et al.* Distinct immunologic effects of different intravenous iron preparations on monocytes. *Nephrol Dial Transplant* 2014; 29(4): 809-822
15. Pai AB, Conner T, McQuade CR, *et al.* Non-transferrin bound iron, cytokine activation and intracellular reactive oxygen species generation in hemodialysis patients receiving intravenous iron dextran or iron sucrose. *Biometals* 2011; 24(4): 603-613
16. Serbina NV, Jia T, Hohl TM, *et al.* Monocyte-mediated defense against microbial pathogens. *Annu Rev Immunol* 2008; 26: 421-452
17. Woollard KJ, Geissmann F. Monocytes in atherosclerosis: subsets and functions. *Nat Rev Cardiol* 2010; 7(2): 77-86
18. Auffray C, Sieweke MH, Geissmann F. Blood monocytes: development, heterogeneity, and relationship with dendritic cells. *Annu Rev Immunol* 2009; 27: 669-692
19. Martinez FO, Gordon S, Locati M, *et al.* Transcriptional profiling of the human monocyte-to-macrophage differentiation and polarization: new molecules and patterns of gene expression. *J Immunol* 2006; 177(10): 7303-7311
20. Zawada AM, Rogacev KS, Muller S, *et al.* Massive analysis of cDNA Ends (MACE) and miRNA expression profiling identifies proatherogenic pathways in chronic kidney disease. *Epigenetics* 2014; 9(1): 161-172

21. Muller S, Rycak L, Winter P, *et al.* omiRas: a Web server for differential expression analysis of miRNAs derived from small RNA-Seq data. *Bioinformatics* 2013; 29(20): 2651-2652
22. Li H, Durbin R. Fast and accurate short read alignment with Burrows-Wheeler transform. *Bioinformatics* 2009; 25(14): 1754-1760
23. Wang L, Feng Z, Wang X, *et al.* DEGseq: an R package for identifying differentially expressed genes from RNA-seq data. *Bioinformatics* 2010; 26(1): 136-138
24. Vlachos IS, Kostoulas N, Vergoulis T, *et al.* DIANA miRPath v.2.0: investigating the combinatorial effect of microRNAs in pathways. *Nucleic Acids Res* 2012; 40(Web Server issue): W498-504
25. Paraskevopoulou MD, Georgakilas G, Kostoulas N, *et al.* DIANA-microT web server v5.0: service integration into miRNA functional analysis workflows. *Nucleic Acids Res* 2013; 41(Web Server issue): W169-173
26. Vlagopoulos PT, Tighiouart H, Weiner DE, *et al.* Anemia as a risk factor for cardiovascular disease and all-cause mortality in diabetes: the impact of chronic kidney disease. *J Am Soc Nephrol* 2005; 16(11): 3403-3410
27. Regidor DL, Kopple JD, Kovesdy CP, *et al.* Associations between changes in hemoglobin and administered erythropoiesis-stimulating agent and survival in hemodialysis patients. *J Am Soc Nephrol* 2006; 17(4): 1181-1191
28. Locatelli F, Pisoni RL, Combe C, *et al.* Anaemia in haemodialysis patients of five European countries: association with morbidity and mortality in the Dialysis Outcomes and Practice Patterns Study (DOPPS). *Nephrol Dial Transplant* 2004; 19(1): 121-132
29. Drueke TB, Locatelli F, Clyne N, *et al.* Normalization of hemoglobin level in patients with chronic kidney disease and anemia. *N Engl J Med* 2006; 355(20): 2071-2084
30. Singh AK, Szczech L, Tang KL, *et al.* Correction of anemia with epoetin alfa in chronic kidney disease. *N Engl J Med* 2006; 355(20): 2085-2098
31. Pfeffer MA, Burdmann EA, Chen CY, *et al.* A trial of darbepoetin alfa in type 2 diabetes and chronic kidney disease. *N Engl J Med* 2009; 361(21): 2019-2032
32. Padhi S, Glen J, Pordes BA, *et al.* Management of anaemia in chronic kidney disease: summary of updated NICE guidance. *BMJ* 2015; 350: h2258
33. Zager RA, Johnson AC, Hanson SY, *et al.* Parenteral iron formulations: a comparative toxicologic analysis and mechanisms of cell injury. *Am J Kidney Dis* 2002; 40(1): 90-103
34. Kamanna VS, Ganji SH, Shelkovnikov S, *et al.* Iron sucrose promotes endothelial injury and dysfunction and monocyte adhesion/infiltration. *Am J Nephrol* 2012; 35(2): 114-119
35. Kuo KL, Hung SC, Lee TS, *et al.* Iron sucrose accelerates early atherogenesis by increasing superoxide production and upregulating adhesion molecules in CKD. *J Am Soc Nephrol* 2014; 25(11): 2596-2606
36. Kartikasari AE, Visseren FL, Marx JJ, *et al.* Intracellular labile iron promotes firm adhesion of human monocytes to endothelium under flow and transendothelial migration: Iron and monocyte-endothelial cell interactions. *Atherosclerosis* 2009; 205(2): 369-375
37. Murray PJ, Wynn TA. Protective and pathogenic functions of macrophage subsets. *Nat Rev Immunol* 2011; 11(11): 723-737
38. Suttles J, Stout RD. Macrophage CD40 signaling: a pivotal regulator of disease protection and pathogenesis. *Semin Immunol* 2009; 21(5): 257-264
39. Taylor PR, Gordon S, Martinez-Pomares L. The mannose receptor: linking homeostasis and immunity through sugar recognition. *Trends Immunol* 2005; 26(2): 104-110
40. Aderem A, Underhill DM. Mechanisms of phagocytosis in macrophages. *Annu Rev Immunol* 1999; 17: 593-623

41. Ichii H, Masuda Y, Hassanzadeh T, *et al.* Iron sucrose impairs phagocytic function and promotes apoptosis in polymorphonuclear leukocytes. *Am J Nephrol* 2012; 36(1): 50-57
42. Ziegler-Heitbrock L, Ancuta P, Crowe S, *et al.* Nomenclature of monocytes and dendritic cells in blood. *Blood* 2010; 116(16): e74-80
43. Haniffa M, Shin A, Bigley V, *et al.* Human tissues contain CD141^{hi} cross-presenting dendritic cells with functional homology to mouse CD103⁺ nonlymphoid dendritic cells. *Immunity* 2012; 37(1): 60-73
44. Jongbloed SL, Kassianos AJ, McDonald KJ, *et al.* Human CD141⁺ (BDCA-3)⁺ dendritic cells (DCs) represent a unique myeloid DC subset that cross-presents necrotic cell antigens. *J Exp Med* 2010; 207(6): 1247-1260
45. Collin M, McGovern N, Haniffa M. Human dendritic cell subsets. *Immunology* 2013; 140(1): 22-30
46. Davis M, Clarke S. Influence of microRNA on the maintenance of human iron metabolism. *Nutrients* 2013; 5(7): 2611-2628
47. Wong N, Wang X. miRDB: an online resource for microRNA target prediction and functional annotations. *Nucleic Acids Res* 2015; 43(Database issue): D146-152
48. Andolfo I, Liguori L, De Antonellis P, *et al.* The micro-RNA 199b-5p regulatory circuit involves Hes1, CD15, and epigenetic modifications in medulloblastoma. *Neuro Oncol* 2012; 14(5): 596-612
49. O'Connell RM, Taganov KD, Boldin MP, *et al.* MicroRNA-155 is induced during the macrophage inflammatory response. *Proc Natl Acad Sci U S A* 2007; 104(5): 1604-1609
50. Taganov KD, Boldin MP, Chang KJ, *et al.* NF-kappaB-dependent induction of microRNA miR-146, an inhibitor targeted to signaling proteins of innate immune responses. *Proc Natl Acad Sci U S A* 2006; 103(33): 12481-12486
51. Schaar DG, Medina DJ, Moore DF, *et al.* miR-320 targets transferrin receptor 1 (CD71) and inhibits cell proliferation. *Exp Hematol* 2009; 37(2): 245-255
52. Chan SY, Zhang YY, Hemann C, *et al.* MicroRNA-210 controls mitochondrial metabolism during hypoxia by repressing the iron-sulfur cluster assembly proteins ISCU1/2. *Cell Metab* 2009; 10(4): 273-284
53. Yoshioka Y, Kosaka N, Ochiya T, *et al.* Micromanaging Iron Homeostasis: hypoxia-inducible micro-RNA-210 suppresses iron homeostasis-related proteins. *J Biol Chem* 2012; 287(41): 34110-34119
54. Brookhart MA, Freburger JK, Ellis AR, *et al.* Infection risk with bolus versus maintenance iron supplementation in hemodialysis patients. *J Am Soc Nephrol* 2013; 24(7): 1151-1158

TABLES

Table 1. Expression of CD68 (M1/M2 marker), CD40, CD64, CD80, CD86 (M1 markers) and CD14, CD16, CD32, CD163, CD206 (M2 markers) after *in vitro* differentiation of monocytes.

M1 macrophages													
	Control	IS [mg/mL]			SFG [mg/mL]			FCM [mg/mL]			IIM [mg/mL]		
		0.133	0.266	0.533	0.133	0.266	0.533	0.133	0.266	0.533	0.133	0.266	0.533
CD68	6421 ± 754	8932 ± 798	9016 ± 770	6599 ± 633	9194 ± 1066	7413 ± 837	8675 ± 956	6145 ± 1081	6716 ± 384	6807 ± 438	6016 ± 579	6601 ± 692	7032 ± 539
CD40	21013 ± 2754	17786 ± 1693	15861 ± 1360	7122 ± 984**	16660 ± 1296	12785 ± 1439**	11241 ± 889**	16496 ± 3145	18066 ± 2640	16887 ± 2232	19804 ± 4041	19658 ± 2956	20154 ± 2921
CD64	720 ± 92	785 ± 71	820 ± 59	540 ± 42	715 ± 58	615 ± 74	575 ± 50	642 ± 61	685 ± 64	727 ± 81	705 ± 122	676 ± 88	749 ± 96
CD80	288 ± 36	268 ± 16	268 ± 15	198 ± 18*	275 ± 16	246 ± 21	274 ± 18	238 ± 15	251 ± 28	252 ± 20	276 ± 45	267 ± 35	274 ± 31
CD86	898 ± 94	742 ± 81	744 ± 66	454 ± 36*	699 ± 71	640 ± 57	523 ± 37	742 ± 169	810 ± 150	746 ± 104	960 ± 112	901 ± 163	848 ± 151

M2 macrophages													
Control		IS [mg/mL]			SFG [mg/mL]			FCM [mg/mL]			IIM [mg/mL]		
		0.133	0.266	0.533	0.133	0.266	0.533	0.133	0.266	0.533	0.133	0.266	0.533
CD68	5031 ± 593	7989 ±	8712 ±	7472 ±	8157 ±	7883 ±	8745 ±	6361 ±	5997 ±	6693 ±	5875 ±	5979 ±	6447 ±
		796**	681**	407*	842	1362	1583*	341	754	1158	468	146	501
CD14	461 ± 294	34 ± 6	30 ± 7	31 ± 10	76 ± 31	21 ± 5	24 ± 3	415 ± 230	263 ± 149	74 ± 26	345 ± 213	413 ± 229	312 ± 182
CD16	2073 ± 928	333 ±	272 ±	259 ±	429 ±	362 ±	373 ±	2194 ±	1570 ±	799 ±	2027 ±	2334 ±	1620 ±
		72*	46*	46*	134	135*	82	904	725	334	955	1090	746
CD32	18849 ± 8129	5096 ± 773	4435 ± 806	4318 ± 717	8273 ± 1750	5080 ± 883	4421 ± 667	15693 ± 5657	11668 ± 4840	7847 ± 1957	15349 ± 5999	16057 ± 5522	12808 ± 5142
CD163	14222 ± 7952	2280 ± 248	2398 ± 243	2387 ± 252	2620 ± 316	2930 ± 507	3170 ± 517	13730 ± 5374	8016 ± 3015	4378 ± 1212	11972 ± 5403	14704 ± 7033	9979 ± 4165
CD206	6379 ± 700	5035 ± 715	4675 ± 532	3342 ±	4535 ± 557	5044 ± 506	3713 ±	8069 ± 1302	6854 ± 1966	6292 ± 1397	5823 ± 857	6450 ± 1212	6329 ± 1242

Indicated is mean fluorescence intensity [MFI] ± SEM; 4 ≤ n ≤ 6; Significant changes are presented as bold numbers, *P < 0.05, **P < 0.01.

Table 2a. MiRNA analysis of monocyte derived mature dendritic cells after iron sucrose stimulation.

miRNA	Control (tpm)	Iron sucrose (0.266 mg/mL, tpm)	Log2(fold change)	p-value
hsa-miR-146a-5p	18913	24992	-0.40	0
hsa-miR-142-5p	16923	8986	0.91	0
hsa-miR-19b-3p	14993	9102	0.72	0
hsa-miR-29a-3p	30909	21275	0.54	0
hsa-let-7g-5p	12486	7140	0.81	0
hsa-let-7i-5p	10423	5092	1.03	0
hsa-miR-23b-3p	3403	455	2.90	0
hsa-miR-210	5033	412	3.61	0
hsa-miR-146b-5p	30093	16402	0.88	0
hsa-miR-103a-3p	13309	7088	0.91	0
hsa-miR-21-5p	421617	523388	-0.31	0
hsa-miR-155-5p	30697	7440	2.04	0
hsa-miR-340-5p	3013	5596	-0.89	8.39×10^{-284}

hsa-miR-378c	1335	299	2.16	1.43×10^{-254}
hsa-miR-101-3p	26845	21223	0.34	7.17×10^{-243}
hsa-miR-223-3p	4400	7086	-0.69	1.83×10^{-229}
hsa-miR-374a-5p	6200	9308	-0.59	1.82×10^{-227}
hsa-miR-191-5p	7835	5059	0.63	2.54×10^{-218}
hsa-miR-320a	1661	539	1.62	6.30×10^{-216}
hsa-miR-148b-3p	2302	4205	-0.87	3.98×10^{-204}

P = 0 for P < 9.99×10^{-307}

Table 2b. MiRNA expression analysis of monocyte derived mature dendritic cells after iron isomaltoside 1000 stimulation.

miRNA	Control (tpm)	Iron isomaltoside 1000 (0.266 mg/mL, tpm)	Log2(fold change)	p-value
hsa-miR-142-3p	58843	67993	-0.21	0
hsa-miR-155-5p	30697	26222	0.23	7.47×10^{-195}
hsa-miR-210	5033	3487	0.53	1.01×10^{-152}
hsa-miR-29a-3p	30909	27629	0.16	9.47×10^{-103}
hsa-miR-103a-3p	13309	11242	0.24	7.24×10^{-96}
hsa-let-7g-5p	12486	10526	0.25	5.43×10^{-92}
hsa-miR-21-5p	421617	430105	-0.03	2.18×10^{-80}
hsa-miR-146a-5p	18913	16694	0.18	6.74×10^{-77}
hsa-miR-27a-3p	8077	9519	-0.24	1.81×10^{-65}
hsa-miR-24-3p	9987	11457	-0.20	3.51×10^{-56}
hsa-miR-30e-5p	14552	16267	-0.16	1.51×10^{-53}
hsa-miR-3676-5p	53	151	-1.51	4.91×10^{-28}
hsa-miR-101-3p	26845	28415	-0.08	3.17×10^{-26}

hsa-miR-221-3p	5844	5172	0.18	1.05×10^{-23}
hsa-miR-93-3p	1488	1163	0.36	5.10×10^{-23}
hsa-miR-92a-3p	3370	2905	0.21	3.72×10^{-20}
hsa-miR-29b-3p	7721	8465	-0.13	4.01×10^{-20}
hsa-miR-3676-3p	120	226	-0.91	3.71×10^{-19}
hsa-miR-25-3p	1553	1257	0.31	1.89×10^{-18}
hsa-miR-7-5p	937	717	0.39	2.56×10^{-17}

P = 0 for P < 9.99×10^{-307}

LEGENDS TO FIGURES

Figure 1. Monocytic adhesion on activated HUVECs and transmigration through 8 μ M cell culture inserts (after CD45-labelling and in the presence of 50 ng/ml MCP-1) after stimulation with 0.133 mg/mL iron sucrose (IS), sodium ferric gluconate (SFG), ferric carboxymaltose (FCM) or iron isomaltoside 1000 (IIM). Blood was collected from control subjects and evaluated by phase contrast microscopy (adhesion) and by fluorescence microscopy (transmigration). Numerical analyses were evaluated in 10 microscopic fields per approach. **A; B:** Representative examples of monocytic adhesion (**A**) and transmigration (**B**); bar scales 100 μ m for all images. **C; D:** Mean \pm SEM of 4 independent experiments for adhesion (**C**) and transmigration (**D**); controls (in the absence of iron) are defined as 100%. Statistical analysis was performed by using ANOVA followed by Dunnett's multiple comparison test as post-hoc test.

Figure 2. Capacity of M1 macrophages to phagocyte opsonised carboxylate microspheres (0.75 μ m, Yellow Green) within 30 min. Macrophages were *in vitro* differentiated from monocytes under stimulation with three different concentrations (0.133 mg/mL, 0.266 mg/mL, 0.533 mg/mL) of iron sucrose (IS), sodium ferric gluconate (SFG), ferric carboxymaltose (FCM) or iron isomaltoside 1000 (IIM). Blood was collected from control subjects. Counts of FITC-positive cells as phagocytosing macrophages (shown on the right-hand side of each histogram) were determined flow-cytometrically. Histograms depict representative examples from one single individual, and mean \pm SEM of at least 5 independent experiments. Statistical analysis was performed using ANOVA and the Dunnett's multiple comparison test as post-hoc test.

Figure 3. Phenotypical and functional analysis of mDCs that were *in vitro* differentiated from monocytes under stimulation with iron sucrose (IS), sodium ferric gluconate (SFG), ferric carboxymaltose (FCM) or iron isomaltoside 1000 (IIM) (0.133 mg/mL, 0.266 mg/mL, 0.533 mg/mL). Blood was collected from control subjects. Statistical analysis was performed

by using ANOVA and the Dunnett's multiple comparison test as post-hoc test; data of 5 independent experiments are presented as mean \pm SEM; *P < 0.05, **P < 0.01. **A-H:** Protein expression analysis of mDC surface markers CD1c (**A**), CD141 (**B**), CD80 (**C**), CD83 (**D**), CD86 (**E**), CD1a (**F**), CD40 (**G**) and HLA-DR (**H**) were measured as mean fluorescence intensity (MFI) by flow-cytometry. **I; J:** For T-cell proliferation analysis mDCs were co-cultured with autologous, CFDA-SE-labelled T-cells at the ratio of 5:1 and activated with 2.5 μ g/mL staphylococcal enterotoxin B. After 3 days, counts of proliferating T-cells (shown on the left-hand side of each histogram) were analysed flow-cytometrically by their FITC-fluorescence intensity, identifying total T-cells by CD3-expression (**I**) and CD8⁺ T-cells by CD3/CD8 expression (**J**).

Figure 4. miRNA expression analysis (smallRNA-seq and omiRas [21]) of mDCs, *in vitro* differentiated from monocytes under stimulation with 0.266 mg/mL iron sucrose and iron isomaltoside 1000. Statistical analysis of miRNA expression was performed with the DEGseq bioconductor package [23]. A p-value of $< 10^{-10}$ was considered statistically significant. Presented scatter plots show tags per million (tpms) of 631 analysed miRNAs in iron sucrose stimulated mDCs, compared to control approach as well as in iron isomaltoside 1000 stimulated mDCs, compared to control (**A**). Presentation of significantly different expressed miRNAs between the 3 approaches control, iron sucrose and iron isomaltoside 1000 (**B**).

FIGURES

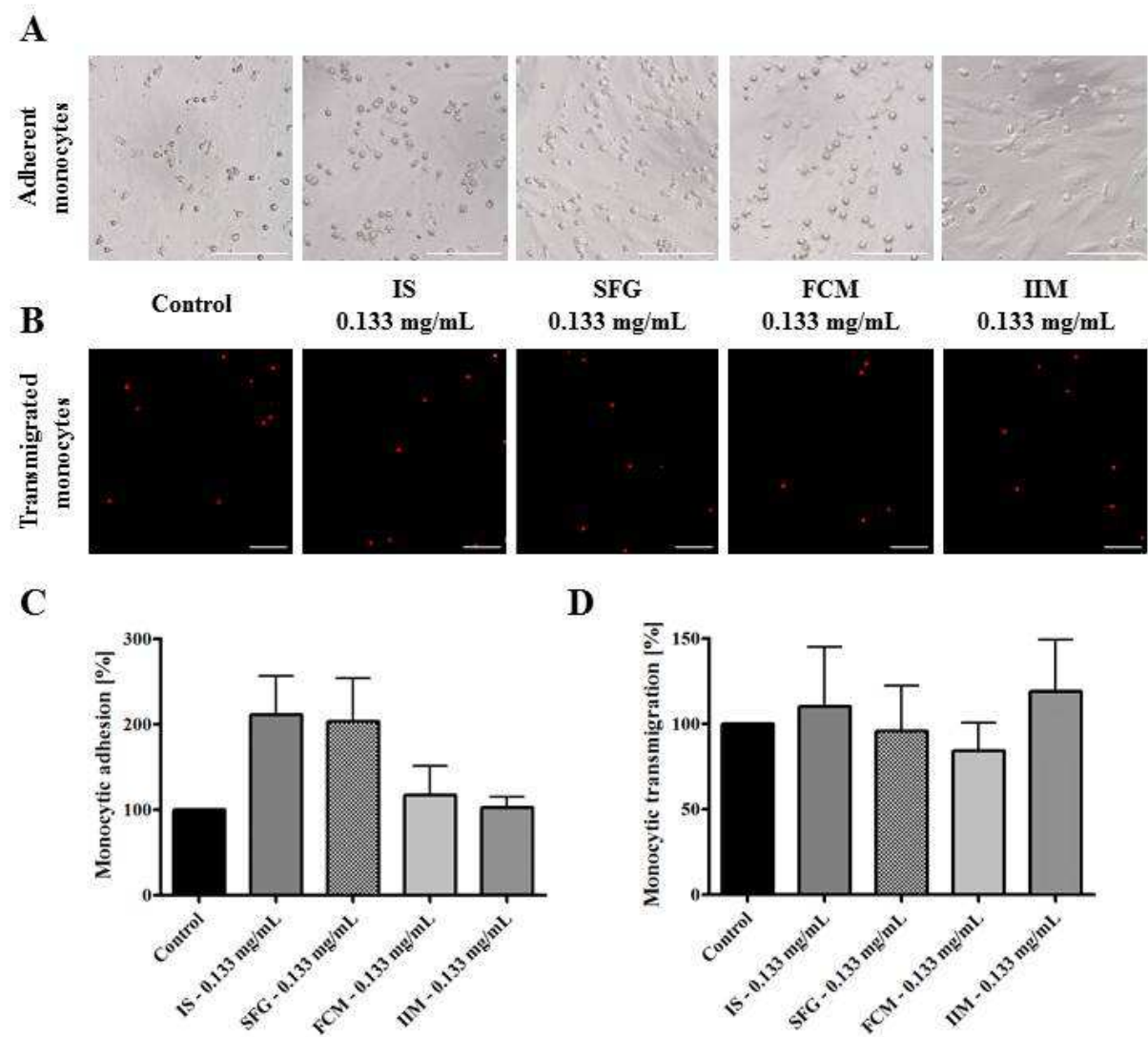
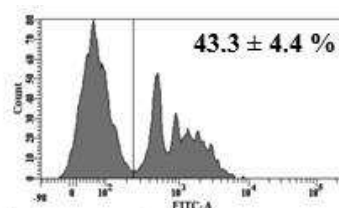


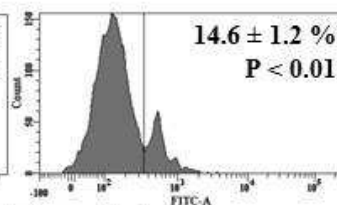
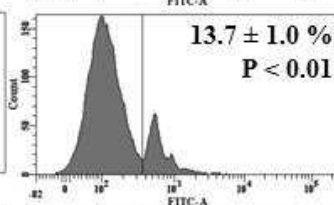
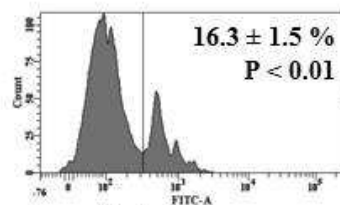
Figure 1

M1 macrophages

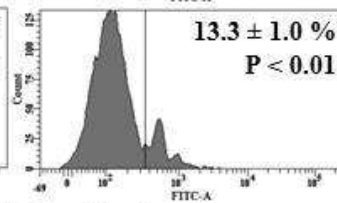
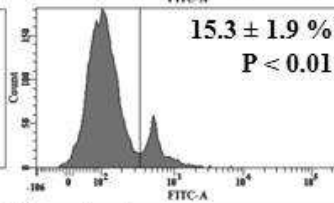
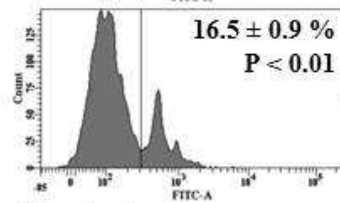
Control



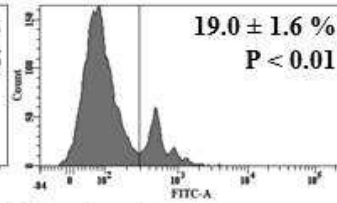
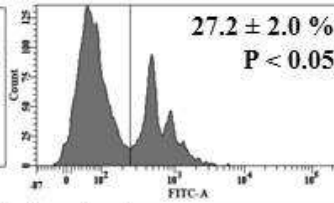
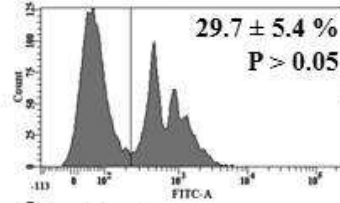
IS



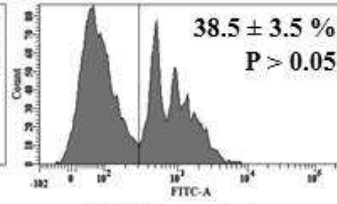
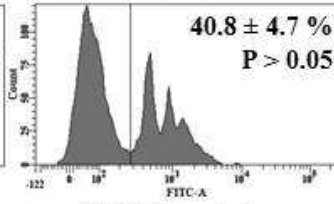
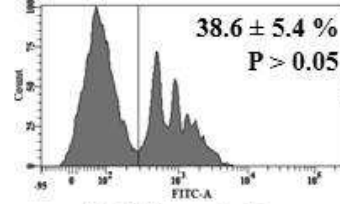
SFG



FCM



IIM



0.133 mg/mL

0.266 mg/mL

0.533 mg/mL

Figure 2

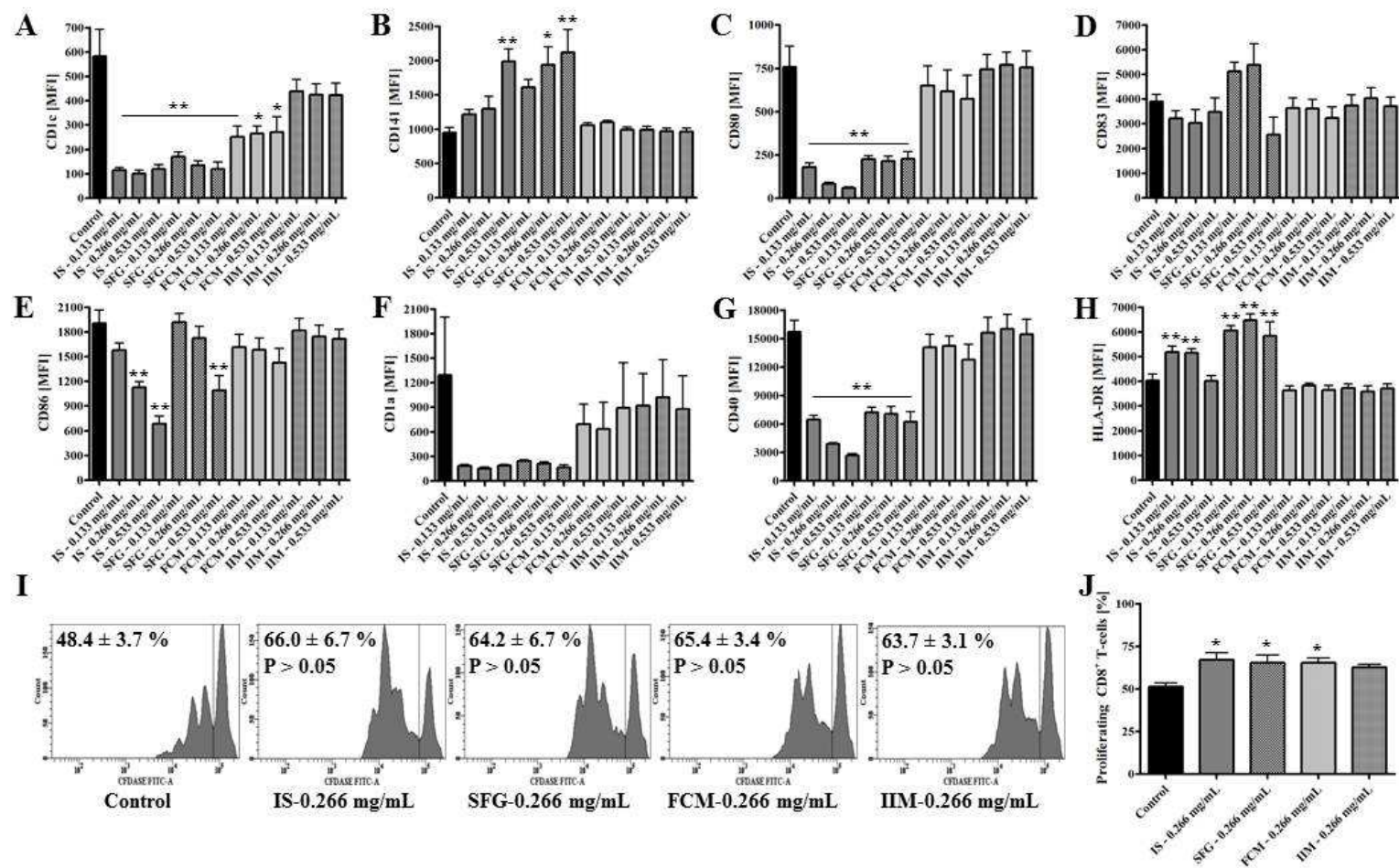


Figure 3

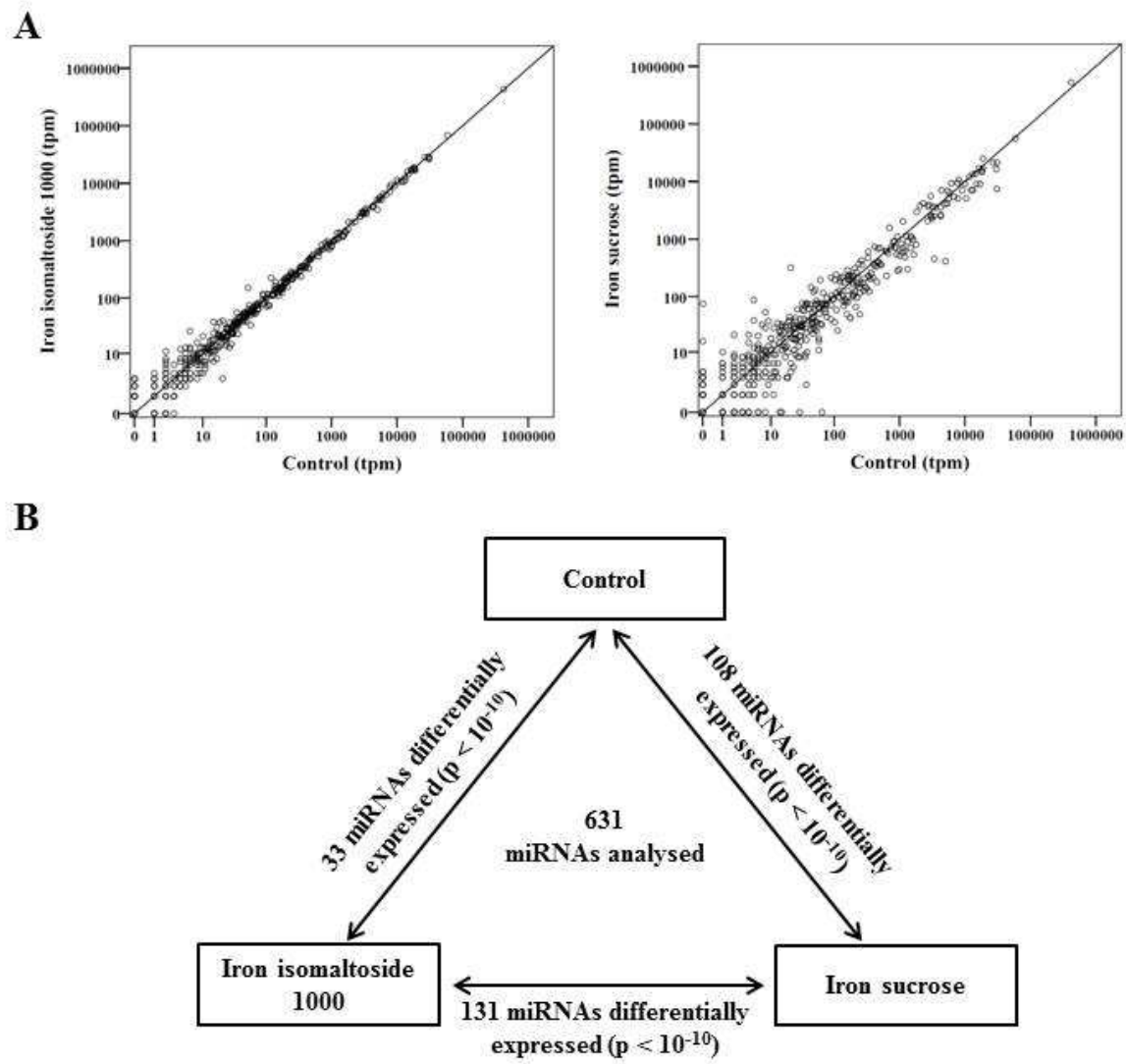


Figure 4

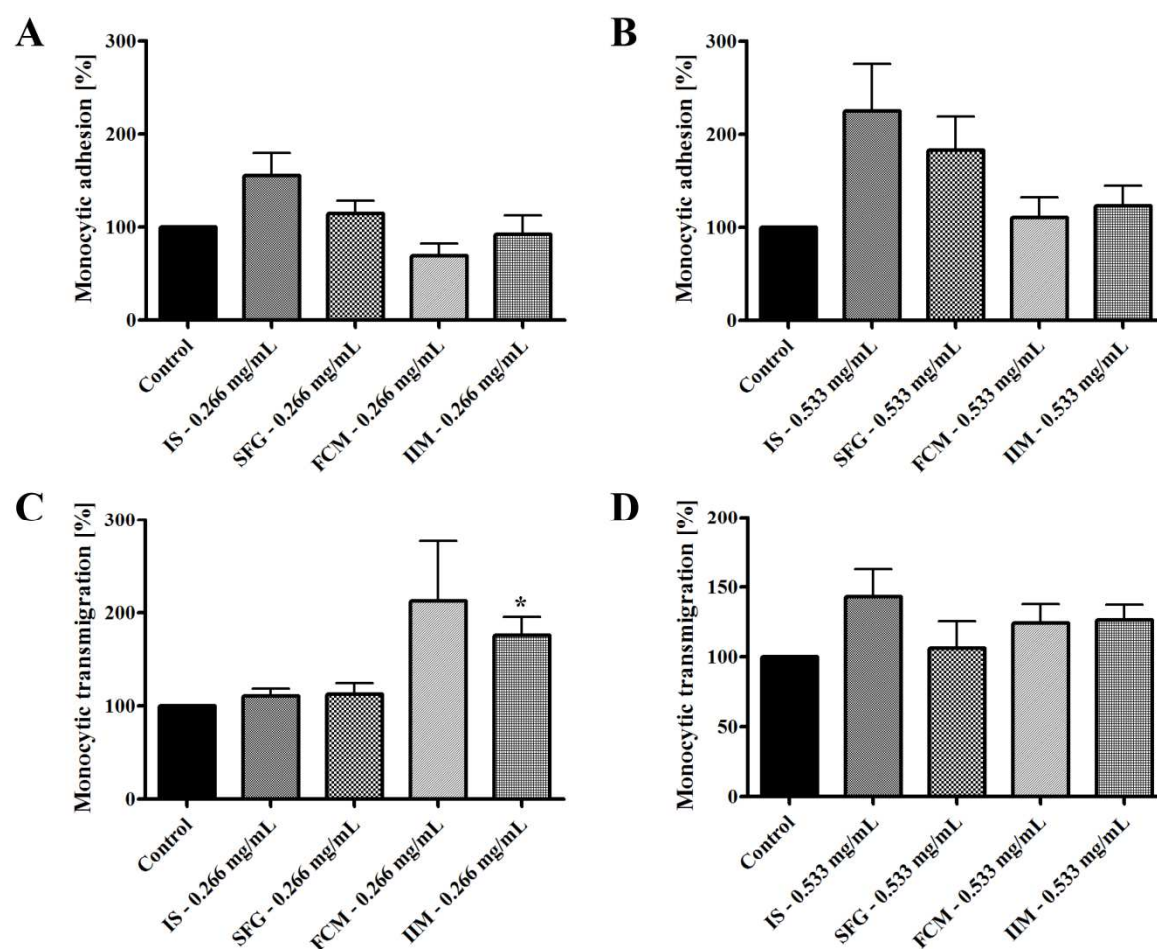


Figure S1

Figure S1. Monocytic adhesion on activated HUVECs (**A**, **B**) and transmigration of CD45 labelled monocytes through 8 μ M cell culture inserts in the presence of 50 ng/ml MCP-1 (**C**, **D**) after stimulation with 0.266 mg/mL and 0.533 mg/mL iron sucrose (IS), sodium ferric gluconate (SFG), ferric carboxymaltose (FCM) or iron isomaltoside 1000 (IIM). Blood was collected from control subjects. In each approach, cell numbers were evaluated either by phase contrast microscopy (adhesion) or by fluorescence microscopy (transmigration) in 10 fields and indicated in comparison to control. Statistical analysis was performed by using ANOVA followed by Dunnett's multiple comparison test as post-hoc test; data of 4 independent experiments are presented as mean \pm SEM; *P < 0.05.

M2 macrophages

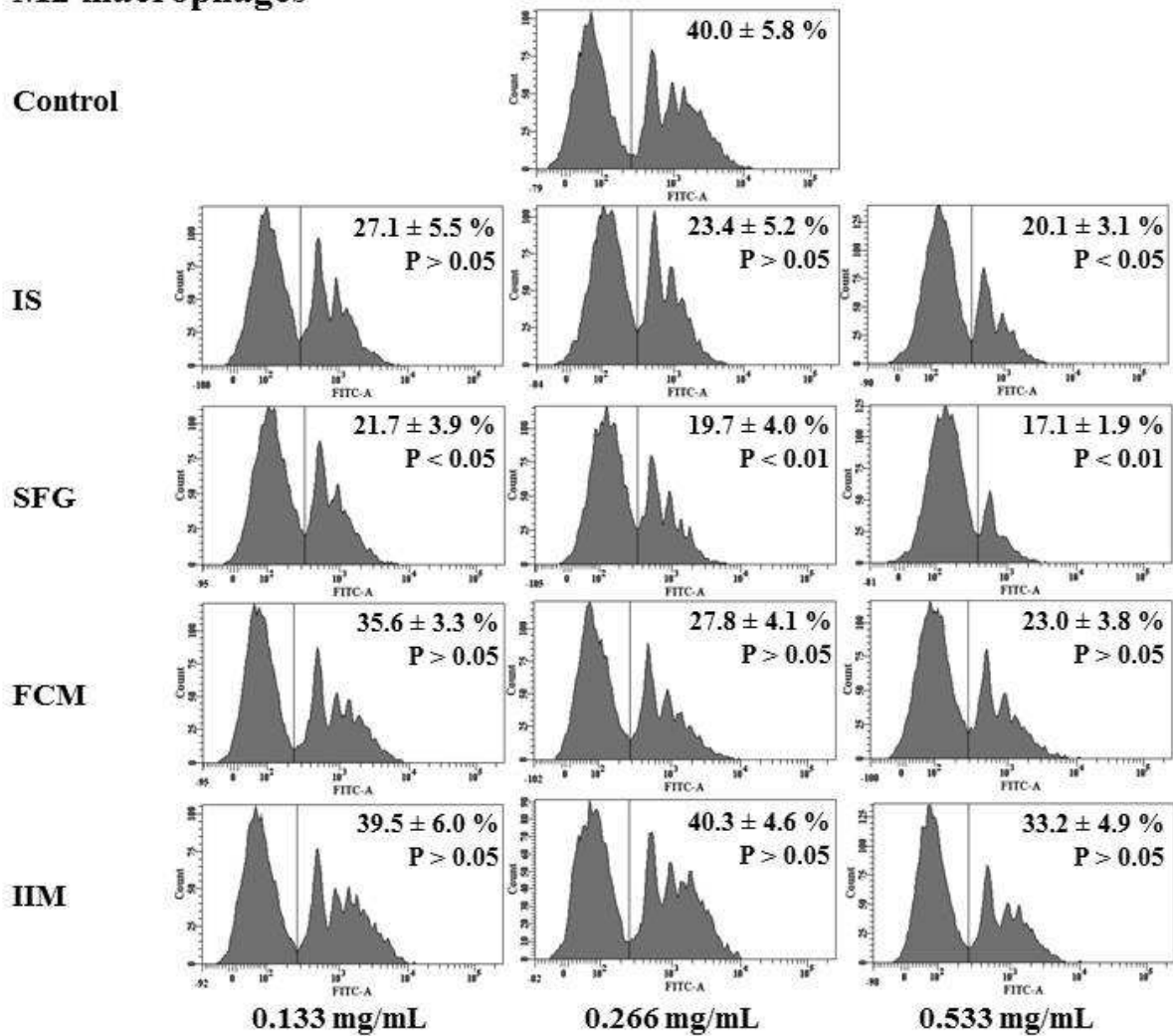


Figure S2

Figure S2. Capacity of M2 macrophages to phagocyte opsonised carboxylate microspheres (0.75 μ m, Yellow Green) within 30 min. Macrophages were *in vitro* differentiated from monocytes under stimulation with iron sucrose (IS), sodium ferric gluconate (SFG), ferric carboxymaltose (FCM) or iron isomaltoside 1000 (IIM) (0.133 mg/mL, 0.266 mg/mL, 0.533 mg/mL). Blood was collected from control subjects. Counts of FITC-positive cells as phagocytosing macrophages (shown on the right-hand side of each histogram) were determined flow-cytometrically. Histograms show representative examples from one individual and the mean \pm SEM of at least 5 independent experiments. Statistical analysis was performed using ANOVA and the Dunnett's multiple comparison test as post-hoc test.

Table S1. Antibodies used in this study.

Molecule	Conjugate	Clone	Source
CD45	PE	H130	BD Biosciences
CD14	PerCP	MφP9	BD Biosciences
CD16	PE/Cy7	3G8	BD Biosciences
CD86	PE	HA5.2B7	Beckman-Coulter
HLA-DR	APC	Immu-357	Beckman-Coulter
CD141	APC	M80	Biolegend
CD83	PE/Cy7	BH15e	Biolegend
CD1c	FITC	L161	Biolegend
CD40	PE/Cy7	5C3	Biolegend
CD1a	PerCP	HI149	Biolegend
CD80	FITC	2D10	Biolegend
CD32	APC	Fun-2	Biolegend
CD68	PE	Y1/82A	Biolegend
CD64	FITC	10.1	Biolegend
CD163	PE/Cy7	GHI/61	Biolegend
CD206	APC	15-2	Biolegend
CD3	APC	SK7	Biolegend
CD4	Pe/Cy7	OKT4	Biolegend
CD8a	PE	HIT8a	Biolegend

Table S2. Raw data of microRNA analysis of monocyte derived mature dendritic cells in the control approach and after stimulation with iron sucrose and iron isomaltoside 1000.

Table S3. Comparative miRNA analysis of monocyte derived mature dendritic cells after iron sucrose and iron isomaltoside 1000 stimulation.

miRNA	Iron isomaltoside 1000 (0.266 mg/mL, tpm)	Iron sucrose (0.266 mg/mL, tpm)	Log2(fold change)	p-value
hsa-miR-378c	1358	299	2.18	0
hsa-miR-146a-5p	16694	24992	-0.58	0
hsa-miR-101-3p	28415	21223	0.42	0
hsa-miR-223-3p	4135	7086	-0.78	0
hsa-miR-142-5p	16909	8986	0.91	0
hsa-miR-19b-3p	14403	9102	0.66	0
hsa-miR-29a-3p	27629	21275	0.38	0
hsa-let-7g-5p	10526	7140	0.56	0
hsa-miR-148b-3p	2139	4205	-0.98	0
hsa-let-7i-5p	10379	5092	1.03	0

hsa-miR-23b-3p	3117	455	2.77	0
hsa-miR-210	3487	412	3.08	0
hsa-miR-146b-5p	28838	16402	0.81	0
hsa-miR-103a-3p	11242	7088	0.67	0
hsa-miR-340-5p	3218	5596	-0.80	0
hsa-miR-21-5p	430105	523388	-0.28	0
hsa-miR-155-5p	26222	7440	1.82	0
hsa-miR-142-3p	67993	55756	0.29	0
hsa-miR-34a-5p	2053	3789	-0.88	4.34×10^{-275}
hsa-miR-374a-5p	6581	9308	-0.50	1.98×10^{-248}

P = 0 for $P < 9.99 \times 10^{-307}$